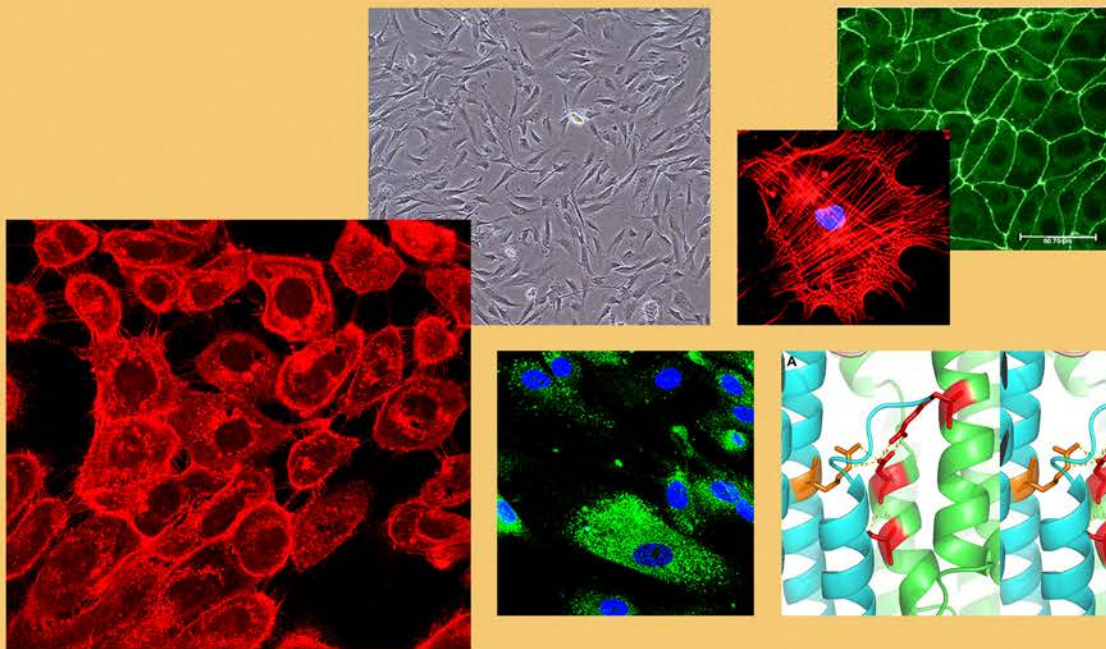


ANNUAL REPORT

2020-2021



RESEARCH IN OPHTHALMIC SCIENCES
Aravind Medical Research Foundation

ARAVIND MEDICAL RESEARCH FOUNDATION

Aravind Medical Research Foundation is recognised as Scientific and Industrial Research Organization (SIRO) by the Department of Scientific and Industrial Research (DSIR), Government of India

MISSION

To eliminate needless blindness by providing evidence through research and evolving methods to translate existing evidence and knowledge into effective action.

RESEARCH IN OPHTHALMIC SCIENCES

Dr. G. Venkataswamy Eye Research Institute

Annual Report 2020 - 2021

ARAVIND MEDICAL RESEARCH FOUNDATION

BOARD OF MANAGEMENT



DR. P. NAMPERUMALSAMY,
MS, FAMS



DR. G. NATCHIAR, MS, DO



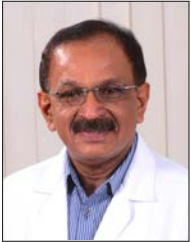
ER. G. SRINIVASAN, BE, MS



MR. R.D. THULASIRAJ, MBA



DR. S.R. KRISHNADAS,
DO., DNB



DR. R. KIM, DO., DNB



DR. N. VENKATESH PRAJNA
DO., DNB., FRCophth



DR. S. ARAVIND, MS, MBA

FACULTY



PROF. K. DHARMALINGAM
Director - Research



PROF. V.R. MUTHUKARUPPAN
Advisor-Research



DR. P. SUNDARESAN
Senior Scientist
Molecular Genetics



DR. C. GOWRI PRIYA
Scientist, Immunology &
Stem Cell Biology



DR. S. SENTHILKUMARI
Scientist, Ocular Pharmacology



DR. A. VANNIARAJAN
Scientist, Molecular Genetics



DR. J. JEYA MAHESHWARI
Scientist, Proteomics



DR. D. BHARANIDHARAN
Scientist, Bioinformatics



DR. O.G. RAMPRASAD
Scientist, Proteomics



DR. DAIPAYAN BANERJEE
Scientist - I, Proteomics



DR. SWAGATA GHOSH
Associate Faculty, Microbiology



DR. SIDDHARTH NARENDHAN
Associate Faculty

ARAVIND MEDICAL RESEARCH FOUNDATION

CLINICIAN-SCIENTISTS



DR. P. VIJAYALAKSHMI, MS
Professor of Paediatric
Ophthalmology



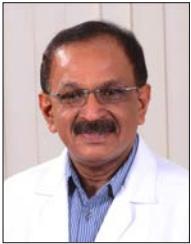
DR. S.R. KRISHNADAS,
DO., DNB
Professor of Ophthalmology



DR. SR. RATHINAM,
MNAMS, PH.D
Professor of Ophthalmology &
HOD - Uvea Services



DR. HARIPRIYA ARAVIND, MS
HOD - IOL & Cataract Services



DR. R. KIM, DO., DNB
Professor of Ophthalmology &
Chief Medical Officer



DR. N. VENKATESH PRAJNA
DO., DNB., FRCophth
Professor of Ophthalmology
& HOD - Cornea Services



DR. USHA KIM, DO, DNB
Professor of Ophthalmology
& HOD - Orbit, Oculoplasty &
Ocular Oncology Services



DR. LALITHA PRAJNA,
MD., DNB
HOD - Microbiology



DR. R. SHANTHI, MD
Pathologist



DR. R. SHARMILA, DNB
Medical Consultant
Glaucoma Services



DR. MADHU SHEKAR, DNB
Chief - Cataract Services



DR. MAHESH KUMAR, DO, DNB
Chief - Neuro-ophthalmology
Services

RESEARCH COUNCIL MEMBERS



DR. P. NAMPERUMALSAMY
Chairman



DR. P. VENKATACHALAM
Member



PROF. V.R. MUTHUKKARUPPAN
Member



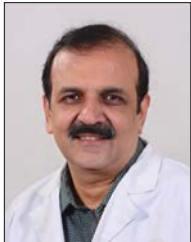
DR. G. KUMARESAN
Member



DR. S. THIYAGARAJAN
Member



PROF. S. KARUTHAPANDIAN
Member



DR. N. VENKATESH PRAJNA
Member



DR. R. KIM
Member



PROF. K. DHARMALINGAM
Member Secretary

INSTITUTIONAL ETHICS COMMITTEE (IEC)

Chairman

PROF. R. VENKATARATNAM M.A., PH.D
Senior Prof. of Sociology (Retired)
Madurai Kamaraj University, Madurai

Member-Secretary

DR. R. SHARMILA, DNB
Medical Officer, Glaucoma Clinic,
Aravind Eye Hospital, Madurai

Members

DR. C. SRINIVASAN M.SC., PH.D
UGC Emeritus Professor
New No. 2/249 (Old No 2/172), 7th Street, Kalvinagar,
Rajambadi, Madurai - 625021

DR. T.S. CHANDRASEKARAN MS, DO
Ophthalmologist,
No.6, N.M.R.Subbaraman Road, Chokkikulam North,
Madurai

MR. M. SENTHILKUMAR M.A., B.L
Advocate
Plot No.32, Sindanayalar Nagar
Senthamil Nagar, Karuppayoorani East, Madurai

MR. R. RAJA GOVINDASAMY M.A., M.A (USA)

Former Principal, Thiagarajar College
169-1, 2nd Cross Street, I Main Road, Gomathipuram,
Madurai - 625020

DR. S. SABHESAN DPM, MNAMS, PH.D

Consultant – Psychiatrist, Apollo Specialty Hospitals
Lake view Road, K.K.Nagar, Madurai

DR. A. AMIRTHA MEKHALA BDS, MPH, MFDSRCPS

Private Practice - Dental Services
208 Karpaga Nagar 8th Street, K.Pudur, Madurai - 625007

MRS. PREMALATHA PANNEERSELVAM M.A., M.ED

Secretary, Mahatma Montessori Matriculation Hr.Sec.
School, Madurai

DR. J.R. VIJAYALAKSHMI MD (PHARMACOLOGY)

Professor of Pharmacology
CSI college of Dental Sciences, Madurai

MR. ARM. GANESH B.COM., LLB

Advocate, D-3/4, First Cross Street
K.K.Nagar west, Madurai - 625020

DR. LALITHA PRAJNA DNB

Chief - Microbiology, Aravind Eye Hospital, Madurai

CONTENTS

Molecular Genetics	1
Stem Cell Biology	20
Proteomics	28
Ocular Pharmacology	44
Bioinformatics	52
Ocular Microbiology	57
Conferences / Meetings	62
Publications 2020 - 2021	64
Ongoing Research Projects	66

FOREWORD



AMRF is all set to explore new areas of research with the addition of four new faculty members. Age related macular degeneration (ARMD), stem cells for transplantation research, retinal pigment epithelial cell regeneration, Acanthamoeba keratitis are some of the specializations which the new team will focus on. They also will collaborate with the existing scientists to expand the scope of ongoing research programmes. One of the scientists was awarded the prestigious Ramalingaswami re-entry fellowship and he will be working on the use of stem cells in AMD. I hope these developments will rejuvenate the research programmes at AMRF and will produce clinically relevant results.

Many eye diseases are amenable to therapeutic intervention today due to the distinctive characteristics of the eye, such as immune privilege, blood retinal barrier and presence of non-dividing cells. There are at least 17 ophthalmic conditions that could be dealt with by gene therapy and almost 50 clinical trials are in progress. Leber hereditary optic neuropathy, and Choroideremia (CHM) gene therapy clinical trials are in phase III. This is an area where AMRF will have its focus in the immediate future.

Another topic which AMRF plans to explore is cell based therapies for diseases such as ARMD, which is the third major cause of irreversible blindness. The newly hired faculty will be working on using the converted pluripotent stem cells and tailoring the regenerative potential of damaged pigment epithelial cells to deal with this disease.

Bioavailability of the intraocular drugs administered topically is restricted due to the architecture of eye tissue. Use of nanocarriers as nanomedicines for drug delivery is an area that needs our attention. I am aware that a group of investigators from AMRF are exploring the functions of nanovesicles (exosomes) from the eye and their usefulness as nanocarriers of drugs and immune modulators to deal with corneal infections, glaucoma and diabetic retinopathy. All these new initiatives will go a long way in this important area of translational research.

Contributions of AMRF will be more substantial in the near future, with additional human resource, financial input and new areas of research. As in the previous years, AMRF and the Aravind Eye Care System will continue to support and nurture research in order to achieve the goal of our founder, Dr. G. Venkataswamy.

- *Dr. P. Namperumalsamy*
President, AMRF

INTRODUCTION



I am very happy to record that we have recruited four additional faculty members for AMRF this year. With this addition, AMRF hopes to expand its areas of research and take up new projects. Further, existing investigators will continue to explore new avenues for research. Stem cells for age-related macular degeneration, regeneration of retinal pigment epithelium, Acanthamoeba keratitis are some of the new research areas which the team will be pursuing this year onwards. As in the previous years, AMRF continues to receive financial support from industries, government organisations and private donors. AMRF gratefully acknowledges their support and looks forward to a continuing partnership.

Like any other organization, AMRF was severely affected by the COVID pandemic. In spite of the lock downs, the team could keep the labs, freezers and essential equipment running, thanks to the hard work and commitment of the technicians and research scholars. Despite the trying conditions, they continued to come to the lab to make sure that the critical instruments were running smoothly, and the labs were safe.

Various projects, their progress and their potential for clinical utility are highlighted in this report.

Prof. K. Dharmalingam
Director - Research

MOLECULAR GENETICS

Genetics in ocular disorders are becoming increasingly important for an accurate molecular diagnosis and for the development of novel genotype-specific treatments. Molecular Genetics lab currently focuses on the leading cause of inherited retinal dystrophies, understand the molecular mechanism underlying disease pathogenesis in cone-rod dystrophies, retinitis pigmentosa, Stargardt, Leber's congenital amaurosis, Leber's hereditary optic neuropathy and Juvenile X-linked retinoschisis. Furthermore, the lab offers genetic counselling based on moral and ethical values to provide the best possible solution for people at risk.

Translational Genomics of Paediatric Eye Diseases

- Investigators : Dr. P. Sundaresan
Dr. A. Vanniarajan
Dr. D. Bharanidharan
Dr. VR. Muthukkaruppan
Dr. P. Vijayalakshmi, Dr. R. Kim
Dr. Usha Kim
- Project Fellows : Roopam Duvesh, Gowri
Poigaiwar, A.S.Sriee
Viswarubhiny, Susmita
Chowdhury, A. Aloysius
Abraham, K. Jeya Prakash,
A. Mohamed Hameed Aslam,
C. Prakash, K. Manoj Kumar
- Funding Agency : Department of Biotechnology

Introduction

In India, prevalence of blindness is estimated to be 0.8/1000 in the paediatric age group with around 280,000 blind children. Major causes of childhood blindness in India include congenital anomalies and retinal dystrophies together contributing to 40%. Childhood blindness affects the learning and cognitive abilities of individuals and thus impact quality of life. In children, about 29% of abnormalities contributing to blindness has been observed in the retinal tissue, making it the most affected site. Moreover, diagnosis becomes more challenging due to presence of phenotypic heterogeneity in genetic eye diseases. Herein, the team used a unified approach of clinical, genetic and computational analysis to dissect the underlying molecular cause of paediatric eye diseases including Leber Congenital Amaurosis (LCA), Leber's Hereditary Optic Neuropathy (LHON), Retinoblastoma (RB) and Juvenile X-linked Retinoschisis (JXLR) for better understanding towards early detection and possible treatment.

Clinical Exome sequencing of Leber Congenital Amaurosis patients

Leber congenital amaurosis (LCA), primarily characterized by retinal degeneration is the most severe form of inherited retinal dystrophy (IRD) responsible for congenital blindness. The presence of phenotypic heterogeneity made the diagnosis of LCA challenging, especially in the absence of pronounced disease pathognomonic, yet it can be well



comprehended by employing molecular diagnosis. Therefore, the present study aimed to reveal the causative mutations in ten LCA patients with variable phenotypes using clinical exome sequencing. Ophthalmic information of ten unrelated LCA patients and their family history were obtained. Clinical exome sequencing was performed for all patients and the data was analyzed using a bioinformatics pipeline. The identified mutations were further validated by Sanger sequencing. Segregation analysis was also performed on available family members.

Clinical exome sequencing identified disease-causing mutations in nine out of ten patients, of which seven patients harbored mutations in the LCA associated genes, including RPE65, LCA5, CRX, PRPH2, CEP290, and ALMS1. Among these, three mutations (LCA5: c.1823del, p.Leu608TyrfsTer30; CRX: c.848del, p.Met283ArgfsTer88; CEP290: c.2483G>T, p.Ser828Ile) were novel. To the team's knowledge, this is the first report of a mutation of these LCA candidate genes, including PRPH2: c.629C>T, p.Pro210Leu; CEP290: c.2483G>T, p.Ser828Ile; and ALMS1: c.11310_11313del, p.Glu3771TrpfsTer18 from Indian population.

The remaining two patients were identified with other retinal disease genes IFT80 and RP1 (Figure 1). IFT80 mutants are known to cause Jeune syndrome, an autosomal recessive disease characterized by the constricted thoracic cage, respiratory insufficiency, cystic renal disease, polydactyl disease and retinal degeneration. The mutation (c.1936G>T, p.Val646Phe) in the IFT80 gene has not reported yet to associate with the LCA phenotype. Other patient was initially diagnosed with LCA as she presented with poor visual acuity at the age of 1.75 years. Interestingly, molecular diagnosis identified a homozygous frameshift mutation in exon 4 of the RP1 gene, documented to cause retinitis

pigmentosa. Thus, based on the genetic finding and revision of initial clinical data, the diagnosis was re-defined to early-onset retinitis pigmentosa.

In conclusion, the results underline the importance of clinical exome sequencing in clinically diagnosed LCA patients with variable phenotypes. This study established the involvement of new genes in the pathogenesis of LCA and helped re-define the clinical diagnosis.

Whole mitochondrial genome sequencing and haplogroup analysis of Leber's Hereditary Optic Neuropathy (LHON) patients

Leber's hereditary optic neuropathy (LHON) is a matrilineal inherited mitochondrial disorder causing retinal ganglion cell degeneration that leads to central vision loss predominantly in young males. It is caused by mitochondrial DNA (mtDNA) mutations that disrupt the protein complexes involved in Electron Transport Chain.

Whole mitochondrial genome for 100 South Indian LHON patients was analyzed by utilizing Sanger and Next Generation Sequencing approaches. The results revealed the presence of LHON causing primary mutations in 43 samples (43%) including the common primary mutations: m.G11778A (38/43, 88.37%), and m.T14484C (3/43, 6.98%); and the rare primary mutations: m.C4171A (1/43, 2.33%), and m.G11696A (1/43, 2.33%). The potential pathogenic mutations that have been previously reported to be associated with LHON were found in 8% of the patients. They are: m.T4216C (2/8), m.T4216C+m.G7444A (1/8), m.G9139A (1/8), m.T12338C (1/8), m.G13708A (2/8), m.G15077A (1/8). Together, the study identified LHON associated mutations in 51% of the study participants.

Possible Pathogenic Variants: Analysis of variant pathogenicity in samples those were negative for

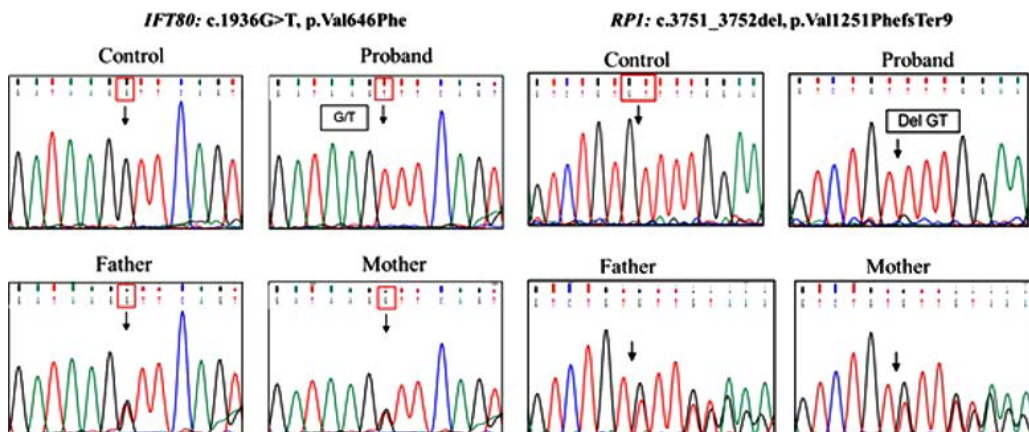


Figure 1: Chromatograms depicting IFT80 and RP1 pathogenic variants identified in LCA patients

Table 1: Possibly pathogenic variants detected in LHON samples

S.No	Variant	Gene	Aminoacid change	SIFT	Polyphen 2	Provean	Genbank frequency	Conservation
1	m.A8396G	MT-ATP8	T11A	A	POD	N	0.186%	40.00%
2	m.A4833G	MT-ND2	T122A	A	POD	N	1.004%	17.78%
3	m.T3398C	MT-ND1	M31T	A	B	D	0.443%	91.11%
4	m.T11544A	MT-ND4	L262H	A	PRD	D	0.006%	53.33%
5	m.T11544A	MT-ND4	L262H	A	PRD	D	0.006%	53.33%
6	m.T15287C	MT-CYB	F181L	A	B	D	0.168%	82.22%
7	m.A4833G	MT-ND2	T122A	A	POD	N	1.004%	17.78%
8	m.A5186T	MT-ND2	W239C	A	PRD	N	0.091%	17.78%
9	m.C8513T	MT-ATP8	P50S	A	PRD	D	0.008%	86.67%
10	m.T11087C	MT-ND4	F110L	A	PRD	D	0.186%	100.00%
11	m.C14990T	MT-CYB	L82F	A	PRD	D	0.043%	73.33%

A-Affect protein function; POD-Possibly damaging; PRD-Probably damaging; D-Deleterious; B-Benign; N-Neutral

LHON mutations, suggested the presence of possibly pathogenic variants (Table 1).

Mitochondrial Haplogroup Classification:
Haplogroup analysis was performed using the tool, HaploGrep2 to predict the group at risk of developing the disease. Phylogenetic analysis revealed that the haplogroup M was predominant in the study cohort (69%) followed by R (14%), U (9%), N (3%), G (2%), H (2%), W (1%). The distribution illustrated that

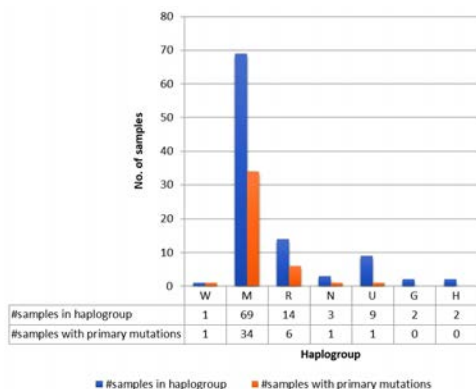


Figure 2: Distribution of primary mutations with respect to different haplogroups

LHON mutations appear across all these haplogroups except HG-G and HG-H (Figure 2).

Interestingly, haplogroup U was identified with lowest frequency of primary mutations. Out of 9 patients, only one patient (11.11%) harboured the predominant primary mutation m.11778G>A, while the other potentially pathogenic LHON variants were detected in 3 patients (33.33%) the U group. Primary mutations were absent in the haplogroups G and H.

Hospital-based Prevalence of LHON

In addition, the prevalence of LHON in Aravind Eye Hospital was estimated based on the 5-year patient statistics, from 2015-2019. On the basis of clinical evaluation and genetic testing for the three common primary mitochondrial DNA mutations (m.G3460A, m.G11778A, m.T14484C) in LHON patients from 2015-2019 (Table 2, Figure 3), the prevalence of the disease was estimated at a rate of 1:1689 or 5.92 per 10,000 patients (95% CI 3.78–8.81 per 10,000) in the Neuro-Ophthalmology Clinic, Aravind Eye Hospital, Madurai.

Table 2: Number of new patients attended Aravind Eye Hospital (AEH), Madurai

Year	Outpatients attended AEH	Patients referred to the Neuro-Ophthalmology	Clinically confirmed LHON patients	Genetically confirmed LHON patients
2015	325,730	9112	11	4
2016	349,356	9580	10	5
2017	326,297	8141	9	3
2018	309,344	6902	14	7
2019	287,714	6792	11	5
Total (2015–2019)	1598441	40527	55	24

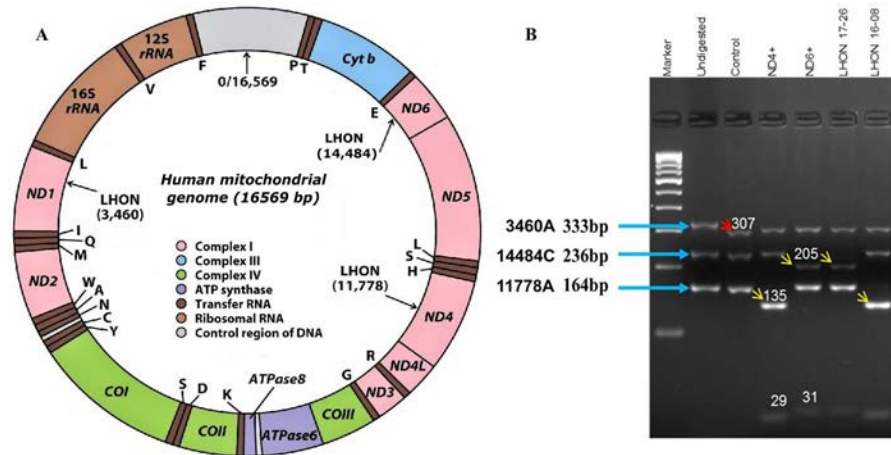


Figure 3: Human mitochondrial genome and detection of primary mutations in LHON samples. A: Schematic representation of the human mtDNA map indicating 37 genes including MT-ND1, MT-ND4 and MT-ND6 as well as the positions of primary mutations. B: The red arrow demonstrates the internal control of digestion in the MT-ND1 gene product. The yellow arrows indicate the MaeIII restriction, detecting the corresponding mutations marked in blue arrows.

Mito-nuclear genes involvement in LHON patients

LHON is frequently associated with defective expression of the electron transport complex I genes that subsequently decrease ATP production, increases ROS accumulation and finally cause bioenergetic failure of mitochondria. In humans, the electron transport complex I of mitochondria is composed of 45 sub units. Among them, 7 subunits are encoded by mitochondria and the remaining 38 subunits encoded by nucleus. Hence, mutations in nuclear encoded mitochondrial genes have also been important to consider the modulation of phenotypic expression in LHON.

Mitocarta 2.0 database holds list of 1158 nuclear genes showed strong evidence in mitochondrial localization across 14 different tissues. On this account, the current study primarily focuses the complex involvement of 1158 mito-nuclear genes using a targeted mito-nuclear gene panel for identifying the pathogenesis involved in LHON.

For this study, totally 15 samples were subjected to characterize the impact of mito-nuclear gene involvement in LHON patients through a targeted gene panel using Nextseq 550 platform. All 15 samples have been clinically diagnosed as LHON (Table 3). Whole mitochondrial DNA sequencing results revealed that four of the fifteen samples were positive for ND4 and ND6 primary mitochondrial DNA mutations, respectively (Figure 4). Six samples were positive for secondary mitochondrial DNA mutations associated with LHON and the remaining five samples showed no primary and secondary mitochondrial DNA mutations in the LHON affected individuals. Targeted exome sequencing results of these 15 samples showed no nuclear gene mutation in the primary mutation positive samples. Three of the six secondary mitochondrial DNA mutation affected individuals harbor nuclear gene mutation in MTFMT, NDUFS7 and PDSS1 and finally, 3 out of 5 individuals with no mitochondrial DNA mutation showed mutations in nuclear genome regulating

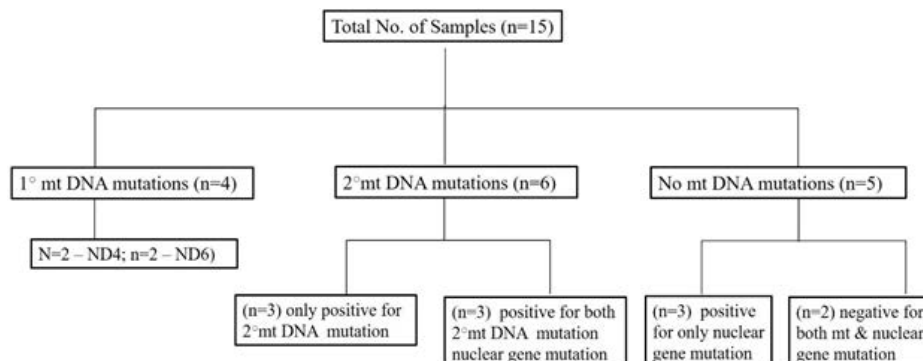


Figure 4: NGS sample details

mitochondria including NDUFV1, SLC25A46 and OPA1.

All the pathogenic variants identified in the targeted exome sequencing were tightly associated with complex I deficiency disorder. The details of the nuclear gene mutations was given in the table below (Table 4). This study provides an insight of the factors underlying incomplete penetrance modulating the phenotypic expression of LHON affected individuals.

Mutational screening of retinoschisin (RS1) gene in the patients with Juvenile X-linked retinoschisis (JXLR)

Juvenile X-linked retinoschisis (JXLR) is an X-linked recessive retinal disorder, characterized by splitting of the retina's neurosensory layer leading to progressive retinal degeneration and thus vision deterioration. With the reported estimated prevalence of 1 in 15000

to 25000, JXLR has been associated with early vision impairment in first decade of life. Classically, the clinical phenotype observed in retinoschisis patients includes foveal schisis resulting from inner retinal layer splitting, thus representing an archetypal spoke-wheel appearance and a negative electroretinogram (ERG). Mutations in the candidate gene-retinoschisin (RS1) have been reported for JXLR patients. RS1 encodes an adhesive 24kDa retinoschisin protein reported to involve in cellular adhesion and cell-cell interactions, thus preserving the structure and functional integrity of the retina. Hence, mutations affecting retinoschisin protein might result in schisis formation across retinal layers.

Sanger sequencing approach was undertaken to screen entire RS1 gene for the identification of mutations in 27 JXLR patients recruited from paediatric clinic, Aravind Eye Hospital, Madurai after

Table 3: Clinical demographics of LHON affected individuals

S.No	Study No	Age/Gender	Mitochondrial gene	Nuclear gene	Clinical data	Consanguinity	Family history
1	10-173-1	27/M	ND6 (1 ^o)	-	NA	Yes	No
2	11-196-1	12/F	ND1 (2 ^o)	-	NA	No	No
3	15-4-1	18/M	LDYT (2 ^o)	NDUFS7	NA	Yes	No
4	15-5-1	15/F	ND1 (2 ^o)	MTFMT	NA		No
5	17-17-1	27/M	ND2 (2 ^o)	-	NA	Yes	No
6	17-22-1	27/M	ND5 (2 ^o)	-	Fundus	Yes	No
7	17-24-1	23/M	No mutation	-	Fundus	Yes	No
8	18-30-1	16/F	No mutation	OPA1	Fundus	No	No
9	18-38-1	21/M	ND4 (1 ^o)	-	OCT, Fundus	No	No
10	18-39-1	16/M	No mutation	NDUFV1	OCT, Fundus	Yes	No
11	18-41-1	16/M	ND5 (2 ^o)	PDSS1	OCT, Fundus	Yes	No
12	19-43-1	26/M	No mutation	-	OCT, Fundus	No	No
13	19-44-1	35/M	ND6 (1 ^o)	-	OCT, Fundus	No	No
14	19-48-1	15/M	No mutation	SLC25A46	OCT, Fundus	Yes	No
15	19-49-1	22/M	ND6 (1 ^o)	-	OCT, Fundus	No	Yes

Table 4: Nuclear gene mutations and its clinical phenotype associated with mitochondrial disorders

Sample No	Nuclear genes	c.DNA change	Aminoacid change	Phenotype associated with mitochondrial disease
18-39-1	NDUFV1	c.C1156T	p. R386C	Mitochondrial complexI deficiency nuclear type4
18-30-1	OPA1	c.526-527 del	p. K176Rfs	Dominant hereditary optic atrophy
18-41-1	PDSS1	c.A854G	p. D285G	Co-enzymeQ10 deficiency, Primary 2
19-48-1	SLC25A46	c.A670G	p. T224A	Neuropathy, hereditary motor and sensory typeVIB
15-5-1	MTFMT	c.T476C	p. V159A	Mitochondrial complexI deficiency nuclear type 27
15-4-1	NDUFS7	c.C431T	p. P144L	Mitochondrial complexI deficiency nuclear type 3

comprehensive ocular examinations. Out of the 27 study subjects, 7 harbored RS1 gene mutations which include c.422G>A, c.305G>A, c.608 C>T, c.637C>T, c.7C>G, c.214G>A, c.305G>A (Table 5

Genetic screening was performed in the siblings clinically diagnosed as GA along with their parents (Figure 6). Sanger sequencing revealed a nonsense mutation in exon 11 of the OAT gene

Table 5: Identified RS1 gene mutations in JXLR patients

S. No.	Exon	Variant Type	cDNA Change	Number of patients identified with mutation	Amino acid Changes	ID
1	5	Missense	c.422G>A	1	R141H	rs61752159
2	4	Missense	c.305G>A	2	R102Q	rs61752068
3	6	Missense	c.608 C>T	1	P203L	rs104894930
4	6	Missense	c.637C>T	1	R213W	rs281865365
5	1	Missense	c.7C>G	1	R3G	rs374672514
6	4	Missense	c.214G>A	1	E72R	rs104894928

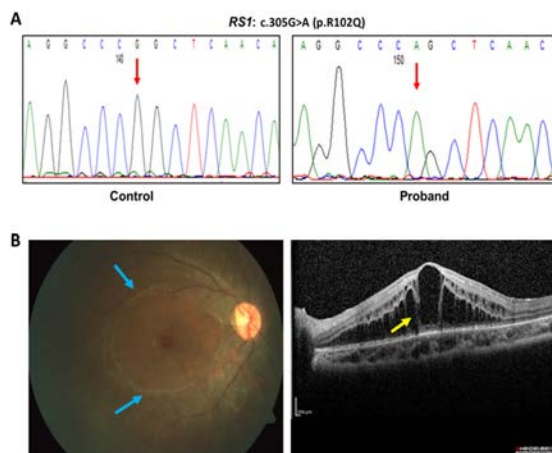


Figure 5: A. Representative chromatogram showing RS1 mutation 305G>A in a JXLR proband (right) compared to control (left). B. Fundus image showing typical spoke wheel like pattern (left; blue arrows) and retinal tear seen on optical coherence tomography (OCT) scan (right; yellow arrow) in retinoschisis phenotype.

and Figure 5). Further, samples negative for RS1 mutations will be screened through whole exome sequencing to explore the potential involvement of other genes underlying JXLR pathogenesis.

Genetic analysis of Gyrate Atrophy- a chorioretinal dystrophy with defective mitochondrial matrix enzyme

Gyrate atrophy (GA) of the choroid and retina, a rare congenital metabolic disorder results from the deficiency of the mitochondrial matrix enzyme ornithine- δ -aminotransferase (OAT). This autosomal recessive condition presents with progressive chorioretinal degeneration, myopia, night blindness, and eventually complete blindness in the fourth or fifth decade. In humans, OAT enzyme is encoded by OAT gene located on chromosome 10q26. This study aims to correlate the clinical and genetic findings in this metabolic disorder of mitochondria.

(c.1192C>T; p.Arg398Ter) in all the family members with a homozygous mutation in the patient and sibling, and heterozygous mutation in the parents (Figure 7). Variable phenotype was observed among the siblings. Older sibling did not have any ocular complaints other than myopia with varied ornithine levels (892.8 μ mol/L in the patient and 572.3 μ mol/L in the sibling), despite having the same homozygous mutation. Generally, intrafamily heterogeneity has been observed to be associated with clinically less severe manifestations of GA as compared to interfamilial heterogeneity.

In this study, a rare case of gyrate atrophy is presented with vitreous hemorrhage and nonsense OAT gene mutation, inherited in the autosomal recessive pattern. Phenotypic variability among the siblings with the same mutation in OAT gene is also documented.

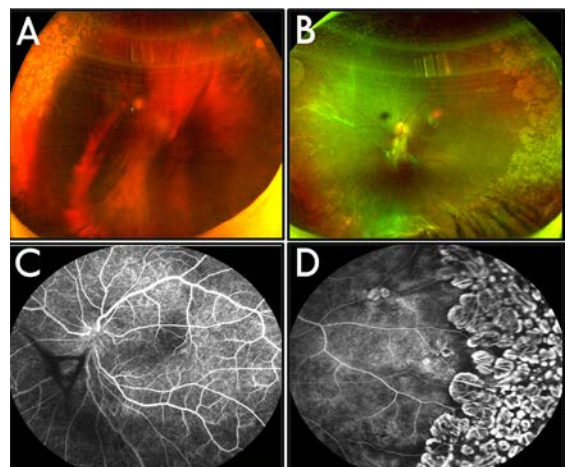


Figure 6. Clinical features of patient with gyrate atrophy: Pseudocolour wide-field fundus imaging of both eyes of the patient showing vitreous hemorrhage with peripheral chorioretinal atrophic patches (A,B). Fluorescein angiography OS showing staining in peripheral chorioretinal atrophic patches (C, D)

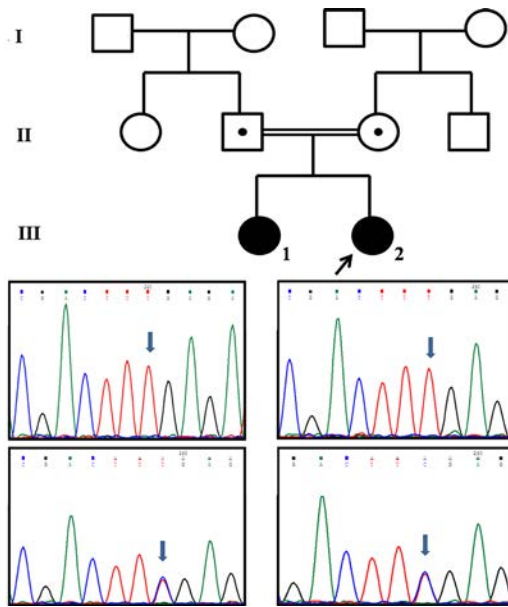


Figure 7. Genetic details of patient with gyrate atrophy: Pedigree chart with phenotypes and proband marked with arrow (A). Electropherogram indicating homozygous OAT gene mutation c.1192C>T in patient (B) and sibling (C) and heterozygous mutation c.1192C>T in parents (D, E). Blue arrows denote the mutation.

Annotation of non-canonical splice variants and miRNAs from retinoblastoma whole exome data

Retinoblastoma (RB) has long been considered as a paradigm of cancers and loss of *RB1* gene is considered as an initiating event in retinoblastoma. Other than pathogenic variants, a variety of intragenic mutations, loss of expression by methylation and chromosomal deletions can lead to *RB1* loss. In this study, whole exome sequencing (WES) of six RB tumors are examined for variant in the intragenic and intronic regions of functional significance.

The six samples were analyzed for *RB1* mutations categorically in the order of stop gain mutations, splice changes, frameshift and indels with

the inhouse data analysis pipeline. Four samples had mutations with deleterious effect predicted by the bioinformatics tools like SIFT, Polyphene, GERP, CADD scores. Two samples which did not show any such mutations were further taken up and reanalyzed. One sample had a synonymous mutation in Exon 13: c.1332 G>A in *RB1* gene p.Q444Q in a homozygous state which was confirmed by Sanger sequencing. To understand the effect of this synonymous mutation, RNA was isolated from this sample and subjected for sequencing. RT-PCR amplification revealed two bands of approximately 130bp difference. When these two bands were cut and sequenced separately, the mutant band was found to have exon 13 skipped due to altered splicing (Figure 8).

Sequence data were checked for the mutations in miRNAs associated with *RB1* gene. Prominent miRNAs such as miR-100, miR-1178, miR-5089, miR-519, miR-149, miR-3909 were found to be mutated. The effect of these miRNA mutations on the *RB1* and other target genes needs further functional studies.

These results prove that the analysis of *RB1* gene mutations should not be restricted to just the pathogenic variants. It was shown that even synonymous mutations have certain effect on the reading frame due to altered splicing and hence on the total protein, corroborating earlier studies.

Genetic investigation of Human papilloma virus in non-familial retinoblastoma

Retinoblastoma (RB) is known to be primarily caused by genetic aberrations of both copies of *RB1* gene in retinal progenitor cells. Over the past two decades, multiple studies have suggested the role of Human papillomavirus (HPV) in RB pathogenesis. However, it is still debatable and the study of HPV DNA in *RB1* genotyped sporadic RB is very limited. Hence, this study is aimed at investigating whether HPV is a risk factor in the etiology of RB.

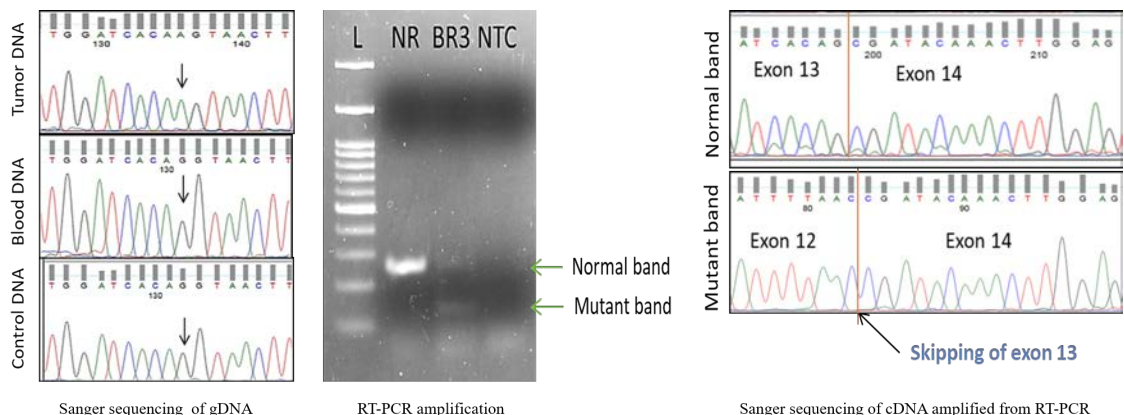


Figure 8. Altered splicing identified by RT-PCR in a retinoblastoma patient

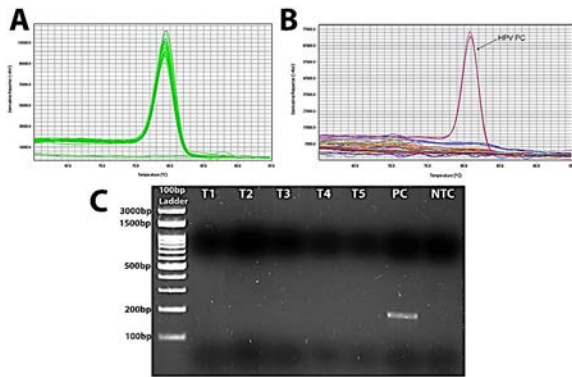


Figure 9. Molecular analyses of HPV DNA in tumor genome. A) Melt curve plot for B2M gene B) Melt curve plot for HPV L1 consensus shows amplification only in positive control (HPV PC, black arrow). C) HPV detection by semi-nested PCR. Lane 1: 100 bp ladder (GeneDireX®), Lane T2 to T5: RB DNA samples, Lane PC: HeLa DNA (HPV 18 positive) and NTC- non-template control. HPV quantification by TaqMan probe assay.

During 2012 to 2019, 106 patients were diagnosed as sporadic RB by clinical examination. Of 106 RB patients, 83% had unilateral and 17% had bilateral disease. The male (n= 55) to female (n= 51) ratio was 1.07:1, with mean age at diagnosis was 26.77 ± 15.36 (mean \pm Std.dev) months (ranges from 2 to 72 months). HPV screening was performed using semi-nested PCR with HPV L1 consensus primers and real-time quantitative PCR (RT- qPCR) targeted two different genes of HPV (1) L1 consensus and (2) E6 or E7 gene in RB tumor DNA samples that had already been *RB1* genotyped.

RB1 screening by Sanger sequencing and Multiplex ligation-dependent probe amplification (MLPA) identified 98 tumors with *RB1* mutations

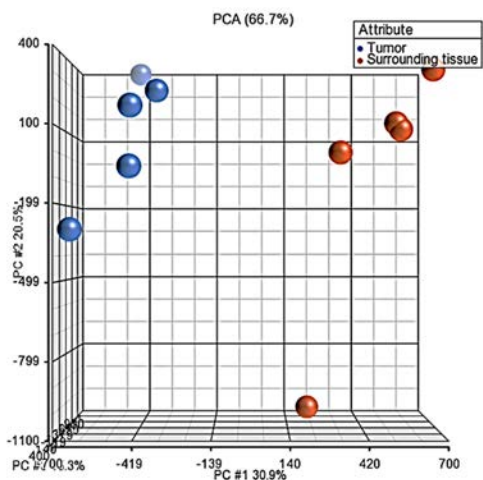


Figure 10: PCA plot showing the clear segregation of Tumor sample and the surrounding tissue samples as an individual group

and 8 tumors with no detectable *RB1* mutation. HPV investigation by real time PCR with HPV L1 gene showed none of RB samples were positive (Figure 9A and 9B). This was further confirmed by a semi-nested PCR targeted HPV L1 region (Figure 9C). A total of 40 blinded RB DNA samples were analysed for 14 oncogenic HPV types and found no positivity.

From this study, it is clear that HPV is neither a cofactor nor an independent risk factor in the RB development or pathogenesis. Other mechanisms underlying *RB1* inactivation further need to investigate in especially retinoblastoma lacking *RB1* mutations.

Epigenetic mechanisms underlying tumor progression in retinoblastoma

Retinoblastoma is known to be caused by genetic and epigenetic events. Hence, it is important to elucidate the epigenetic mechanisms underlying the tumor progression. MS-MLPA and bisulfite sequencing were used for analyzing the *RB1* promoter methylation. This study is aimed to identify the genome-wide methylation and its impact on tumor progression.

Illumina Infinium® Methylation EPIC 850K Array that can quantify methylation at 850,000 different CpG sites was used for the analysis of 13 samples including 8 RB tumors and 5 surrounding tissues. The IDAT files generated were used for analysis with R Statistical Software-ChAMP. First step of analysis excluded sex chromosomes, failed probes and SNPs from the analysis and 7,38,615 probes were taken for further analysis. Functional normalization and beta-mixture quantile normalization were performed and

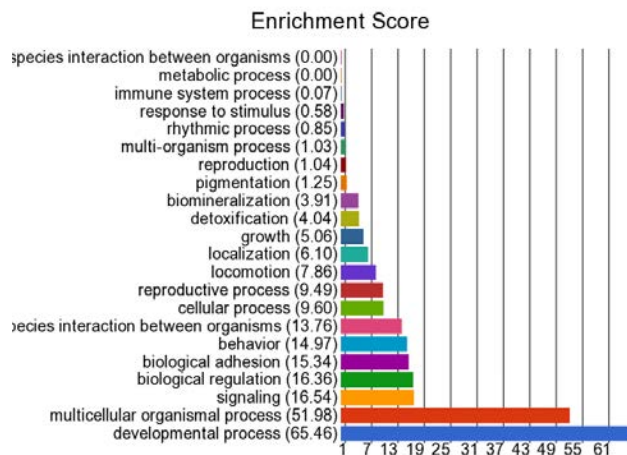


Figure 11: Gene ontology analysis for the significant DMPs showed the enriched biological processes. Genes were over represented for the developmental process and least represented for the species interaction between organisms as indicated by enrichment score

checked with multidimensional scaling plots of the 5000 most variable CpG sites. Principal component analysis showed clear segregation of the tumor samples from the surrounding tissues and helped to adjust confounding factors (Figure 10).

The differentially methylated positions (DMPs) were identified and gene ontology analysis revealed the genes enriched for biological processes like development process, multicellular organismal process, signalling etc. (Figure 11). The DMPs of these genes were taken for DAVID that identified the cancer pathways like: TGF- β signalling pathway, Rap1 signalling pathway, Neutrophin signalling pathways.

Whole genome methylation identified several cancer pathways that are differentially methylated. The significance of these pathways will be further checked with the transcriptomic data that can reveal functional alterations due to the altered methylation patterns.

Molecular genetics of ABCA4 gene in autosomal recessive Cone rod dystrophy and Retinitis Pigmentosa

Investigators : Dr. P. Sundaresan,
Dr. Rupa Anjanamurthy
Research Scholar : R.Kadarkarai Raj
Funding : Aravind Medical Research
Foundation

Introduction

Inherited Retinal Dystrophies (IRDs) are a group of heterogeneous retinal disorders that cause severe progressive vision loss in children. It mainly affects the photoreceptor cells, either, predominantly, the cones (responsible for detailed vision and colour), rods (responsible for night and peripheral vision) or both at the same time that leads to Stargardt disease, retinitis pigmentosa or cone-rod dystrophy,

respectively. The prevalence was estimated to be 1 in 3000. To date, more than 271 genes have been associated with IRDs (RetNet: <https://sph.uth.edu/retnet/>). Among the 271 genes, adenosine triphosphate (ATP)-binding cassette transporter 4 gene (ABCA4) has a high genetic prevalence and carrier frequency in six ethnic groups worldwide. Mutations in this gene are responsible for the spectrum of IRDs including Stargardt-I (STGD-I), autosomal recessive Cone rod dystrophy (AR-CRD) and AR-Retinitis Pigmentosa (AR-RP). ABCA4 located in chromosome 1p13, contains 50 exons and involved in the hydrolyzing of N-retinylidene-phosphatidylethanolamine to all-trans-retinal and phosphatidylethanolamine in visual cycle pathway. So far, only one study in India has shown that AR-RP was caused by mutations in ABCA4 gene. Therefore, the team intended to further explore the involvement of ABCA4 in AR-CRD and AR-RP phenotypes in South Indian patients through Sanger sequencing method.

Results and Conclusion

A total of nineteen patients have been recruited for this study. The ophthalmic examination of all the proband were carefully evaluated by a paediatric ophthalmologist. Ten out of nineteen patients were presented with AR-CRD like disease phenotype and the remaining nine patients represented as AR-RP like disease phenotype. Five ml of peripheral blood sample was collected from all the proband and the genomic DNA was extracted by modified salting out precipitation method. The genetic analysis of ABCA4 gene was performed using Sanger sequencing method and the SNP associated with ABCA4 in both AR-CRD and AR-RP patients were enlisted in Table 1. Out of 19 probands, 17 had no disease-causing pathogenic variant in ABCA4 gene. This is the first study which shows the association of two missense variants in ABCA4 gene in AR-CRD patients (rs1390936521, rs770439859) belongs to the South Indian population. The details were given in Table 2.

Table:1 List of ABCA4 – SNPs associated with AR-CRD and AR-RP patients

Exon	Nucleotide Change	Amino acid Change	Variant class	ClinVar Interpretation	SNP ID	Frequency (%)	Allele Frequency in 1000G
3	c.302+26A>G	-	IVR	Benign	rs2297634	89	0.4531
4	c.442+80G>T	-	IVR	-	rs11165073	68	0.4573
6	c.635G>A	p.R212H	Missense	Benign	rs6657239	5	0.0533
7	c.769-86A>T	-	IVR	-	rs574741	21	0.2526
	c.769-32T>C	-	IVR	Benign	rs526016	10	0.1977
10	c.1356+11T>G	-	IVR	-	rs113055350	16	-
	c.1240-14C>T	-	IVR	Benign	rs4147830	31	0.51478
	c.1268A>G	p.H423R	Missense	Benign	rs3112831	10	0.2208
	c.1269C>T	p.H423H	Synonymous	Benign	rs4147831	10	0.1146
14	c.2160+49T>C	-	IVR	Benign	rs56197337	5	0.05431
19	c.2828G>A	R943Q	Missense	Benign	rs1801581	5	0.01538
22	c.3191-10G>T	-	IVR	SNP	-	5	-
26	c.3814-62G>A	-	IVR	-	rs547369977	5	0.0006
29	c.4352+54A>T	-	IVR	-	rs547806	47	0.0118
	c.4256T>C	p.M1419T	Missense	Benign	rs142673376		
16	0.0028						
33	c.4773+48C>T	-	IVR	Benign	rs472908	16	0.37046
38	c.5460+62G>A	-	IVR	-	rs2275033	21	0.3271
40	c.5585-70C>T	-	IVR	-	rs537831	21	0.3085
	c.5682G>C	p.L1894L	Synonymous	Benign	rs1801574	5	0.20068
41	c.5715-25A>C	-	IVR	-	rs4147856	5	0.1877
42	c.5844A>G	p.P1948P	Synonymous	Benign	rs2275029	5	0.16713
	c.5836-11G>T	-	IVR	Benign	rs1800739	5	0.1833
44	c.6069T>C	p.I2023I	Synonymous	Benign	rs1762114	89	0.2300
45	c.6282+79G>A	-	IVR	-	rs189091964	37	0.0004
	c.6282+7G>A	-	IVR	Benign	rs17110761	28	0.1340
	c.6249C>T	p.I2083I	Synonymous	Benign	rs1801359	26	0.1340
46	c.6285T>C	p.D2095D	Synonymous	Benign	rs1801555	21	0.3011
48	c.6729+51C>G	-	IVR	-	rs7518454	5	0.1156
49	c.6730-3T>C	-	IVR	Benign	rs1800717	10	0.1486
	c.6764G>T	p.S2255I	Missense	Benign	rs6666652	10	0.1769
	c.6816+28G>C	-	IVR	Benign	rs6666559	10	0.1480
	c.6816+73T>A	-	IVR	-	-	10	-
50	c.*299G>C	-	3 prime UTR	Benign	rs538804441	5	0.00220

Table: 2 List of disease causing ABCA4 variants identified in AR-CRD patients

Exon	Nucleotide Change	Amino acid Change	Variant class	Variant type	Zygosity	SNP ID	Allele Frequency (%)	Disease Phenotype	Reference
3	c.302T>C	p.I101T	Missense	Disease causing	Homozygous	rs1390936521	0.000004	Cone Rod dystrophy	This study
10	c.1319A>G	p.Y440C	Missense	Disease causing	Homozygous	rs770439859	0.000143	Cone Rod dystrophy	This Study

GENETICS OF OCULAR TUMORS

Eye Cancer is a major debilitating disease that affects sight, eye and even life. Every year, about 10,000 new eye cancer cases are diagnosed in India. Major challenges of these ocular tumors include their diverse disease course, varied response to the chemotherapeutic drugs, recurrence of tumor even after multimodal treatment and metastasis. In order to address these challenges, detailed molecular analyses are done and interpretations are made with clinical investigations. A snapshot of the recent findings of AMRF is presented here along with the scope for future work.

Genetic testing of retinoblastoma

Investigators : Dr. A. Vanniarajan,
Dr. Usha Kim,
Prof. VR. Muthukkaruppan
Project Fellow : V. Senthil Nathan
Funding Agency : Aravind Eye Care System,
Madurai

Introduction

Retinoblastoma (RB) is the most common primary intraocular malignancy of infancy and the incidence is 1 in 15,000 to 30,000 live births. The pivotal genetic event in all retinoblastoma tumors is the inactivation, due to mutations or deletions, of both copies of *RB1* at the chromosomal locus 13q14. Genetic testing and counseling are therefore essential components of care for all children diagnosed with RB. *RB1* gene analysis will influence surveillance or clarify recurrence risks for family members. Identification of the *RB1* mutation status of a patient allows

differentiation between sporadic and heritable retinoblastoma variants and to predict the risk of inheritance.

Results

During the last year, 29 samples including 21 unilateral and 8 bilateral RB were analysed. One patient had a positive family history. Sanger sequencing of *RB1* gene including promoter and exons 1 to 27, as well as nearby flanking intronic regions detected the genetic alteration in *RB1* gene of 22 patients. Using Multiplex Ligation Dependent Probe Amplification (MLPA), the whole-exon/multi-exon deletions and duplications in the *RB1* gene were determined in 3 patients. No mutations or deletion in 4 blood samples suggest the somatic event of RB which could not be identified due to non-availability of tumor sample.

Genetic analysis was also helpful for the older patients to know the risk of RB in the offspring, apart from the newly enrolled patients. One patient diagnosed with unilateral RB in 2001 had her eye enucleated as a treatment procedure. When she came for follow-up and replacement of prosthetic eye, she was willing to know the risk of RB in her future offspring. Her blood sample was collected and genetic analysis showed a deletion of one allele of *RB1* (Figure 1). The presence of germline *RB1* deletion is rare in a unilateral patient without any family history. Genetic counselling was given to the family stating the 50% chance of inheritance of RB to the next generation. It is also suggested to bring the future offspring for screening immediately after birth and early intervention to save the vision and



child. This evidence displayed the strength of genetic testing in clinical practice and also in patient welfare.

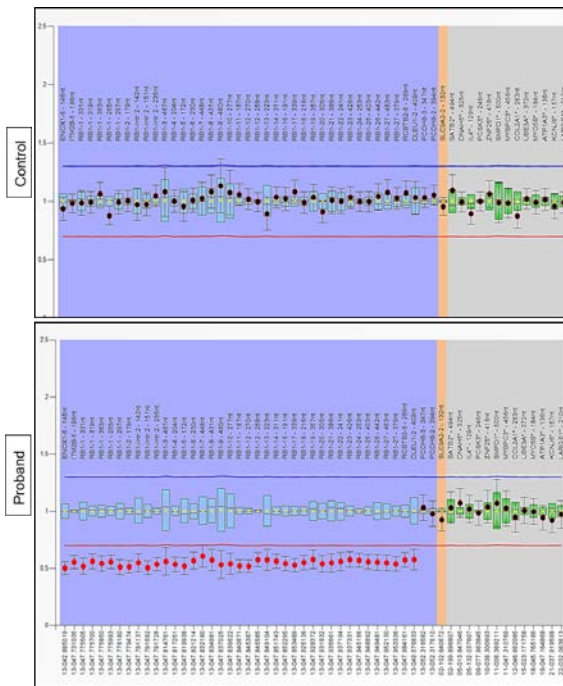


Figure 1. MLPA showed heterozygous deletion of RB1 gene in which the ratio point lying below the deletion cutoff range whereas the control showed normal range

Genomic characterization of kinome related genes in retinoblastoma

Investigators : Dr. A. Vanniarajan,
Dr. Usha Kim,
Prof.VR. Muthukkaruppan
Research scholar : K. Jeyaprakash
Funding agency : Department of Biotechnology

Introduction

Retinoblastoma (RB) is developed upon biallelic inactivation of RB1 gene in the retinal progenitor cells. This RB1 inactivation has been reported primarily due to mutations, deletion or promoter methylation in multiple cancers mainly in RB. However, a subset of retinoblastoma with no such detectable RB1 alteration is also reported. The phosphorylation of pRB had been described as an alternative mechanism for RB1 inactivation in RB. RB1 mutations were already identified in over 90% of RB patients using Sanger sequencing and MLPA methods. To define the alternate mechanisms of inactivation, pRB expression was evaluated in RB with no mutations.

Results

First, the protein extraction buffers were optimized employing neural retina tissues obtained from cadaver eye. The mouse monoclonal anti-human pRB (#9309, Cell signalling) were initially validated using MDA-231 cell lysate (pRB positive) and employed in RB cell line (WERI-Rb1) to evaluate pRB expression.

Among the two buffers used, 1X Laemmli yielded better protein concentration in neural retina tissue than the RIPA buffer (Figure 1A). Analysis of pRB antibody at different protein concentrations showed gradual increased intensity of band around 110Kda with increasing amount of protein (Figure 1B). Western blot analysis of pRB showed desired band in MDA231 lysate but not in WERI-Rb1 (Figure 1C).

Conclusion

The conditions for pRB antibody for western blotting are optimized now and further it will be optimized for IHC. This protocol will be employed for RB samples for expressional analysis of pRB.

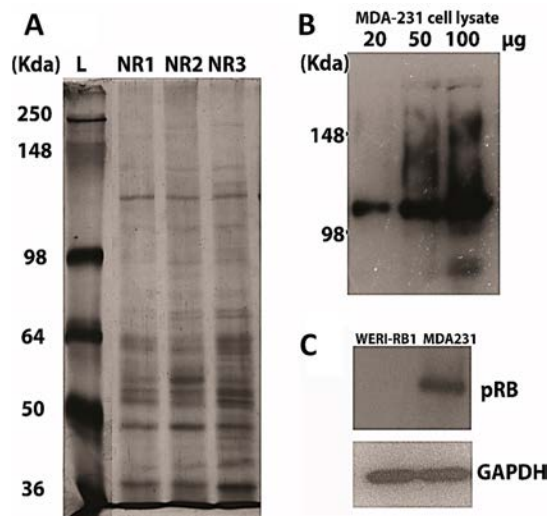
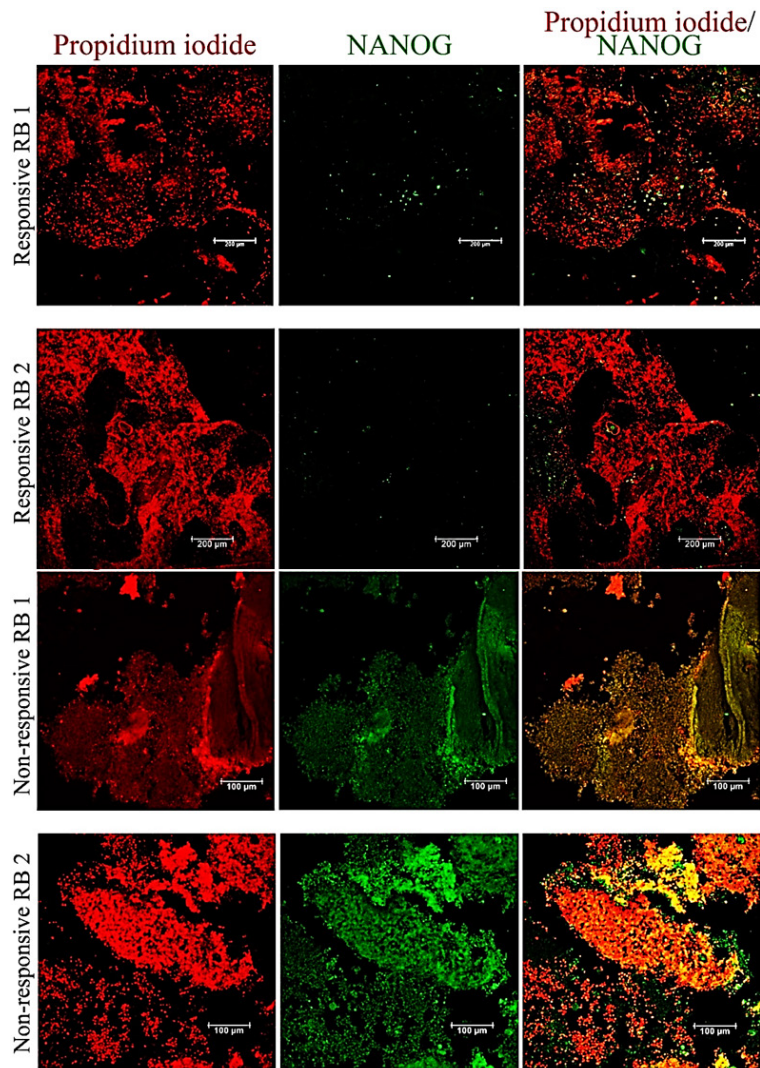


Figure 1. A) Total proteins extracted from neural retina using laemmli buffer B) Validation of pRB antibody using MAD231 cell lysate C) RB1 protein expression analysis in WERI-Rb1 cells and MDA231 (pRB positive control).

Understanding the molecular mechanisms of chemoresistance in retinoblastoma

Investigators : Dr. A. Vanniarajan,
Dr. Usha Kim, Dr. R. Shanthy,
Prof. V.R. Muthukkaruppan
PhD Scholar : T.S. Balaji
Funding Agency : Council of Scientific & Industrial Research (Fellowship)



Scattered positivity in responsive RB and strong nuclear positivity in nonresponsive RB was detected. Nucleus was counterstained with propidium iodide. Scale bar: 200 μm.

Introduction

Poor differentiation of cells is a prominent marker for poor prognosis in a variety of solid tumors. This poor differentiation of tissues may be correlated with the cancer stem cells present in the tumor and expression of specific markers serves as indicators of chemoresistance. One such prominent molecular marker involved in aggressiveness of solid tumors is NANOG. Hence, evaluating the protein expression of NANOG in tumor sections can provide a better understanding of poor tissue differentiation and its correlation with clinical features.

Results

Immunohistochemistry was performed in 2 FFPE sections, each of responsive RB and non-responsive RB. Non-responsive RB showed poor differentiation

and a high level of scleral/choroidal, optic nerve head invasion. Conversely, responsive RB showed well differentiation and scleral/choroidal invasion. Responsive RB showed a very weak expression of NANOG protein with no signal from nucleus. Non-responsive RB showed strong positivity with anti-NANOG in nucleus. This indicates the elevated expression and nuclear localization of NANOG in chemoresistant RB tumors (Figure 1).

Conclusion

Nuclear positivity of NANOG was strong in non-responsive RB with poorly differentiated pattern. Hence targeting NANOG would be a useful strategy to overcome chemoresistance in RB.

Copy number changes and differential expression of modifier genes with therapeutic potential

Investigators : Dr. A. Vanniarajan,
Dr. Usha Kim,
Prof. VR Muthukkaruppan
Research Scholar : A. Aloysius Abraham
Funding Agency : Department of Biotechnology

Introduction

Gross alterations or copy number changes in at least 4 different loci (1q, 2p, 6p, 16q) other than *RB1* have been frequently associated with retinoblastoma (RB) tumorigenesis. To understand the importance of candidate genes involved in such pathways, gene copy number data along with expression data need to be analyzed. It is also essential to study the correlation of these data with the histopathological differentiation pattern of tumors.

found to have upregulation correlating with genomic data. Tumor suppressor gene *TP73* was found to have increased expression in all tumors and it is speculated that altered transcripts of *TP73* may have an oncogenic potential.

Transcription factor *E2F3* was found to have copy number gain in 70% of the tumors at DNA level and increased expression was seen in 7 tumors at RNA level as well. *E2F3* is a direct binding partner of pRB and chief regulator of cell cycle at G1-S interphase and controls genes involved in S-phase. Apart from the 4 genes, differential regulation of *DDX1* was observed with increased significance between the well-differentiated and poorly differentiated tumors. *DDX1* is a helicase protein gene involved in a variety of biological processes. *DDX1* is also an activator of NF- κ B transactivation pathway and its downregulation is evident in well differentiated samples.

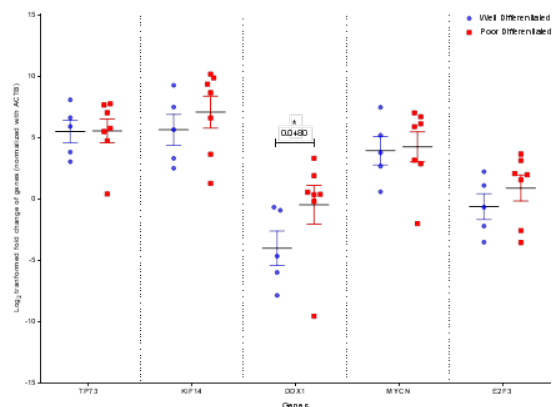
Table 1: Copy number gain and loss found in RB tumor samples

ID	Differentiation pattern	Copynumber gain	Copynumber loss
NGS-1	Poorly differentiated	<i>KIF14, MDM4, DEK, E2F3, CHFR, TP53</i>	<i>BAZ1A, CDH11, CDH13, ATM</i>
NGS-2	Poorly differentiated	-	-
NGS-20	Well differentiated	<i>KIF14, MDM4, MYCN, DEK, E2F3, GATA5, CCND1, E2F1, CCNE1</i>	<i>CDH11, CDH13</i>
NGS-23	Poorly differentiated	<i>TP73, KIF14, MDM4, DEK, E2F3, CHFR, GATA5, E2F2, CCND1, CCNE1</i>	<i>CDH11, CDH13, BCOR</i>
NGS-27	Poorly differentiated	<i>TP73, KIF14, MDM4, DDX1, MYCN, E2F3, SYK, CHFR, OTX2, GATA5, E2F2, CCND1, CCNE1, E2F1</i>	-
NGS-29	Poorly differentiated	<i>TP73, KIF14, MDM4, MYCN, DEK, E2F3, OTX2, GATA5, E2F2, CCND1, CCNE1</i>	<i>CDH11, CDH13, ATM</i>
NGS-55	Poorly differentiated	<i>DDX1, MYCN, DEK, E2F3, E2F1</i>	<i>TP73, CDH11, CDH13, TP53, E2F2</i>

Results

Tumor samples (n=12) were analyzed for CNVs by targeted NGS (Table 1). Same samples were subjected for expression studies for selective candidate genes *KIF14*, *TP73*, *DDX1*, *MYCN*, *E2F3* using 2- $\Delta\Delta$ Ct method with RT-qPCR with neural retina as control. Real-time PCR was performed in triplicates and Ct values were normalized using the Valid Prime analysis method.

There was definite correlation of the genomic data with the gene expression data for *TP73*, *KIF14*, *MYCN* and *E2F3*. *KIF14*, a mitotic kinesin involved in cytokinesis, which accelerates tumor progression in murine model, was upregulated in the all the samples. Similarly, developmental gene *MYCN* was



Expression pattern of genes in well and poorly differentiated RB

Conclusion

Consistent copy number gain at genomic level and increased expression at transcript level of *KIF14*, *MYCN* and *E2F3* confirm its modifier role in tumor progression and therapeutic potential in retinoblastoma. In addition, *DDX1* was found to be differentially regulated in poorly differentiated RB tumors correlating with poor prognosis. Hence *DDX1* could be an effector gene and an ideal drug target for retinoblastoma.

Molecular characterization of tumor progression in Retinoblastoma

Investigators : Dr. A. Vanniarajan,
Dr. Usha Kim,
Prof. V.R. Muthukkaruppan
PhD Scholar : T. Shanthini
Funding Agency : DST-INSPIRE (Fellowship)

Introduction

Deletion of *RB1* gene is a well-established mechanism of *RB1* inactivation, resulting in the defective protein (pRb). pRb is responsible for a major G1 checkpoint, blocking S-phase entry and cell growth. Hence, deletion of *RB1* gene leads to the defects in the cell cycle that turns a normal cell to a malignant phenotype. Deletion of *RB1* along with the contiguous genes was called as 13q deletion syndrome. In this study, MLPA was used to detect the spectrum of *RB1* deletions including 13q deletion syndrome.

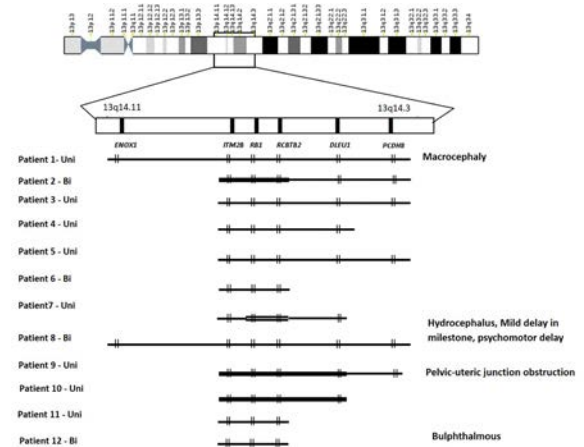
Results

Genetic data of the 271 patients over the period of last 7 years were analysed and MLPA data was segregated based on the extension of deletion beyond *RB1* gene. MLPA probes for *RB1* also comprises the probes for the *RB1* flanking genes in the close proximity of *RB1* namely *ENOX1*, *ITM2B*, *RCBTB2* (48 kb upstream; 35 kb downstream) as well as a probe for the *DLEU1* gene and two probes for *PCDH8* gene 1.6 Mb and 4.5 Mb downstream from *RB1*, respectively. Extended deletion was found in 12 patients and details are given in Fig.1. Clinical details of these 12 patients were reviewed and 4 cases were associated with other systemic illness and one had motor delay.

Conclusion

This study shows the effectiveness of the MLPA technique in the analysis of interstitial deletion in Chr 13q and provides some insights into the clinical heterogeneities. This study also provides

the necessity of genotype-phenotype correlation to eventually define the most appropriate follow-up options.



Extent of deletion was mapped by the single horizontal line for monoallelic deletions and double horizontal line for the biallelic deletions. Breakpoints in the genes were marked by vertical double lines.

Identification and Validation of Dysregulated Pathways in Retinoblastoma

Investigators : Dr. A. Vanniarajan,
Dr. Usha Kim, Dr. R. Shanthi,
Prof. V.R. Muthukkaruppan
Project Fellows : Anindita Rao and T.S. Balaji
Funding Agency : DST-SERB

Introduction

It is becoming increasingly evident that apart from *RB1* loss, other genetic, epigenetic and gene expression alterations are necessary for tumour development. Big data from high throughput techniques like RNA sequencing have paved the way for identification of novel RNA species or aberrant RNA processing events in RB tumors. Potential causal mechanism that renders certain features of acute tumor biology can be identified by pathway/network analysis. Hence, assessing the mRNA profiles of the cancer hallmark pathways is necessary to obtain a holistic view. The present study aims at investigating the expression profile of cancer-specific genes in retinoblastoma tumors as compared to normal tissues using real-time PCR arrays with multiple internal controls.

Results

Dysregulation of cancer-related genes in RB tumors:
Analysis of relative fold-change from the real-time PCR data revealed dysregulation of genes in 13 RB

tumor tissues compared to 3 non-RB tissues. Among 84 cancer-related genes, 68 were differentially regulated in 13 RB tumors with up regulation of 55 and down regulation of 13 genes. Almost 50% of tumor samples had 65 genes altered with 52 upregulated and 13 downregulated genes. Among those, 30 genes were dysregulated in more than 11 tumors indicating the increased transcriptional alterations of cancer-related genes in RB. Among 68 dysregulated transcripts, 6 genes (*CDC20*, *MCM2*, *MK167*, *PGF*, *WEE1* and *COX5A*) had differentially expressed in almost all the tumors studied. *CDC20* was upregulated ($\log_2FC = 4.98 \pm 1.14$; $p = 0.044$) and *COX5A* was downregulated with statistical significance (Figure 1).

expression of these genes clustered in these pathways would favor RB tumorigenesis.

Conclusion

In this targeted transcriptome analysis of cancer-related genes, the team identified many transcriptional alterations that drive tumor propagation upon RB initiation by biallelic loss-of-function of *RB1*. It was also noted that most of the deregulated genes cluster under three main pathways of cell cycle, angiogenesis and apoptosis with notable upregulation of *CDC20* in all tumors studied. *CDC20* can therefore be a potent drug target, which may ameliorate prognosis of RB patients.

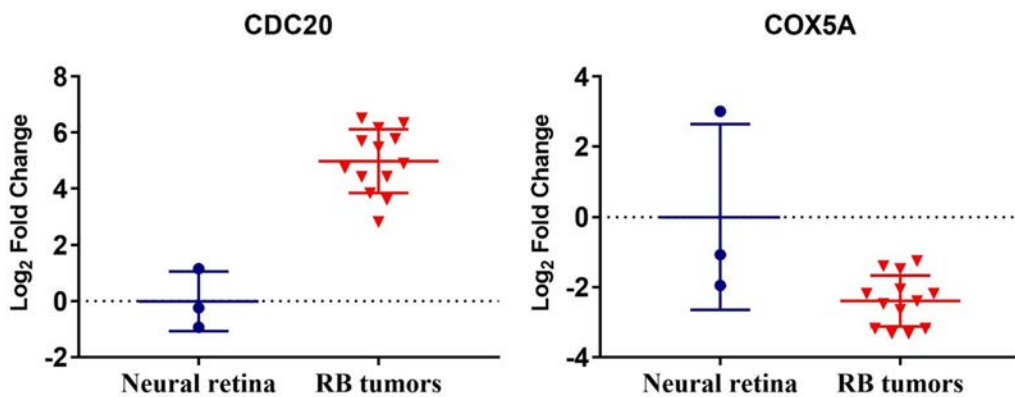


Figure 1. Differential expression of *CDC20* and *COX5A* in all RB tumours with statistical significance

For in silico prediction of protein-protein interaction through STRING, dysregulated genes with statistical significance (*CDC20*, *CASP9*, *COX5A*, *IGFBP7*, *KDR*, *SERPINF1*, *SOD1*, *TBX2*, *TERF2IP*, *XIAP*) and differentially expressed genes in all 13 RB tumors (*MCM2*, *MK167*, *PGF*, *WEE1*) were included. An additional layer of the genes related to deregulated genes with differential expression in more than 11 tumors (*AURKA*, *E2F4*, *STMN1*, *ANGPT2*, *APAF1*, *BCL2L11*, *CASP2*, *TEP1*, *ATP5A1*) was added. These closely interacting partners were highlighted in the STRING network of 84 cancer-related genes (Figure 2). The dysregulated genes were found to cluster in 3 pathways such as cell cycle (Figure 2A), angiogenesis (Figure 2B) and apoptosis (Figure 2C). Differential

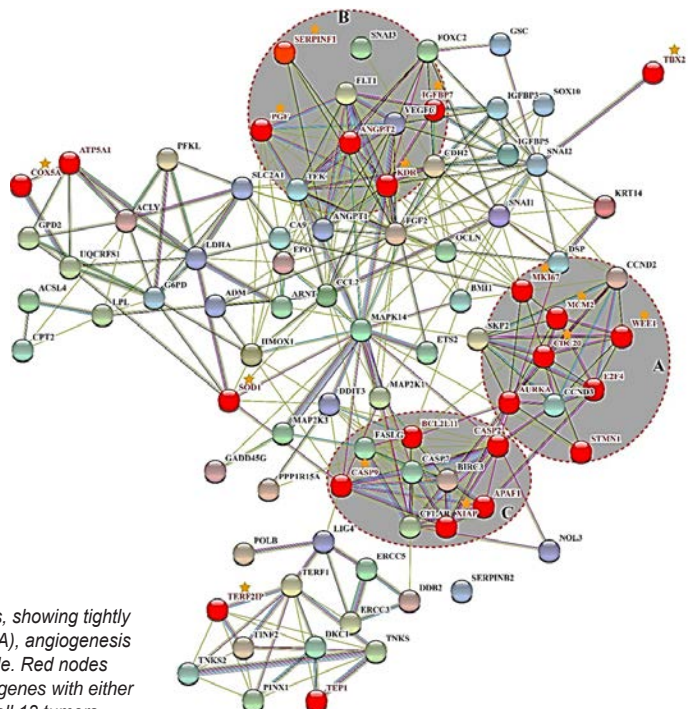


Figure 2. STRING analysis of 84 cancer-related genes, showing tightly interconnected network. Genes involved in cell cycle (A), angiogenesis (B) and apoptosis (C) are highlighted with grey circle. Red nodes represent deregulated genes and yellow star denotes genes with either statistical significance or differential expression in all 13 tumors.

Translational Genomics of Ocular Cancers

Investigators : Dr. A. Vanniarajan
Dr. Usha Kim, Dr. R. Shanthy,
Dr. D. Bharanidharan,
Prof. VR. Muthukkaruppan
Project fellow : K. Saraswathi
Funding Agency : Aravind Eye Foundation, USA

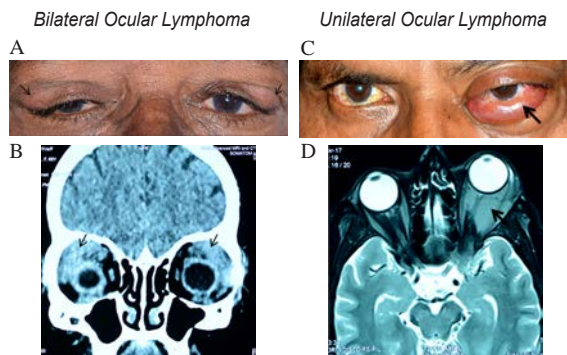
Introduction

Ocular Adnexal Lymphoma (OAL) is the most common orbital malignancy originating from lymphoid cells accounting for 55% of all orbital tumors and 8–10% of all extranodal lymphomas. The diagnosis of OAL is often challenging because of nonspecific clinical sign or symptom and requires confirmation by all ophthalmic and systemic evaluation. Most of the ocular lymphoma (OL) is Non-Hodgkin's type with clonal proliferation of either B-cell or T-cell, and rarely NK-cells. Treatment modalities depend on histological grade, the extension of tumor and the metastatic status. Hitherto, the clinical outcome of OAL has not been studied extensively in India. Hence, retrospective analysis of OAL patients presented at Aravind Eye Hospital over a period of 5 years was made to review the clinical characteristics and outcome.

Results

Patient data were collected from January 1, 2014 to December 31, 2018. Clinical data included complete ophthalmic, physical examination, bone marrow aspiration and computed tomography for initial diagnosis and to assess the progression state. For histopathologic examination, all the specimens were stained against hematoxylin-eosin and analyzed immunohistochemically using leukocyte common antigen (LCA), B- cell marker (CD20), T- cell marker (CD3) and classified according to World Health Organization (WHO) classification (2016) of tumors of Hematopoietic and Lymphoid Tissues.

A total of 71 patients with a histological verified ocular lymphoma were included. The primary end points were overall survival, disease-specific survival and progression-free survival. The median age was 54 years, and 72% of patients were male. 91% were unilateral. The majority of lymphomas were of B-cell origin (96%, n = 71). Proptosis was the most common clinical sign followed by swelling. Common site of involvement was orbit followed by lacrimal gland, conjunctiva and eyelid. OAL were treated with COP or CHOP regimen. Long-term follow-up is required to study the adverse effect of chemotherapy.



A. Clinical examination revealed superolateral mass in both eyes
B. Computed Tomography revealed heterogeneously enhancing mixed density lesion in both lacrimal fossa replacing lacrimal gland
C. Patient presented with conjunctival lesion
D. MRI showed lesion in the left orbit encasing the lateral rectus and optic nerve, involving the intraconal and extraconal compartments.

Conclusion

Clinical studies of lymphoma patients revealed them as B-cell lymphoma mostly. Further investigations on genetic and transcript data in correlation with clinical and histopathological features will help understand the disease pathogenesis.

Targeted Modulation of E2F3 and KIF14 pathway in Retinoblastoma refractory to existing chemotherapeutic drugs

Investigators : Dr. A. Vanniarajan
Dr. Usha Kim,
Prof. K. Dharmalingam
Project Fellow : Mr. R. Sethu Nagarajan

Introduction

Retinoblastoma (RB) is a rare form of intraocular cancer with prevalence of about 3-5% among childhood cancers. The incidence of RB is predominant in developing countries like India which owes about 20% of world RB cases. Due to the lack of awareness and low socio-economic status, large proportion of RB patients present with late stage of the disease. For late stages of RB, enucleation of the affected eye is still the primary choice of treatment. Chemotherapy is the better choice for treating patients and drugs like vincristine, etoposide, carboplatin have been used as combinational approach in systemic therapy. Current regimen was not successful in a subset of patients and hence newer therapy will make the treatment better.

Table 1 Clinical details of Ocular Lymphoma Patients

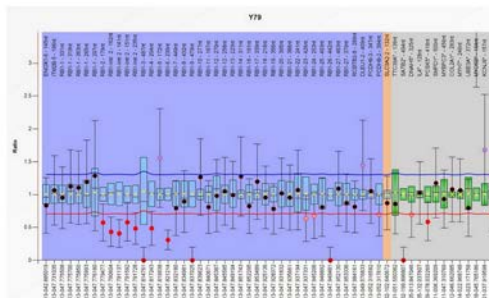
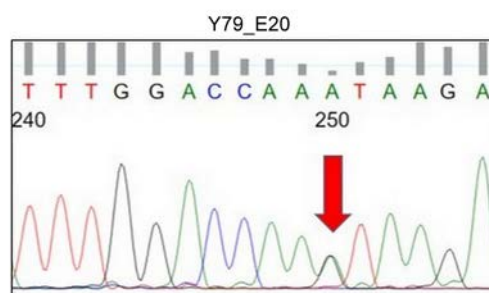
Features	n=71
Sex	
Male	51
Female	20
Age at presentation, yrs	
≤45	15
>45	56
Laterality	
Unilateral	65
Bilateral	6
Histopathology-IHC	
B-cell	68
T-cell	2
Burkitts	1
Treatment	
COP+CHOP	8
COP	26
CHOP	4
CHOP + Rituximub	1
Defaulter/Not Stated	32
Location in the ocular adnexal region	
Orbit	36
Conjunctiva	9
Lacrimal gland	12
Eyelid	7
Not Stated	6
Symptom	
Protrusion	35
Tumor or swelling or mass	27
Irritation or pain	3
Ptosis	1
Decreased visual acuity	1
Redness	2
Not Stated	2

Earlier studies from the lab found frequent copy number gains of cell cycle modulators such as *E2F3* and *KIF14* which are well studied oncogenes. *E2F3* is a direct target for *RB1* gene and an essential regulatory element in the cell cycle at the G1-S phase transition. *KIF14* is a mitotic kinesin vital for the M-G1 phase entry of the cell further enhancing cytokinesis. Targeting these cell cycle modulators could be a competent treatment approach for RB. In this study, small molecule inhibitors against the target genes are used.

Results

Primarily, the cell lines were characterized and expression study was done to confirm the over expression of target genes. The Y79 cell line with passage 33 and WERI-Rb1 with passage 22 were retrieved using the RPMI complete medium. Morphological characterization showed round spherical Y79 cells and irregular rod shaped WERI-Rb1 cells respectively. Molecular characterization was done for identifying the status of *RB1*. Sanger sequencing of Y79 showed G>A splice mutation in intron 20 and MLPA showed deletion of exon 2-6. Loss of both alleles of *RB1* was confirmed by MLPA in WERI-Rb1 cells (Figure1). The pRB protein null status in these cells was confirmed by using western blot.

(a) Mutation and Deletion profile for Y79



(b) Deletion of RB1 confirmation for WERI-Rb1

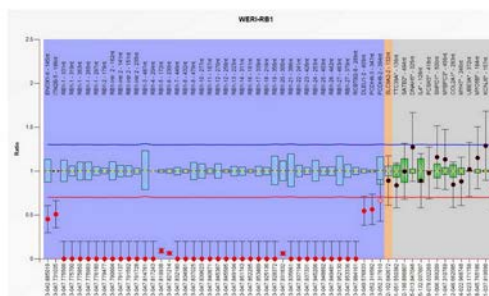


Figure 1: Characterization of Y79 and WERI-Rb1 cell lines (a) Sanger sequencing confirmed the presence of mutation in intron 20 at Splice site (cDNA 2107-1G>A) and MLPA confirmed the presence of deletion in Exon 2-6 for Y79 (b) MLPA confirmed the homozygous deletion in WERI-Rb1

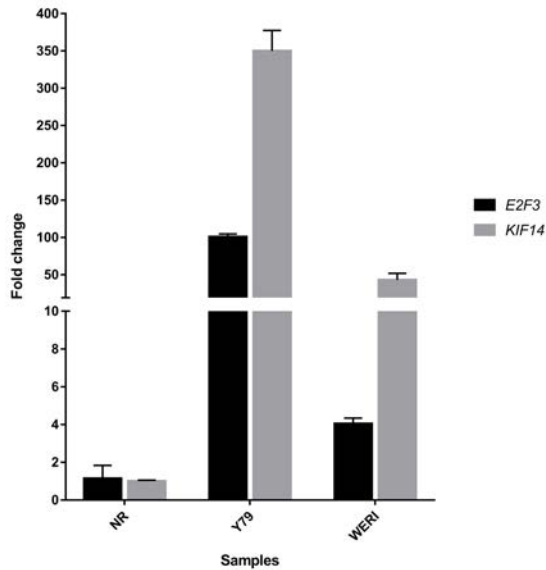


Figure 2: Relative quantification of *E2F3* and *KIF14* showed increased expression in Y79 and WERI-Rb1 cells

Cells were cultured with standard conditions and cell pellet was collected. RNA isolation was done by modified method using Trizol and Qiagen kit columns. cDNA was synthesized using Verso-kit and checked with housekeeping genes. Gene of interest primers was used for amplification and amplicons were confirmed by Sanger sequencing. Gene expression study for two genes *E2F3* and *KIF14* was carried-out using SYBR green dye with the optimized conditions and *B2M* was used as housekeeping gene to normalize the result. Relative expression was calculated by $\Delta\Delta C_t$ method. Higher expression of both genes Y79 and WERI-Rb1 was confirmed (Figure 2).

Conclusion

Overexpression of *E2F3* and *KIF14* was confirmed. Further the cytotoxic effect of the drug will be determined using MTT assay and validated by Western Blot at protein level. The efficient drug combination, derived from in vitro studies will ameliorate the efficacy of RB treatment, thereby improving the chances of vision and life salvage.

STEM CELL BIOLOGY

Adult tissue resident stem cells are quiescent, slow cycling cells with the ability to self-renew and differentiate into tissue specific cell type. These stem cells play a critical role in the maintenance of tissue homeostasis throughout life. Understanding the basic biology of adult ocular stem cells – identification of stem cells and their niche, elucidating their role in the maintenance of tissue homeostasis, characterizing the changes with ageing and in diseased condition to develop better stem cell based therapies at affordable cost is the focus of research in this department.

Title of the project: Limbal miRNAs and their potential targets associated with the maintenance of stemness

Investigator : Dr. Gowri Priya Chidambaranathan
Co-Investigators : Dr. Bharanidharan Devarajan
Prof. VR. Muthukkaruppan
Dr. N. Venkatesh Prajna
Collaborator : Prof. Julie T Daniels, University College London, UK
Research Scholar : Ms. Lavanya Kalaimani
Funding : Department of Biotechnology, New Delhi.
Commonwealth Scholarship Commission, UK (INCN-2018-72)

Introduction including background

Corneal epithelial homeostasis is maintained by the corneal epithelial stem cells (CESCs) that reside in the basal layer of the limbus at the corneo-scleral

junction. Understanding the molecular regulatory function of microRNAs (miRNAs) specific to CESCs will enable us to develop better treatment options for patients with limbal stem cell deficiency caused due to loss/dysfunction of these stem cells.

Previous report from this group identified six microRNAs (hsa-miR-3168, hsa-miR-21-5p, hsa-miR-143-3p, hsa-miR-150-5p, hsa-miR-1910-5p and hsa-miR-10a-5p) to be highly expressed in enriched CESCs compared to central corneal epithelial cells (CCECs) by small RNA sequencing. MiRNA transfection studies with hsa-miR-150-5p and hsa-miR-143-3p indicated their potential to increase the colony forming ability with more holoclones. Further, at the transcriptional level, with the increased expression of hsa-miR-143-3p, the cells exhibited increased the expression of stem cell markers (ABCG2, Δ NP63, NANOG, OCT4 and KLF4) but reduced expression of differentiation marker (Cx43) and Wnt signaling regulators (β -catenin and AXIN2). Further studies were carried out to understand the functional regulation of hsa-miR-143-3p at protein level.

Results

The primary limbal epithelial cells were transfected with hsa-miR-143-3p mimics and inhibitors to evaluate their effect at translational level by Western blotting and immunostaining.

The primary limbal epithelial cells upon transfection with hsa-miR-143-3p mimics had reduced expression of (i) hsa-miR-143-3p targets: DVL3, KRAS, MAPK1, MAPK14 (ii) differentiation marker, Cx43 (iii) Wnt signaling regulators: AXIN2,



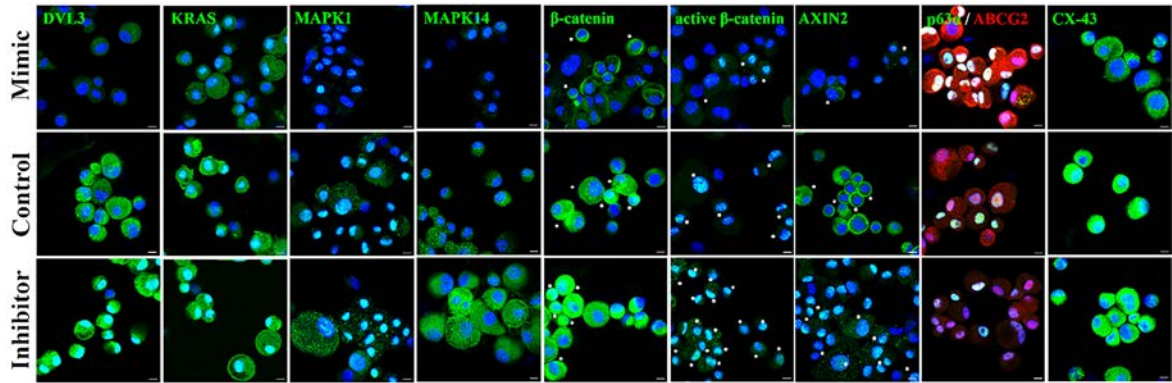


Figure 1: Representative confocal images of transfected limbal primary culture cells immunostained for DVL3, KRAS, MAPK1, MAPK14, β -catenin, active β -catenin, AXIN2, ABCG2, p63 α and Cx43. Nuclei were stained with DAPI (blue) and the protein expression with Alexa Fluor 555 (green) except for ABCG2 with Alexa Fluor 488 (red). The cells with nuclear positivity in Wnt signaling regulators (β -catenin, active β -catenin and AXIN2) were marked with asterisks. Nuclear localization of active β -catenin indicated activation of Wnt signaling. Scale bar 50 μ m.

β -catenin, active β -catenin and (iv) MAPK signaling regulators: p-ERK1/2, p-p38, p-c-JUN, p-c-FOS, p-ATF2, p-p53. However, the expression of stem cell markers ABCG2 and Δ Np63 α were increased in mimic transfected cells compared to that of the control (Figure 1 & 2).

Immunostaining revealed that the cells with nuclear positivity for β -catenin (39.65 \pm 5.42%, $p < 0.05$) and active β -catenin (73.62 \pm 10.01%, $p < 0.05$) expression were higher in inhibitor transfected cells than the control cells (Fig 1) In contrast, the number reduced in mimic transfected cells:

β -catenin (0.77 \pm 0.67%, $p < 0.05$) and active β -catenin (22.42 \pm 4.33%, $p < 0.05$). The nuclear localization of active β -catenin is an indication of Wnt signaling activation in the cells.

Conclusion

Based on the results obtained, the probable mechanism of action of hsa-miR-143-3p on WNT- β -catenin and MAPK signaling has been summarized in Fig 3. A regulatory role for hsa-miR-143-3p in maintenance of stemness by inhibiting WNT and MAPK signaling pathway was thus indicated.

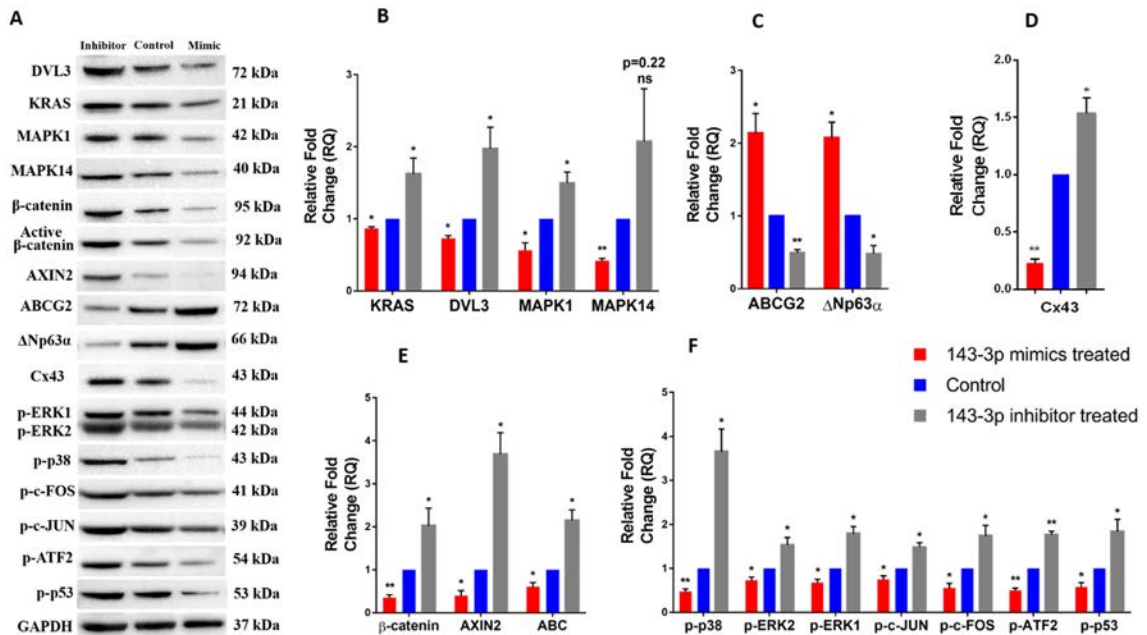


Figure 2: (A) Representative Western blots of protein of interest in three groups-hsa-miR-143-3p mimic, inhibitor and control (n=3). GAPDH was used as normalising reference and loading control. Bar graphs indicating the relative expression profile of the proteins quantified by Western blotting (B) hsa-miR-143-3p targets (C) Stem cell markers (D) Differentiation marker (E) Wnt signaling regulators (F) MAPK signaling regulators. * $P < 0.05$; ** $P < 0.001$.

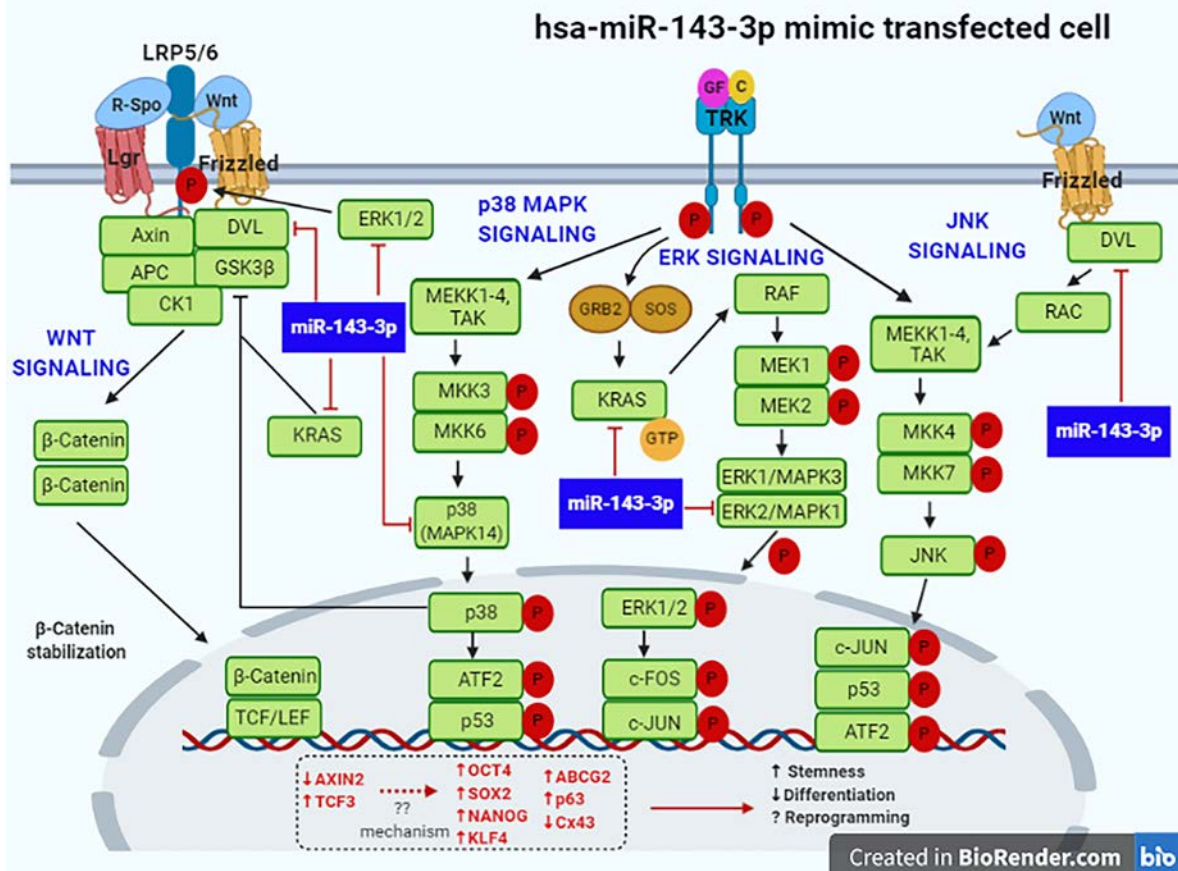


Fig 3: Hsa-miR-143-3p inhibits WNT signaling by downregulating the expression of its targets (i) DVL3- activates WNT signaling by dissociating the destruction complex (ii) MAPK1 (ERK2)- activates the WNT co-receptor LRP6 through phosphorylation and initiates WNT signaling (iii) MAPK14 (p38) and KRAS- inhibits GSK3β, a repressor of WNT signaling.

Hsa-miR-143-3p inhibits MAPK signaling by downregulating the expression of its targets (i) DVL3- initiates JNK MAPK signaling through activation of RAC protein (ii) KRAS- activates ERK MAPK signaling through activation of RAF protein (iii) MAPK14- activator of p38 ERK MAPK signaling and (iv) MAPK1- activator of ERK MAPK signaling.

Title of the project: Characterization and Functional Evaluation of Trabecular Meshwork Stem Cells in Glaucoma Pathogenesis

Investigator : Dr. Gowri Priya
Chidambaranathan
Co-Investigators : Dr. VR. Muthukkaruppan
Dr. S. Senthilkumari
Dr. Neethu Mohan
Dr. SR. Krishnadas
Research Scholar : R. Iswarya, Yogapriya
Sundaresan
Funding : Science and Engineering
Research Board (SERB)

Introduction including Background

Trabecular meshwork (TM), a tiny porous tissue located in the iridocorneal angle of the eye is

responsible for maintaining IOP homeostasis.

Previous studies from this laboratory identified that the stem cells for human TM (ABCG2⁺⁺p75⁺) are present in the Schwalbe's line region. An age-related reduction in the TM stem cells (TMSCs) was reported to be significantly correlated with the reduction in total TM cell content. The percentage of TMSCs was further reduced significantly in glaucomatous donor TM along with a drastic reduction in total TM cells, compared to age-matched controls. These results indicated a probable role of TMSCs in TM cell loss resulting in increase in IOP and in glaucoma.

Results

Stem Cell Growth Medium Maintains stemness upon culturing the TM cells

TM cells were isolated and cultured in -TM medium (DMEM+10%FBS), Modified Embryonic Stem Cell Medium (MESCM) and Stem Cell Growth

Medium (SCGM). Immunostaining of cultured cells revealed that the stem cells (ABCG2++p75+) are maintained only in SCGM (65.6±6.68%) and in MESCM (16.9 ± 4.25%). On passaging in both medium, the stem cell content reduced to 12-14% (Table 1).

Property / Media	Normal TM	MESCM	SCGM
Time taken to reach confluency	3-4 weeks	6-8 weeks	3- 4 weeks
Stem cell content (ABCG2++/ p75+)	P0=0%	P0= 16.9 ± 4.25% P1= 11.96 ± 0.67	P0=65.6±6.68% P1= 14.33±2.31
Sphere forming ability	0.028%	0.062%	0.18%

Table: Comparison of TM cells cultured in different media. The cells cultured in SCGM had greater ability to maintain stemness.

Functionally, the cells from SCGM had more sphere forming efficacy (0.18%) compared to the other media (Table). Hence, cells cultured in SCGM were taken for further studies.

Saponin to establish TM cell loss model in Human Organ Culture for Anterior Segment (HOCAS)

The concentration of saponin required to cause a 36±9% cell loss equivalent to glaucomatous condition was identified using TM cell cultures. At 0.002% concentration, 30.28±3.54% cells were dead while with higher concentrations >90% cell death was observed in comparison with control. Saponin treatment of the anterior segment in HOCAS at

0.002% resulted in 25.55±1.63% cell death. Further studies are being carried out to evaluate whether this TM cell loss will increase the pressure, to establish the cell loss glaucoma model.

Transplanted TM cells Home to TM tissue

In HOCAS, Qtracker 655 labelled passage1 TM cells were transplanted. Immunohistochemistry analysis of anterior segment revealed the ability of transplanted human cells to home to both filtering and non-filtering regions of TM while the cells were also found in ciliary body (Figure).

Conclusion

The current study revealed that

- SCGM has greater ability to maintain stemness without compromising the functional efficacy of TMSCs.
- Upon transplantation the cultured TMSCs home to both filtering and non-filtering regions of TM.

Characterization of adult human lens epithelial stem cells in the maintenance of tissue homeostasis throughout life and their functional status in cataractous lens

Investigator : Dr. Madhu Shekhar
 Co-Investigators : Dr. Gowri Priya
 Chidambaranathan
 Dr. Haripriya Aravind
 Prof. VR. Muthukkaruppan
 Research Scholar : P. Saranya
 Funding : Science and Engineering
 Research Board (SERB)

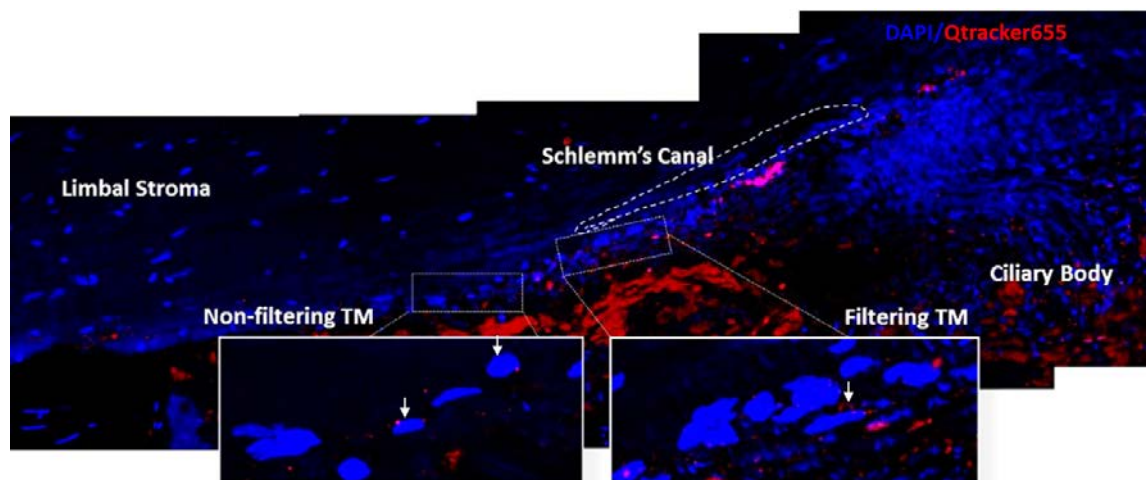


Figure: Montaged confocal images of human anterior segment after transplantation with Qtracker labelled cells. Nucleus counter stained with DAPI (Blue), Qtracker 655 labelled cells (Red). The transplanted cells (red) had the ability to home to TM both non-filtering and filtering regions (inset - higher magnification, arrow indicates transplanted cells).

Introduction including Background

The anterior lens epithelium (central, germinative, transitional and equatorial zones) has the ability to differentiate into lens fibres throughout life with the inductive action of neural retina, the mouse anterior lens epithelium develops a complete lens *in vitro*. This study aims to characterize the adult human lens epithelial stem cells and to understand its role in tissue homeostasis. The presence of stem cells in the whole mounts of native human lens epithelium was identified based on the expression of the stem cell marker SOX-2 but negative for the differentiated cell marker – connexin-43 (Cx-43). Such stem cells were located in the central zone of human anterior lens epithelium. The commencement of the germinative zone was defined by the presence of Cx-43 positive and SOX-2 negative cells; transitional zone by expression of β crystallin, an early elongation cell marker and equatorial zone by the late elongating cell marker - γ crystallin. In continuation, this year, the expression of SOX-2, Cx-43 and Ki-67 (proliferation cell marker) in different zones was confirmed using the human lens paraffin sections. Preliminary studies were carried out to evaluate the regenerative potential of human anterior lens epithelium using human whole lens cultures.

Results

Characterization of the human anterior lens epithelium

The human lens sections were immunostained for SOX-2, Cx-43 and Ki-67 (n=3 donors, 3 sections/donor). The expression of SOX2 was observed both

in the central 1.7 mm (30%) and equatorial (11%) (towards fibre differentiation) zones of the lens epithelium. Except for 67.5% cells in the central zone, all epithelial cells were positive for Cx-43 (Figure 1).

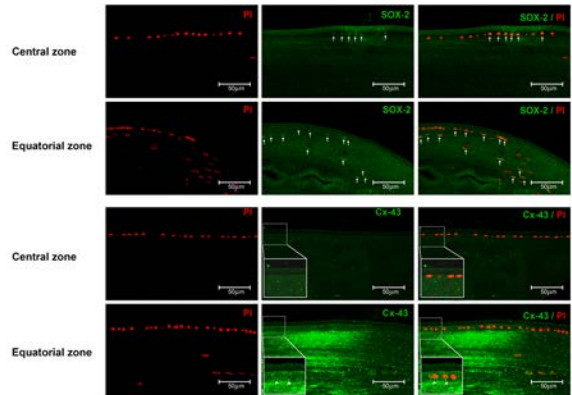


Figure 1: Representative confocal images of lens sections showing expression of SOX2 (arrow) in epithelial cells of both central and equatorial zones. But the expression of connexin-43 (Cx-43, arrow head) was observed to be negative only in cells in the central zone.

The expression of proliferating cell marker Ki-67 was observed in both the central (Figure 2A) and equatorial (Figure 2B) regions (58.9 \pm 10.1% of total epithelial cells). Among the cells in the central 2 mm region, 34 \pm 12.8% of epithelial cells were positive (36% in 3 years; 40.2% in 16 years; 16% in 74 years).

Establishment of human whole lens culture system in the absence of neural retina

In order to evaluate the efficacy of human anterior lens epithelium for the regenerative potential, the whole lens was dissected, placed on a matrigel -

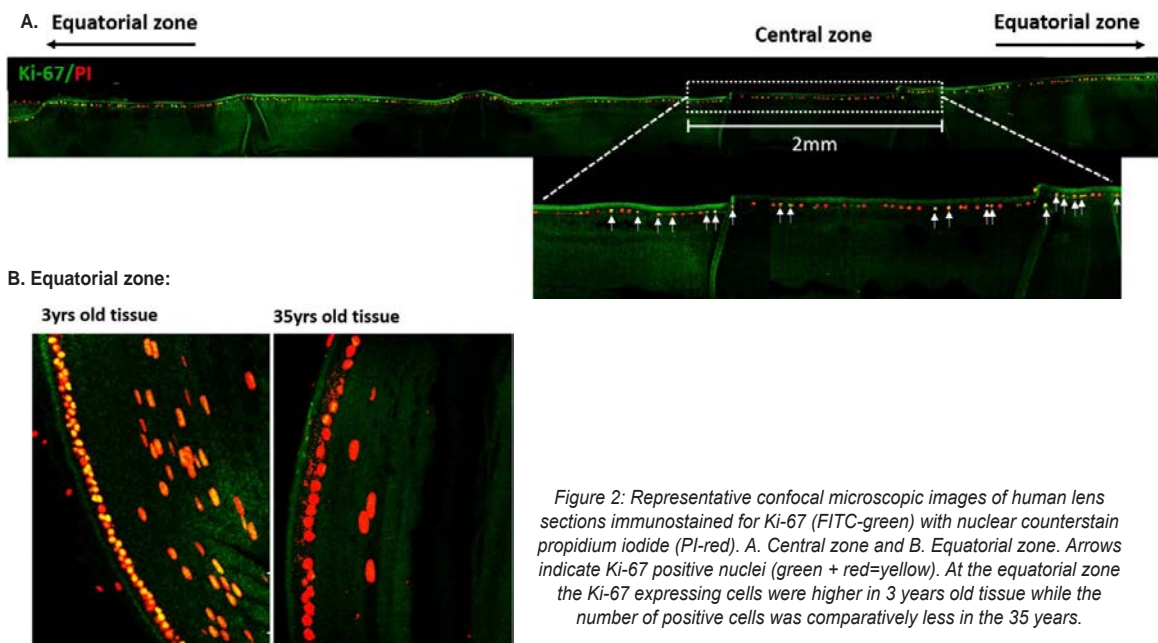


Figure 2: Representative confocal microscopic images of human lens sections immunostained for Ki-67 (FITC-green) with nuclear counterstain propidium iodide (PI-red). A. Central zone and B. Equatorial zone. Arrows indicate Ki-67 positive nuclei (green + red=yellow). At the equatorial zone the Ki-67 expressing cells were higher in 3 years old tissue while the number of positive cells was comparatively less in the 35 years.

Growth Factor Reduced coat with the anterior lens epithelium facing-up and cultured for 19 days in MEM with 20%FBS, 25ng FGF, penstrep and gentamicin.

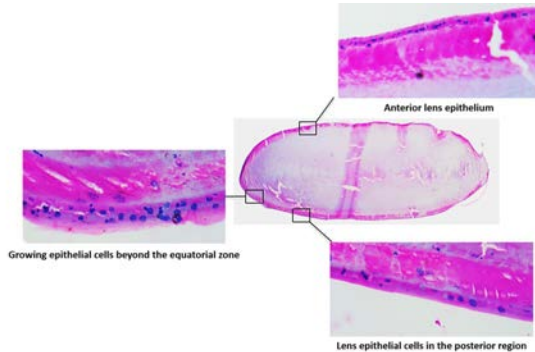


Figure 3: Hematoxylin and eosin stained section of cultured human lens. The cultured whole lens sections revealed the migration of human lens epithelial cells beyond the equatorial zone.

The hematoxylin and eosin stained sections of the cultured human lens indicated the migration of lens epithelial cells towards the posterior capsule (Figure 3).

Analysis of the immunostained human lens sections (Figure 4) revealed Ki-67, the proliferating cell marker to be positive in 30% of lens epithelial cells, including 60% positive cells in the central 1.2 mm region.

Conclusion

- The presence of SOX2+ and CX43– stem cells was confirmed to be located in the central zone of human anterior lens epithelium.
- Whole lens culture system was established. The regeneration potential was evident with the lens epithelial cell proliferation and migration towards the posterior capsule in adult human lens in the absence of neural retina.

Further studies are being carried out on whole lens culture with neural retinal induction to confirm the role of lens epithelial stem cells in lens regeneration and tissue homeostasis.

Identification and Characterization of adult human retinal pigment epithelial stem cells

Investigator : Dr. Gowri Priya
Chidambaranathan
Co-Investigators : Prof. VR. Muthukkaruppan
Dr. K. Naresh Babu
Dr. R. Kim
Research Scholar : A. Waseema

Introduction including Background

Retinal Pigment Epithelium (RPE) is a monolayer of post-mitotic, pigmented cells beneath neural retina, which is actively involved in the visual process by supporting the replenishment of photoreceptors. Dysfunction of RPE is associated with age related macular degeneration, a leading cause of blindness worldwide. In human RPE, stem cells have been identified only in cultured cells. But no report is available on the stem cells in native RPE, their role in tissue homeostasis and in the pathology of age related macular degeneration. Previous report from this laboratory identified a higher expression of embryonic stem cell marker OCT4 in the peripheral RPE compared to central and equatorial RPE by real time PCR. In continuation, cultured human RPE cells from different regions and RPE sections were characterized by immunostaining for stem cell or proliferating cell markers.

Results

Characterisation of cultures from different regions of RPE

RPE cells from the peripheral, equatorial and central regions were isolated with dispase – trypsin treatment and plated onto Primaria dishes, reported to inhibit fibroblast growth. The cultured cells (passage 2) were characterized for the expression of ABCG2, KLF4, connexin43 and RPE-65. Further, passage 2 cells were pulse labelled with BrdU for five days after which the cells were trypsinised and immunostained with anti-BrdU antibody.

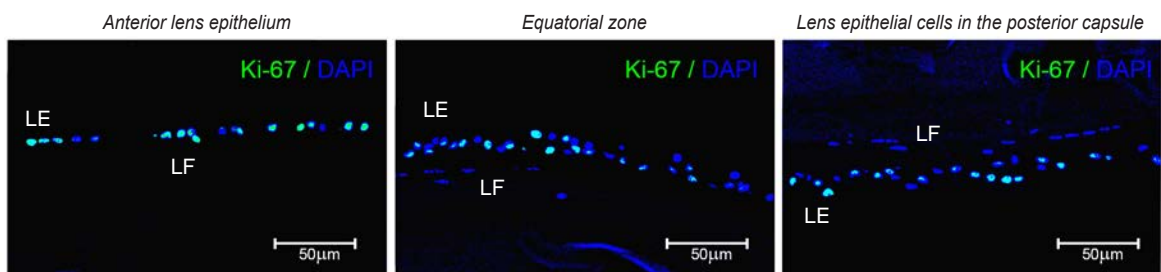


Figure 4: Confocal microscopic images of cultured human lens immunostained for Ki-67(FITC-green) with nuclear counterstain DAPI (Blue). The Ki-67 positive cells (green+blue=cyan blue) indicated the proliferation and migration of lens epithelial cells towards the posterior capsule. LE - Lens Epithelium; LF -Lens Fiber

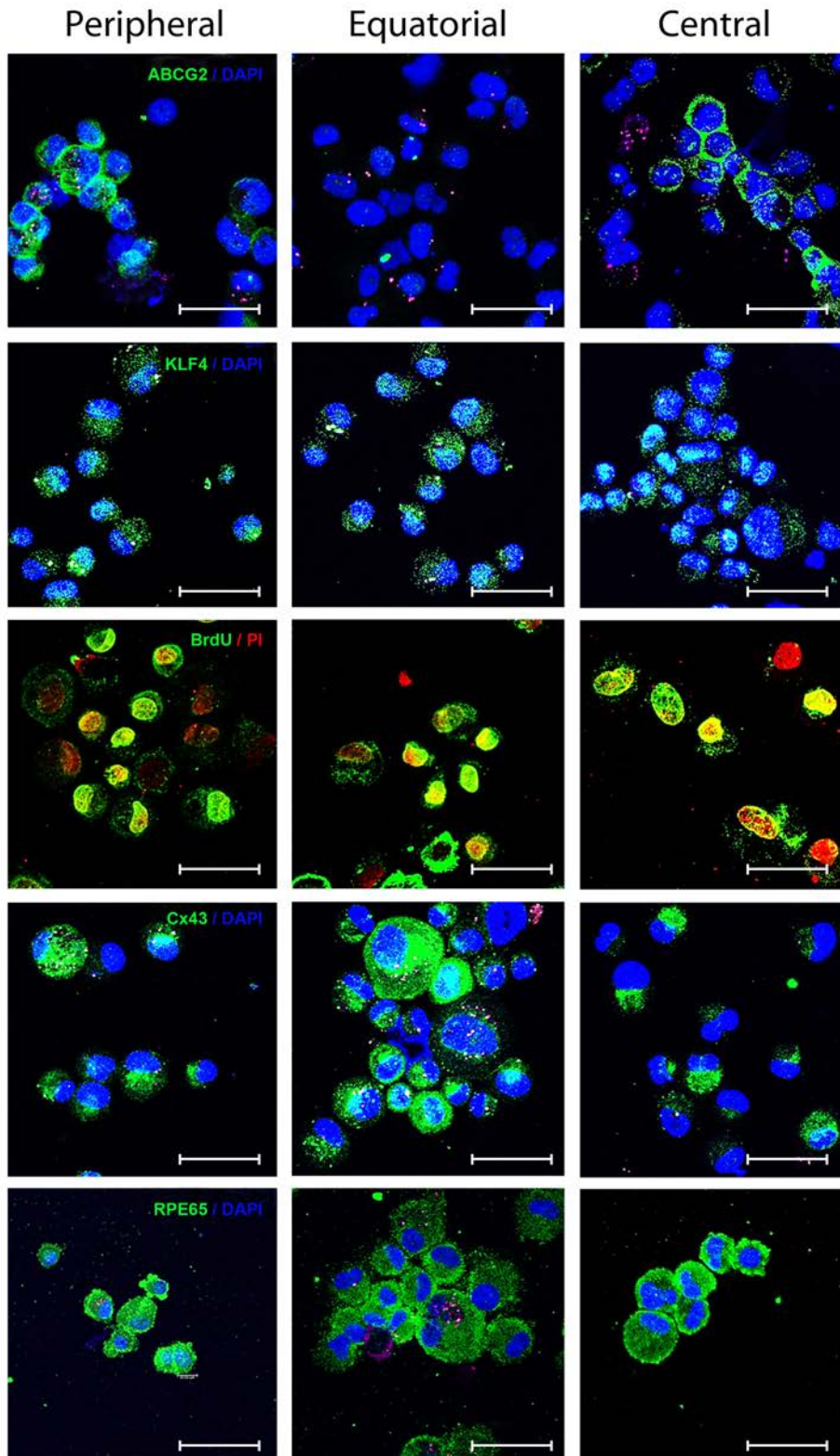


Figure 1: Immunostaining of cultured RPE cells. Representative confocal images of cultured RPE cells (passage 2) cytosmears immunostained (green) for ABCG2, KLF4, BrdU, connexin 43 (Cx43) and RPE65, nuclear counterstain – DAPI (blue)/PI (red). The expression of the stem cell markers was higher in RPE cells cultured from peripheral and central regions compared to equatorial region. Scale bar represents 50 μm .

Markers	Percentage of Positive Cells		
	Peripheral	Equatorial	Central
ABCG2 (high expression)	3	0	9
KLF4	25	12	66
BrdU	69	68	70
Connexin 43	95	100	86
RPE65	96	99	98

Table. Characterization of cells cultured from the three regions of human RPE

Cultures from all regions expressed the RPE specific marker RPE65 (96-99%). The percentage of cells expressing ABCG2, the universal stem cell marker and KLF4, an embryonic stem cell marker was found to be higher in the central and peripheral RPE (Figure 1, Table). Further, all equatorial cells expressed the differentiation marker Connexin 43 while a proportion of cells (5% in peripheral; 14% in central) were negative for the marker in the other two regions.

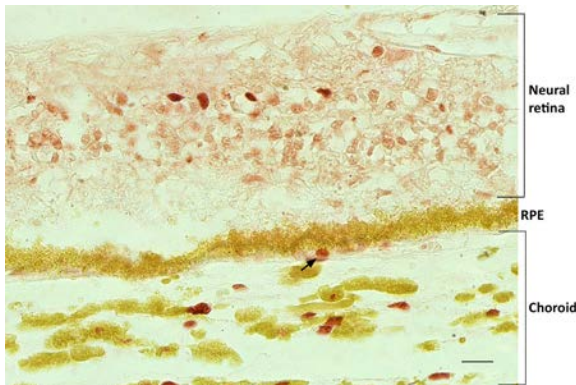


Figure 2: Immunohistochemistry of native human RPE. Representative light microscopic image of a native human RPE section immunostained for Ki67 (red). The expression of Ki67 (arrow) was observed in all regions of human RPE. Scale bar represents 20 μ m.

Immunohistochemistry of Native human RPE

Sections of human retina (n=3 donors) were depigmented with potassium permanganate-oxalic acid treatment and then immunostained for the proliferation marker Ki67. RPE cells expressing Ki67 were observed in peripheral RPE (Figure 2).

Conclusion

The observed regional difference in the expression of stem cell markers in cultured RPE cells indicated that the stem cells for RPE might be present in either the central or peripheral RPE. In addition, the presence of proliferating cells in peripheral region highlighted the existence of a mechanism to maintain tissue homeostasis and confirmed the presence of adult stem cells in RPE.

PROTEOMICS

In the Proteomics Department, our primary focus is to understand the pathological mechanisms underlying various eye diseases and to develop methods or identify biomarkers with diagnostic and prognostic potential. Currently our focus is on four eye diseases, fungal keratitis, diabetic retinopathy, keratoconus, and pterygium. We employ 2D-gel based and mass spectrometry-based proteomics approaches for profiling and comparative analysis of proteome from ocular fluids or tissues from patients. Through this approach, we identify alterations in the proteome as the disease progresses and such alterations include changes in the abundance of proteins and proteoforms as well as post-translational modifications. The state-of-the-art mass spectrometry facility at the proteomics department enabled us to profile complex proteomes in the discovery phase studies from which we shortlist candidate biomarker proteins that are then validated in a larger patient cohort. The proteomics approach is complemented by studies at the genome and transcriptome level. We also have an established cell culture facility where we use cell lines as a model system to test our hypothesis. We collaborate with various national and international institutions such as Vision Research Foundation, Chennai, Moorefields Eye Hospital, UK, and Dartmouth College, USA to broaden our scope of research. The collaborative project on the development of a novel chemical cross-linker with the University of Liverpool is being further extended with a study on the mechanism of action of the cross-linker in stiffening of the keratoconus cornea.

Research on Fungal Keratitis

Interaction of *A. flavus* conidia with human corneal epithelial cells

Investigators : Prof. K. Dharmalingam and Dr. J. Jeya Maheshwari
Clinician Scientists: Dr. N. Venkatesh Prajna and Dr. Lalitha Prajna
Team Member : Ms. A. Divya

Background

Infectious keratitis is the major corneal disease responsible for monocular blindness and affects two million people worldwide every year. *Fusarium* and *Aspergillus* are the predominant pathogens associated with fungal keratitis. Internalization by phagocytosis is a fundamental process of innate immunity, and professional phagocytes such as neutrophils, dendritic cells, monocytes and macrophages and non-professional phagocytes such as epithelial cells, fibroblasts, and endothelial cells are involved. Previously, we have shown that the corneal epithelial cells form actin ring around the conidia and the conidia containing phagosomes matured from early phagosomes to late phagosomes. Further the changes in the immune response genes were analyzed using NanoString assay. Here, the phagocytic efficiency of *A. flavus* conidia by human corneal epithelial (HCE) cells and the phagolysosome acidification were analyzed.



Phagocytic efficiency of HCE cells

HCE cells were infected with *A. flavus* conidia (CI1123) with MOI of ten for 2h at 37°C. CI1123 is an *A. flavus* isolate from a fungal keratitis patient who was not cured with antifungal therapy. In order to examine the efficiency of phagocytosis, the uptake of conidia was determined by distinguishing the internalized conidia and conidia bound to the surface of the cells by staining extracellular conidia by calcofluor white and membrane staining by CM-Dil. The absence of CFW staining of conidia indicates that the added conidia were internalized. A representative picture for the conidial internalization examined using confocal microscopy is shown in figure 1a. The first panel shows the total conidia labeled with FITC (Figure 1a panel A), the second panel (Figure 1a panel B) shows internalized and external bound conidia (green/blue merged), third panel represents the membrane stained HCE cells (Figure 1a panel C) and last panel indicates the merged overlay of all channels (Figure 1a panel D). The white arrows in the panel B (Figure 1a) indicates the green color conidia and the absence of blue fluorescence, which reveals that the absorbed conidia were internalized by RCB2280 cells and the last panel clearly shows the host cell containing the internalized conidia (Figure 1a panel D). CM-Dil staining also shows a ring-like structure around the conidia. For quantitation of internalization, the ring structure, as well as the absence of blue fluorescence, were taken into

account. Around 30% of the total added conidia were internalized by RCB2280 cells. The internalization was inhibited when the cells were treated with cytochalasin D. The phagocytic activity and the phagocytic index of RCB2280 cells for engulfing the *A. flavus* conidia (CI1123) were found to be 15% and 30% respectively.

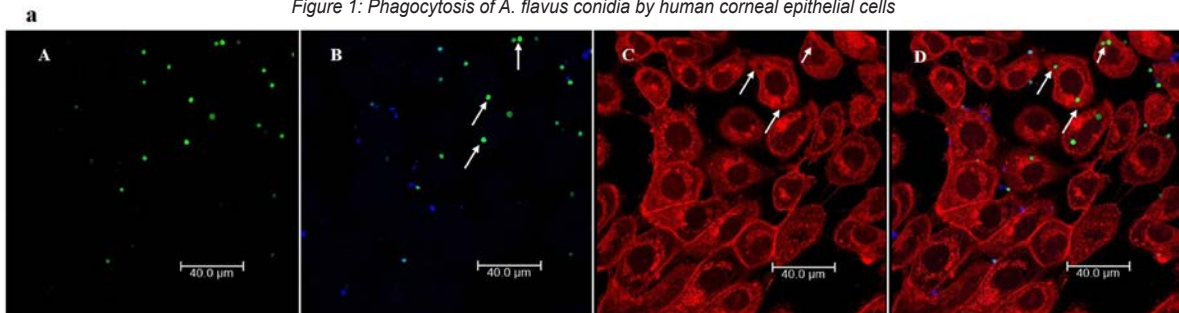
Phagolysosome acidification

As the phagosomes and phagolysosomes are characterized by their acidic nature, acidotropic probe lysotracker red DND-99 was used to examine the pH of the phagosomes. Confocal microscopy revealed a bright red fluorescence was impregnating the conidia containing vacuoles after 4h of post-infection. The merged image shows the lysotracker stained about 25% of the conidia containing vacuoles. Presence of unstained conidia containing vacuoles indicated that some of the phagosomes failed to enter phagolysosomal stage (Figure 2). The treatment with bafilomycin A1, an inhibitor of vacuolar ATPase, completely abolished the colocalization of the red fluorescence (Figure 2).

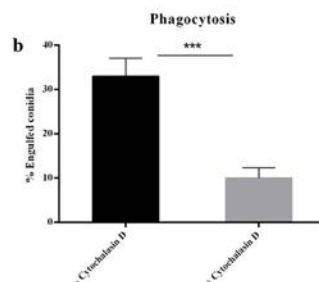
Conclusion

HCE cells phagocytose *A. flavus* conidia and the engulfed conidia were matured into phagolysosome. The fate of conidia in human corneal epithelial cells has to be explored further.

Figure 1: Phagocytosis of *A. flavus* conidia by human corneal epithelial cells



a) Coverslip cultures of HCE cells (RCB2280) were infected with FITC labeled *A. flavus* CI1123 conidia (106) for 2 h at 37 °C. The host cells were stained with CM-Dil, conidia were labeled with FITC and the extracellular conidia were labeled with CFW after infection. A) Green channel (FITC) with all conidia; B) Green (FITC) /blue (CFW) merged layer with internal and external conidia; C) Red channel (CM-Dil) with RCB2280 cells; D) Merged fluorescent image of all channels. White arrows indicate the internalized conidia.



b) % Engulfed *A. flavus* CI1123 after 2 h of exposure in RCB2280 cells with and without cytochalasin D treatment. Bar graph showing significantly decreased engulfment of conidia in the presence of cytochalasin D. % Engulfed conidia is calculated as follows: (the number of conidia engulfed by RCB2280 cells / the total number of conidia associated with HCE cells) * 100. The data were analyzed using two-way ANOVA with Bonferroni multiple comparison test (***) $p < 0.001$.

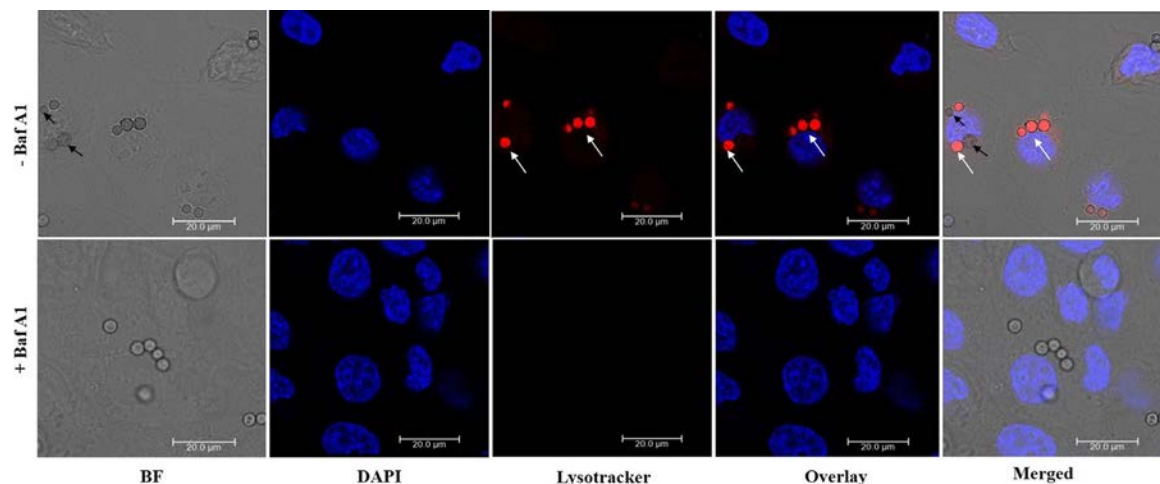


Figure 2: Acidification of *A. flavus* conidia containing phagolysosomes: RCB2280 cells were infected with *A. flavus* C11123 conidia in the lysotracker (200 nM) containing medium in the presence or absence of bafilomycin A1 (250 nM) for 4 h at 37 °C. After infection, the cells were fixed with 4% PFA, mounted on slides and viewed under confocal microscope. Confocal images showing the red color staining of conidia by lysotracker indicating the acidification and was absent in the presence of bafilomycin.

References

- Ibrahim-Granet O, Philippe B, Boleti H, Boisvieux-Ulrich E, Grenet D, Stern M, Latge JP. 2003. Phagocytosis and intracellular fate of *Aspergillus fumigatus* conidia in alveolar macrophages. *Infect Immun* 71:891-903
- Gresnigt MS, Becker KL, Leenders, Alonso MF, Wang X, Meis JF, Bain JM, Erwig LP, Van De Veerdonk FL. 2018. Differential kinetics of *Aspergillus nidulans* and *Aspergillus fumigatus* phagocytosis. *J Innate Immun* 10:145-160

40% failed to show any culture growth. Among the culture positive ulcers, 70% are fungal infection. *Fusarium* and *Aspergillus flavus* are the major fungal pathogens causing fungal keratitis and the patients are treated with anti-fungal drugs such as natamycin, voriconazole etc. However, despite the treatment, in 40-50% of the patients the ulcer worsens requiring a surgical intervention to clear the infection. At present, the ophthalmologists use ulcer characteristics such as ulcer depth, size and location to gauge the severity of infection and disease prognosis. More accurate methods to predict the outcome of the fungal infection would help the clinician to make an informed decision on an early surgical intervention in patients who are unlikely to respond to treatment.

Prediction of treatment outcome in fungal keratitis patients

Investigators : Prof. K. Dharmalingam
 Dr. J. Jeya Maheshwari
 Dr. Bharanidharan
 Clinician Scientists: Dr. NV. Prajna
 Dr. Lalitha Prajna
 Dr. Sankalp Sharma
 Team Member : Ms. Sandhya L
 Ms. Pon Yazhini
 Funding : Cognizant Foundation

Objectives

This study aims

- To validate the potential of tear proteins to be used as indicators of the severity of the fungal infection and the inflammatory status due to the host response
- To use the ulcer characteristics and tear protein levels to build a model to predict whether a fungal keratitis patient will respond to treatment or not

I. Validation of tear biomarkers in fungal keratitis patients

Rationale

Fungal keratitis, an infection of the cornea, is more prevalent in tropical countries such as India. Among the 2000 corneal infections reported each year at Aravind Eye Hospital, Madurai more than

Results

Based on our previous proteomics analysis of the tear from early stage *A. flavus* keratitis patients, various pathways were found to be activated during fungal infection (Kandhavelu et al., 2017). The three key events that contribute to the inflammatory response and eventually to the treatment outcome are complement pathway, coagulation pathway and

Tear protein	Function of the protein	Rationale for selection as marker
Complement factor H (CFH)	Acts as a soluble inhibitor of complement and hence, negatively regulates the activation of complement pathways	Indicator of regulation of complement pathway activation
Complement factor B (CFB)	Activator of alternative complement pathway	Indicator of amplification of complement pathways
Alpha-2 macroglobulin (A2M)	Panprotease inhibitor and acute phase reactant	Indicator of the extent of inflammatory response
Calprotectin - heterodimer of S100A8 and S100A9 (CAL)	The antimicrobial heterodimer protein released in neutrophil extracellular traps that acts as the major antifungal component	Indicator of the extent of neutrophil infiltration
Vimentin (VIM)	Extracellular vimentin has been implicated in mediating repair-cell function in wound repair	Indicator of wound healing response
Zinc-alpha 2 glycoprotein (ZAG)	Multifunctional protein with many functions such as lipid mobilization, RNase activity, inhibitor of tumor proliferation etc	Previous studies indicate differences in ZAG levels between <i>A. flavus</i> and <i>Fusarium</i> keratitis tear

These six tear proteins were quantified in tear samples collected from 72 study subjects (24 *A. flavus* keratitis, 24 *Fusarium* keratitis and 24 healthy controls).

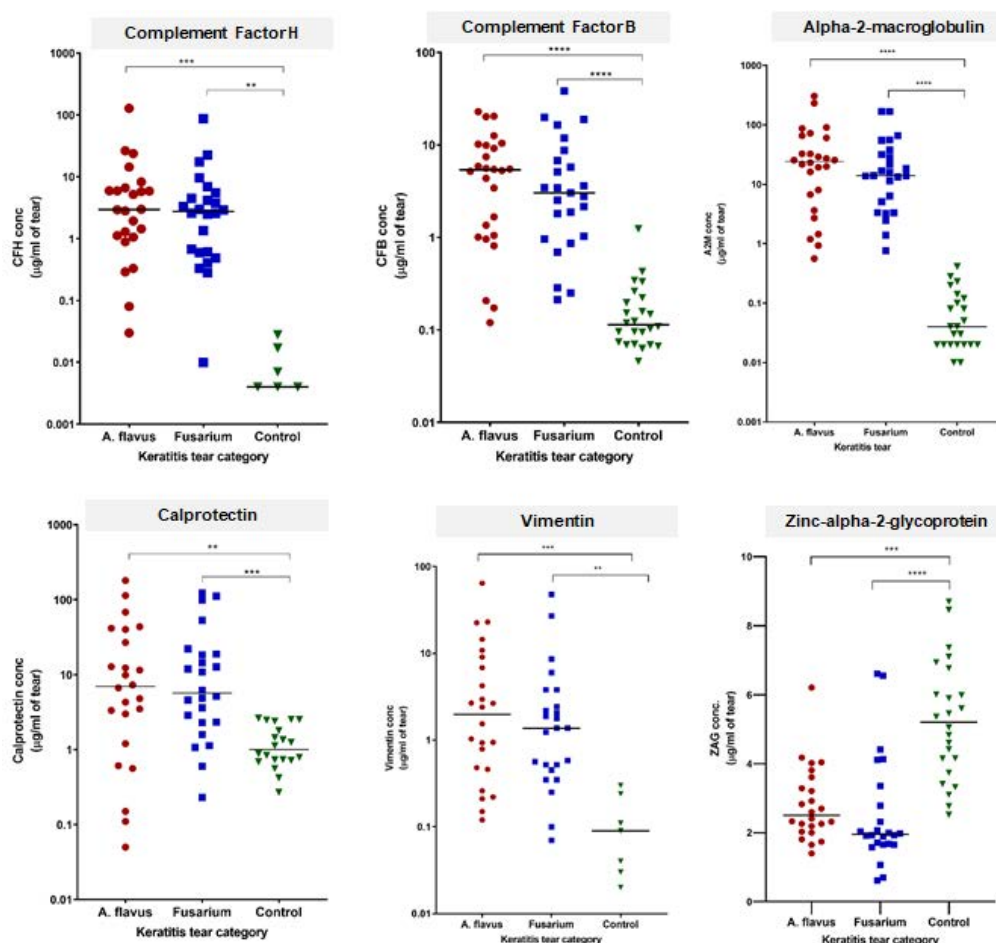


Figure 1.1. ELISA quantitation of six tear proteins. Tear samples from *A. flavus* keratitis, *Fusarium* keratitis and control samples were used for quantifying the six proteins. Each sample was assayed in triplicates during ELISA. Statistical significance, **** $p < 0.0001$; *** $p < 0.0005$; ** $p < 0.005$

neutrophil response in the form of NETosis. Based on this and other earlier studies (Parthiban et al., 2019), six tear proteins were selected for validation in this study.

Among the six markers quantified, five proteins except ZAG showed a significant increase in level in keratitis tear when compared to the control tear. This increase was seen in tear from both the *A. flavus* and *Fusarium* keratitis patients. In case of ZAG, there was a significant decrease in the level of the protein in keratitis patients when compared to the control. No significant difference was observed in the level of any of the six proteins between *A. flavus* and *Fusarium* keratitis patients suggesting that the response to fungal infection may be similar between *A. flavus* and *Fusarium* infections.

Further analysis of the tear protein levels with that of the ulcer characteristics and treatment outcome revealed the following

- ZAG level in tear was significantly lower in keratitis patients with superficial ulcers when compared to those with mid ulcers (Figure 1.2 A)
- Calprotectin and ZAG levels were significantly higher in patients with ulcers that were larger than 5 mm² (Figure 1.2 B & C)
- Patients who did not respond to treatment had higher calprotectin-vimentin ratio when compared to those who responded to treatment (Figure 1.2 D)

- Patients who responded to treatment had higher CFH to CFB ratio when compared to those who did not respond to treatment (Figure 1.2 E).

Data from this study indicate that calprotectin, vimentin, CFH, and CFB levels in tear could be correlated to the treatment outcome in the keratitis patients and hence, will be used for building the predictive model.

Work in progress

The current study examined the changes in six tear proteins and its alterations with reference to the treatment outcome only in *A. flavus* and *Fusarium* keratitis patients. In the second phase of the study, all the six markers will be quantified in a larger cohort of fungal keratitis patients that will include other fungal infections as well. This will enable us to build a robust model to predict the treatment outcome in keratitis patients with any fungal infection.

II. Determination of ocular microbiome profile of keratitis patients using a metagenomics approach

Introduction

Microbial Keratitis is an inflammatory disease, due to bacteria and fungi, mainly filamentous fungi. (Lin et al., 2012). In many patients, the inflammation does not resolve completely, leading to corneal opacification and loss of vision (Thomas 2003). Studies have examined the alteration in the bacterial

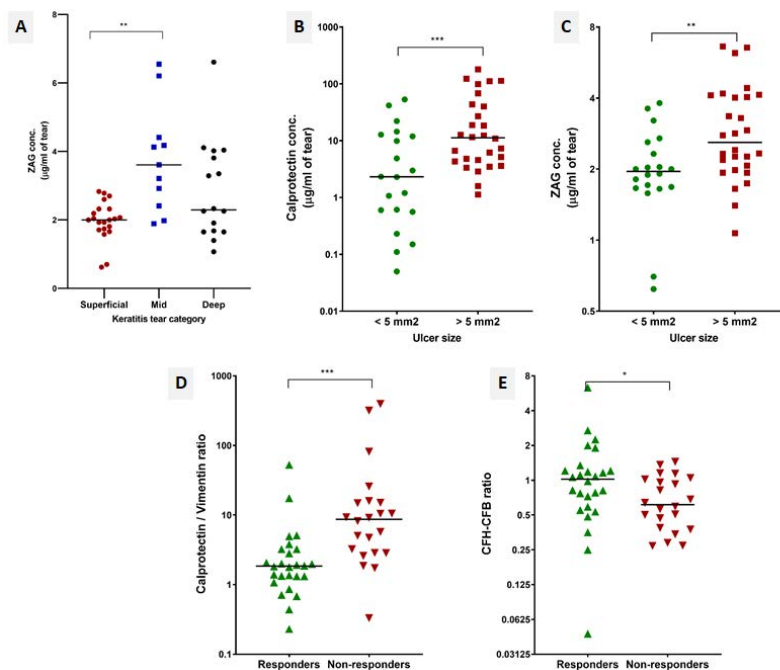


Figure 1.2. Relation between tear protein levels, ulcer characteristics and treatment outcome. Statistical significance, *** $p < 0.0005$; ** $p < 0.005$; * $p < 0.05$

community (Ge, Wei, Yang, Cheng, & Huang, 2019) and whether the antibiotic treatment (Tanure, Cohen, Sudesh, Rapuano, & Laibson, 2000) lead to reduction in the resistance of the eyes to fungal infections. The presence of ocular microbiota strengthens the ocular immunity by increasing various immune effector

molecules. Therefore, it has been demonstrated in the animal-models that colonization of bacterial commensal on the ocular surface has protective role against the pathogen infection. Interestingly, dysbiosis of ocular surface microbiome has been reported widely in several ocular surface disorders

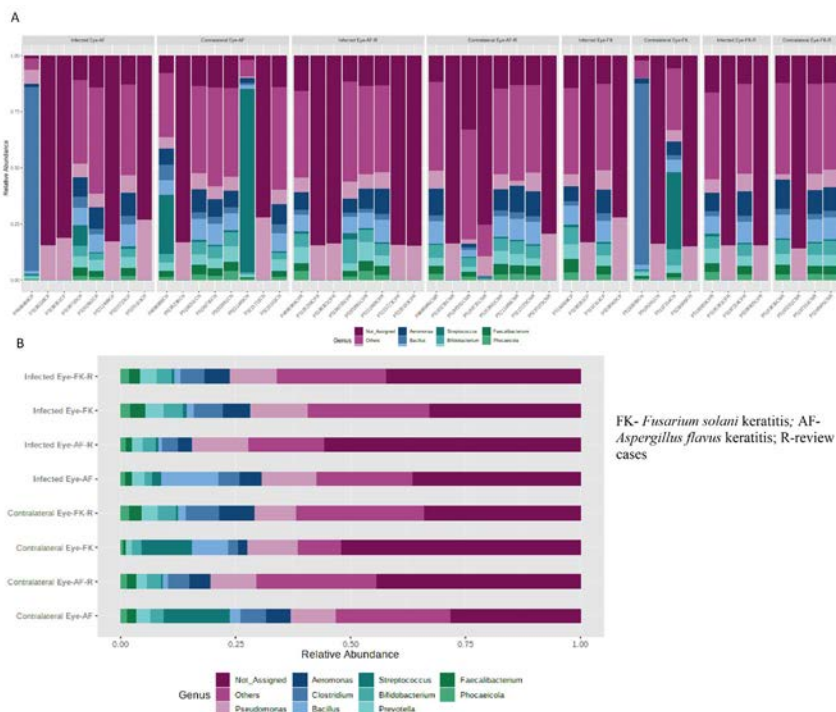


Figure 1. Relative Abundance (A) and average abundance of top 10 bacterial (B) from microbiomes of conjunctival swabs of infected and contralateral eye of *Fusarium solani* and *Aspergillus flavus* keratitis patients as well as review cases.

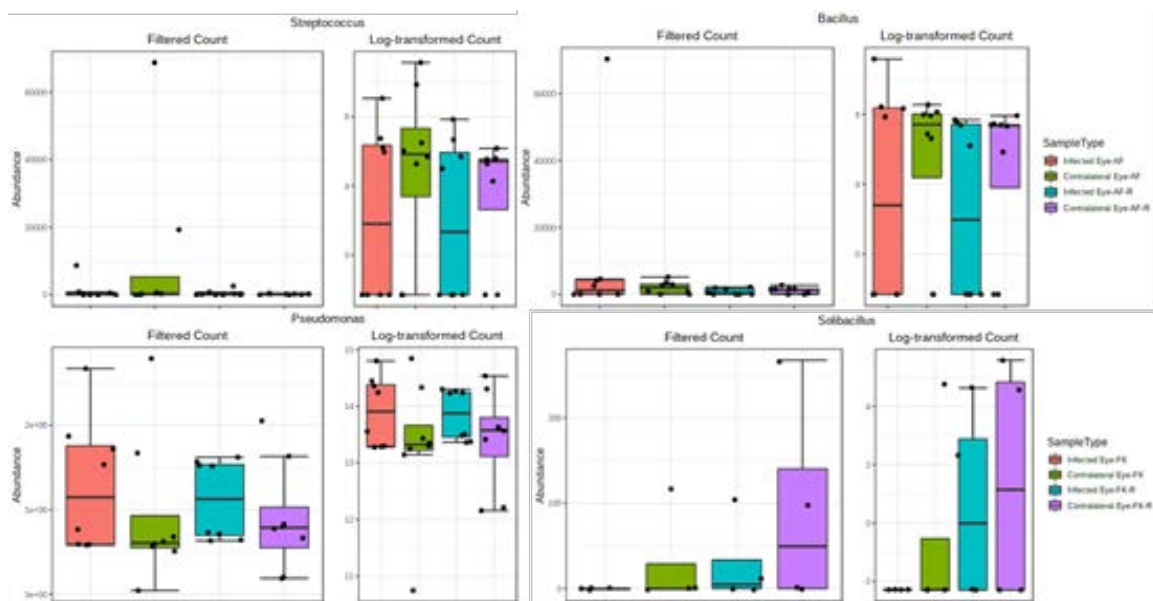


Figure 2. The abundance of three genera *Pseudomonas*, *Streptococcus* and *Bacillus* were differentially observed from microbiomes of conjunctival swabs of infected and contralateral eye of *Aspergillus flavus* keratitis patients as well as review cases, while *Solibacillus* was observed in *Fusarium solani* keratitis patients. Both filter OTU counts and log transformed count were plotted.

and infectious diseases, including fungal keratitis. Despite the fact that dysbiosis exists in fungal keratitis, how the dysbiosis is altered during keratitis progression and after treatment is not studied. In this project, we will be examining the bacterial and fungal microbiome in the initiation, progression and outcome of fungal keratitis mainly caused by *A. flavus* and *Fusarium solani*.

Results and Conclusions

The human eye samples (conjunctival swabs) from fungal keratitis patients were collected to identify all the ocular surface bacterial and fungal species (microbiome) using 16s and ITS metagenomics sequencing. The samples include conjunctival swabs of both eyes and also review samples. Conjunctival swabs from cataract patients were collected as controls for this study. 48 samples, positive for *A. flavus* (32 samples) and *Fusarium solani* (16), were sequenced for both 16s and ITS sequencing. There was a difference in the ocular surface bacterial community between the infected and uninfected eye of fungal keratitis patients. At the genus level, only around 50% of the reads across all the groups were assigned to 253 different genera and the remaining reads were assigned as unclassified genera and others. The figure 1 shows the top 10 genera with variable abundance in each group. The differential analysis of abundance of bacterial genera showed that two bacterial genera *Bacillus* and *Streptococcus* were significantly downregulated in the infected eye of *A. flavus* (Figure 2) as well as after the treatment. While, *Pseudomonas* bacteria was upregulated in the infected eye of patients with before and after treatment. On the other hand, *Solibacillus* bacteria was differentially observed in *Fusarium solani* keratitis patients (Figure 2). *Solibacillus* bacteria was less abundant in infected eye and progress to increase its abundance in the contralateral eye and also infected eye after the treatment.

We also observed variable fungal microbiome in the infected eye compared to uninfected, which requires further analysis and validation on more samples. However, we observed that the *Basidiobolus* fungus dominating the core ocular fungal microbiome.

References

- Kandhavelu, J., Demonte, N. L., Namperumalsamy, V. P., Prajna, L., Thangavel, C., Jayapal, J. M. & Kuppamuthu, D. (2017). J Proteomics 152, 13-21.
- Parthiban, N., Sampath, N. L., JeyaMaheshwari, J., Prajna, N. V., Lalitha, P. & Dharmalingam, K. (2019). Exp Eye Res 186, 107700.

Research on Diabetic Retinopathy

Proteome Profiling of Serum Microparticles in Diabetes and Diabetic Retinopathy Patients: Towards Identification and Validation of Predictive Biomarkers

Investigators : Dr. J. Jeya Maheshwari
Prof. K. Dharmalingam
Clinician Scientists: Dr. R. Kim
Team Member : Mr. Vignesh
Mr. Subash
Funding : Department of Health Research,
Govt. of India

Rationale

A recent statistics from the International Diabetes Federation suggest that as of 2019, approximately 463 million adults across the globe have diabetes mellitus and this number is expected to rise to 700 million by 2045. One-third of the diabetic individuals develop diabetic retinopathy (DR), a microvascular complication of the retina that could lead to visual impairment and blindness. Treatment in the form of anti-VEGF or surgical intervention is usually given only in the advanced stages of the DR. Therefore, early detection and effective management of DR is essential to protect the DR patients from vision loss.

It is speculated that microparticles may be involved in the development of diabetic complications. An increase in microparticle release have been reported under different stimuli that can lead to diabetic complications. Hence, analysis of microparticle proteome will help understand the development and progression of DR. And, more importantly, the altered microparticle proteins have the potential to serve as diagnostic or predictive biomarkers and would be helpful in monitoring the progression of DR to determine the appropriate timing for clinical intervention.

Objectives

The major objectives of this project include

1. Profiling and comparative analysis of serum microparticle proteome from individuals across the DR spectrum (non-diabetic, type 2 diabetics (DM), non-proliferative DR (mild, moderate and severe), and proliferative DR) to identify DM-specific and DR-specific protein changes
2. Validation of selected proteins (that show alterations in DR patients) in a large sample cohort to identify candidate biomarkers

Previous work done

Isolation of circulating microparticles were optimized using a high-speed centrifugation method and enrichment of microparticles was confirmed through the identification of previously reported microparticle proteins by mass-spectrometry based proteomics approach and immunoblot analysis. A TMT-labelled quantitative mass spectrometry approach was used to compare the abundance of the proteins in the microparticles isolated from the serum from individuals representing different stages in the development of DR, namely non-DM, type 2 DM, NPDR-mild, NPDR-moderate, NPDR-severe, and PDR. Based on this analysis, a number of microparticle proteins were found to be altered across the different stages of DR.

Results

Amongst the various proteins that were significantly altered in the microparticle proteome of the DR patients, six proteins were selected for further validation in a large sample cohort. These proteins include CD41-61, fibronectin, alpha-2-macroglobulin, vitronectin and peroxiredoxin. Blood samples were collected from individuals across different stages of DM and DR and serum was separated and stored for microparticle validation study. Blood parameters such as HbA1c, urea, creatinine, lipid profile, ESR, microalbuminuria were determined for all the study subjects. Microparticles were isolated from the serum collected from the study subjects and resuspended in RIPA buffer, aliquoted and stored in -80 °C until ELISA analysis.

CD41-61

Platelet-derived microparticles are the most abundant microparticles in the bloodstream constituting approximately 70% to 90% of circulating microparticles. These microparticles are CD41+ indicative of platelet origin. The CD41 (IIb) and CD61 (IIIa) form a calcium-dependent heterodimeric complex in platelet that can bind plasma proteins, such as fibrinogen, fibronectin, von Willebrand factor, and vitronectin, and plays a critical role in platelet aggregation.

In the discovery phase study, CD41-61, an important platelet-derived microparticle marker, was found to be altered in NPDR. To validate this finding, the level of microparticle CD41-61 was quantified in 202 samples distributed across DR sample groups. Figure 2.1 shows the comparison of the CD41-61 levels across the different DR categories and the trend in the change in the level of this protein.

Kruskal-Wallis test was performed to determine the statistical significance in the difference in CD41-61 levels across the different categories. The analysis indicate that there was a statistically significant decrease in the CD41-61 levels in the microparticles from NPDR-moderate, NPDR-severe and PDR subjects when compared to both DM and Non-DM control individuals.

As per the analysis, the CD41-61 level decreases progressively with the onset of DM with a pronounced change observed in the NPDR moderate to PDR stages. Studies have indicated that platelets show increased microparticle formation

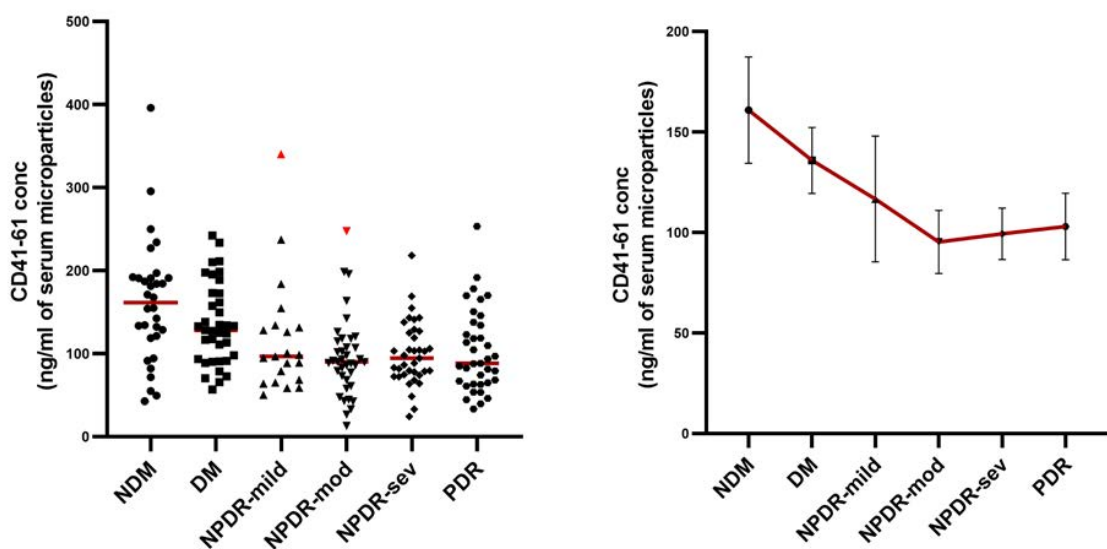


Figure 2.1. CD41-61 levels in serum microparticles in DM and DR patient. A, Microparticles isolated from serum were resuspended in RIPA buffer and CD41-61 was quantified by ELISA and every sample was assayed in triplicates. B, An interval plot showing the confidence interval for the mean of the data across the different categories along with the trend line.

in T2DM and DR conditions. A low level of platelet microparticle CD41-61 despite increased shedding of microparticles is suggestive of a lower expression of these glycoproteins on the platelet surface. As CD41-61 plays a role in thrombin formation, a decrease in this protein abundance could imply a decrease in the efficiency of thrombosis. A recent study has implicated that thrombosis in microaneurysms could be associated with reductions in leakage (Schreur et al., 2018). Therefore, it is important to examine whether decreased CD41-61 levels is correlated to DR progression. Interestingly, although there is a significant difference in CD41-61 in the NPDR-moderate group, a closer look reveals that the data are spread out. This variance within the group indicates that there are individuals who have high CD41-61 level and probably better clotting efficiency as against those with lower CD41-61 levels. To ascertain this, the DR progression in the study subjects would be monitored.

Fibronectin

Fibronectin (FN) is a high-molecular weight glycoprotein produced by endothelial cells, fibroblasts, and other mesenchymal cells. Plasma FN levels were shown to be significantly elevated in diabetic patients (Inoguchi et al., 1986). Yet another study has shown that there was no significant difference in fibronectin between the diabetic and control groups, as well as between the diabetic group with and without retinopathy (Lamberton et al., 1984). In the earlier discovery phase study on microparticles, an increase in the level of fibronectin was observed in NPDR-moderate individuals. Further, as this protein binds to activated platelets and participates in its aggregation, fibronectin was examined in the microparticles from 192 study subjects representing different stages of DM and DR. Comparison of the FN levels across different groups did not reveal any

significant difference between any combination of the sample groups (Figure 2.2).

Unlike the CD41-61 levels, fibronectin level was found to be highly variable within each group that could account for the lack of difference between the groups.

Alpha-2-macroglobulin

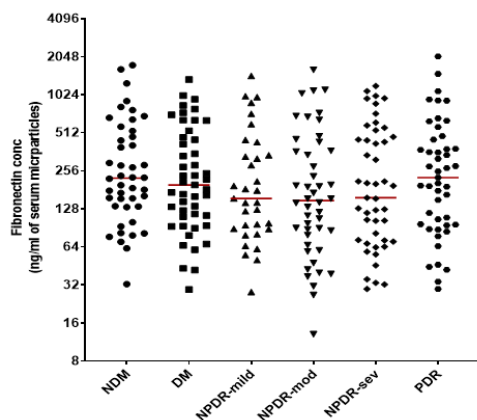
Alpha-2 macroglobulin (A2M) is a major plasma protease inhibitor that also regulates the activity of a variety of bioactive peptides including interleukins and exerts a range of immunomodulatory effects. A2M expression is increased in the eyes of patients diabetic retinopathy along with an enhanced activation of this protein (Sanchez et al., 2007). A2M has been identified in the microparticles and exosomes in plasma and serum. Owing to its multifunctional role, A2M level was analyzed in the microparticles from 148 study subjects across the DR spectrum.

Similar to fibronectin, no significant alteration in the A2M level was observed across the sample groups analyzed. This again could be due to the high variability observed within each group as evidenced by the statistics provided for the data.

The present validation of three markers resulted in the identification of one potential, candidate marker – CD41-61. The alteration in the level of CD41-61 in the microparticles is pronounced with the onset of DM and during progression to DR.

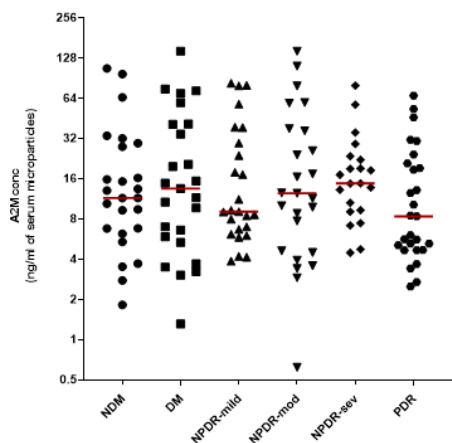
Ongoing work

Three additional microparticle proteins, von Willibrand factor, peroxiredoxin and vitronectin will be validated in the same samples that were used for analyzing CD41-61. Further, correlation studies to understand the variability observed in A2M and FN will also be carried out to identify the systemic factors influencing the level of these markers in individuals across the categories.



	NDM	DM	NPDR-mild	NPDR-mod	NPDR-sev	PDR
Minimum	32.53	29.41	28.18	13.04	0	29.77
Maximum	1755	1349	1443	1614	1203	2061
Mean	378.6	324.3	307.2	295.7	317.5	365.8
Std. Deviation	395.5	305.3	340.4	352.5	328.5	405.8
CV	104.5	94.13	110.8	119.2	103.5	110.9

Figure 2.2. Fibronectin levels in serum microparticles from DM and DR study subjects



	NDM	DM	NPDR-mild	NPDR-mod	NPDR-sev	PDR
Minimum	1.82	1.31	3.87	0.62	4.48	2.5
Maximum	107.4	144.2	83.18	144.4	79.82	67.24
Mean	22.26	27.75	23	28.37	20.54	15.7
Std. Deviation	27.82	33.83	25.61	36.52	18.15	16.83
CV	125.0	121.9	111.4	128.7	88.40	107.2

Figure 2.3. Alpha-2-macroglobulin levels in serum microparticles

References

- Inoguchi, T., Umeda, F., Watanabe, J., Wasada, T. & Ibayashi, H. (1986). Diabetes Res Clin Pract 2, 69-73.
- Lamberton, R. P., Goodman, A. D., Kassoff, A., Rubin, C. L., Treble, D. H., Saba, T. M., Merimee, T. J. & Dodds, W. J. (1984). Diabetes 33, 125-129.
- Sanchez, M. C., Luna, J. D., Barcelona, P. F., Gramajo, A. L., Juarez, P. C., Riera, C. M. & Chiabrand, G. A. (2007). Exp Eye Res 85, 644-650.
- Schreur, V., Domanian, A., Liefers, B., Venhuizen, F. G., Klevering, B. J., Hoyng, C. B., de Jong, E. K. & Theelen, T. (2018). Br J Ophthalmol.

Prospective Multicenter discovery and validation of diagnostic circulating and urinary biomarkers and development of sensor(s) to detect sight threatening diabetic retinopathy

Work package 3 : Biomarker and Biosensor study in UK and India

Funding : Research Councils UK

We have an ongoing multi-institutional Indo-UK Collaborative Project on diabetic retinopathy. We are involved in one of the work packages for biomarker validation in diabetic retinopathy patients with an emphasis on diabetic macular edema (DME). This work package 3 is carried out across three centres – AMRF (Madurai), Vision Research Foundation (Chennai) and University College London (London). This project involves validating 12 markers in type 2

diabetic and diabetic retinopathy patients (with and without diabetic macular edema) across the Indian and the UK population.

Sample category	INDIA		UK
	AMRF	VRF	UCL & Moorefields Eye Hospital
Non-diabetic individuals	25	25	50
Type 2 Diabetics	25	25	50
Non-proliferative diabetic retinopathy with DME	25	25	50
Proliferative diabetic retinopathy without DME	25	25	50
Proliferative diabetic retinopathy with DME	25	25	50
Total/country	250		250
Total for the study	500		

For the biomarker study in Indian population, samples were collected in AMRF and VRF and exchanged to reach the target number as indicated. And, each of the two centers quantified six markers in all the 250 samples from the Indian population. At UCL, quantification of 12 markers is currently ongoing in a sample size of 250 from the UK population.

At the end of the quantification of all 12 markers across 500 samples, statistical analysis will be performed to shortlist a subset of these markers for which biosensors will be developed at Sastra University. These biosensors will be useful to monitor the validated serum markers in the clinic and the field to help assess the risk of onset and progression of DR.

Research on Pterygium

Identification of druggable targets for attenuating the progression of pterygium development

Investigators : Dr. Daipayan Banerjee
Prof. K. Dharmalingam
Clinician Scientists: Dr. N. Venkatesh Prajna
Clinician : Dr. Gonugunta Vishnu Teja
Team Member : Aadithiya T Gr
Funding : Sun Pharmaceuticals

Background

Pterygium is a benign, chronic triangular overgrowth of fibrovascular conjunctiva growing mostly from the nasal side of the conjunctiva onto the cornea. It is a common condition globally with approximately 13% prevalence in Indian population that increases to about 25% in the elderly. Although benign, this abnormal growth protrudes towards the cornea, impairs vision and ultimately affects the quality of life. This lesion of the ocular surface can be compared to neoplastic-like disorder i.e., cancer as it involves cell proliferation, migration, angiogenesis, fibrosis, and extracellular matrix remodeling. In the absence of any pharmacological intervention, surgical removal of the pterygium outgrowth is the only definite treatment constituting the standard of care. Invasive surgical procedure, cost of surgery and high recurrence rate are deterrent factors that affects patient compliance. Upon confirmation, topical steroids and non-steroidal anti-inflammatory drugs (NSAIDs) are used to reduce inflammation. During surgery, mitomycin C (MMC) has been used as a fibroblast proliferation inhibitor to ameliorate the chance of recurrence of the pterygium. However, serious complications of mitomycin C includes necroptosis resulting in corneal edema, corneal perforation, and scleral calcification. 5-fluorouracil (5-Fu) used an anti-proliferative agent has high chances of recurrence. Anti-VEGF drug Bevacizumab had no significant effect on recurrence of primary pterygium excision. Thus, there is an urgent need to find a druggable target that can preclude the need for surgical intervention in pterygium treatment.

While pterygium has been strongly associated with ultraviolet light exposure and evidence implicates several divergent mechanisms like antiapoptotic factors, immunological, cytokines, growth factors, extracellular matrix (ECM) modulators, genetic factors, viral infection as possible causative, the etiology of this disease is still elusive.

Major Objectives

1. Comparative proteomics of pterygium tissue and the control tissue from the contralateral eye of the patients.
2. Transcriptomics analysis to identify altered mRNA transcripts in pterygium.
3. Evaluate the role of Pattern Recognition Receptor's (PRR) role in driving the pro-inflammatory status and contribution in the pathogenesis of pterygium.

Results

Profiling of pterygium conjunctiva tissue proteome

With the broad objective to identify pathways that might be activated and contribute to pterygium development and progression, we took a shotgun proteomic approach.

Method: To detect proteins that are differentially expressed in pterygium tissues in Indian population, we collected excised pterygium conjunctiva tissue sample from the patients undergoing pterygium removal surgery. Age-matched conjunctiva tissues were collected from cataract patients undergoing small incision cataract surgery (SICS). Owing to the age variation within pterygium patients, samples were divided into the following groups: young pterygium (<40 years old, male and female), old pterygium (>60 year's old, male and female), young cataract (<40 years old, male and female) and old cataract (>60 year's old, male and female). Total 30µg pooled protein sample from 3 patients were briefly fractionated on a 10% gel and visualized using colloidal coomassie blue. The entire gel band was excised, subjected to in-gel trypsin digestion and peptides were recovered and desalted as per established protocol. Tryptic digested peptides were analyzed by Orbitrap Velos Pro mass spectrometer (Thermo, USA). Proteins were identified using Proteome Discoverer software with Mascot algorithm

Group		# proteins ≥ 1 peptides	# proteins ≥ 2 peptides
Young Control	M	740	580
	F	752	541
Young Pterygium	M	805	605
	F	821	599
Old Control	M	739	533
	F	857	625
Old Pterygium	M	810	619
	F	676	506

by searching against a database containing the complete human proteome downloaded from the UniProt database. Bioinformatics analysis was performed using DAVID (Database for Annotation, Visualization and Integrated Discovery) to study the gene ontology including biological processes, cellular components and molecular function.

In the common proteins list between pterygium and cataract, 54 proteins were identified that exhibited at least two-fold increase and 73 were identified that showed at least two-fold decrease. Gene ontology analysis using DAVID revealed that in the up-regulated proteins, the biological processes that were altered in pterygium comprised of pathways related to platelet degranulation, response to reactive oxygen species, hydrogen peroxide catabolic process, cell-cell adhesion, complement activation, cellular iron ion homeostasis, acute-phase response and removal of superoxide radicals. Examining the functional relevance of the 314 unique pterygium proteins revealed that the major pathways comprised of platelet aggregation, extracellular matrix organization, integrin-mediated signaling pathway and platelet activation.

Group		# proteins ≥ 1 peptides	# proteins ≥ 2 peptides
Young	Control	1003	817
(M+F)	Pterygium	1148	944
Old	Control	1071	848
(M+F)	Pterygium	1063	870

Platelet activation leads to secretion of angiogenic factors (Kisucka et al, PNAS, 2006) and Reactive oxygen species (ROS) are generated within activated platelets (Qiao et al, Redox Biology, 2018). Further, integrin signaling is vital for pathological angiogenesis (Mahabeleshwar et al, JEM, 2006). These pathways can form a nexus to promote cell migration and pterygium progression.

Work in progress

Future study in this project will comprise of the following:

1. Identify pathways that are altered in young pterygium compared to old pterygium.
2. RNA sequencing to identify altered transcripts in pterygium.
3. Validate the pathways identified in the discovery phase.
4. Using cell culture approach, target the selected pathways by pharmacological inhibitors to halt pterygium progression.

Research on Keratoconus

Understanding the mechanism of action of a novel chemical cross-linker designed to treat keratoconus

Investigators : Dr.O.G.Ramprasad
 Prof. K. Dharmalingam,
 Dr. Venkatesh Prajna and
 Dr. Naveen Radhakrishnan
 Research fellow : Nasrin Banu T.M.
 Funding : ICMR

Introduction including background

Keratoconus is one of the major bilateral corneal dystrophies affecting the working or the young population in the age-group of 25-35 years. It is characterized by the thinning of the cornea followed by the formation of cone shaped central cornea leading to defective vision in the form of severe astigmatism. Decrease in the mechanical strength of the collagen fibrils in the cornea, significant loss of extracellular matrix, defective collagen cross-linking activity lead to keratoconus. The severity of the disease is classified on the basis of radius of curvature of anterior segment of the cornea. Accordingly, mild keratoconus has corneal curvature of 42-47Diopters, moderate keratoconus has a corneal curvature of 47-52D and severe keratoconus has a corneal curvature of >53D. Moderate and advanced forms of keratoconus need conventional corneal crosslinking treatment which serve to slow and, in some cases, halt the progression of the disease by increasing collagen fibril linkages within the cornea, thereby preventing extreme curvature. The conventional crosslinking protocol involves removal of the central corneal epithelium, application of riboflavin and the illumination of the affected eye with UV-A light (370 nm, 3 mW/cm²) for 30 minutes. Removal of epithelium is painful and there is a risk of infection in the form of keratitis.

Our collaborators at the University of Liverpool, UK have developed a novel, PBS soluble chemical cross-linker consisting of EDCI/NHS [1-Ethyl-3-(3-dimethylaminopropyl)carbodiimide/N-hydroxy-succinimide] mediated chemistry and a suberic acid spacer that has the potential to be developed as eye drops. It can cause corneal cross-linking without removing the corneal epithelium, or the use of UV-A irradiation, therefore avoiding the pain associated with the conventional crosslinking treatment of keratoconus and the risk of infection. We, at Aravind Medical Research Foundation and Aurolab have established the proof-of concept in human corneas, wherein treatment of the diseased keratoconus

cornea for 15 minutes at 37°C with the novel chemical cross-linker is able to increase the stiffness of the weak keratoconus cornea by cross-linking collagen molecules. The cross-linker also does not cause cytotoxicity or morphological changes to the corneal cell layers. The details about the investigation are available in the previous progress reports. The mechanism of action of the cross-linker in stiffening the cornea is not clearly understood. By unravelling the mechanism of action of the novel chemical cross-linker solution, this present study will aid in the further development and or refinement of optimal formulation of the cross-linker for further clinical trials.

Results

A preliminary study was conducted on the effect of the cross-linker on human corneal epithelial cell line (HCE) on the regulation of select transcripts. The analysis was done on HCE cells in-lieu of cadaver and keratoconus corneas. Keratoconus is now characterized as an inflammatory disorder. The differential gene expression between the cone and periphery of the keratoconus cornea has been reported (Pahuja et al., 2016). Since corneal epithelium displayed differential expression of a distinct set of inflammatory cytokines in keratoconus, we wanted to analyse the effect of cross-linker on the expression of inflammatory cytokines IL-6, MMP-9, Col1A1 in HCE cells.

Analysis of the effect of Tumour Necrosis Factor- α (TNF- α) in HCE cells

The induction of inflammatory conditions in HCE cells in-vitro was achieved by treating the cells with TNF- α in a range of concentrations from 200 pg/ml of culture medium to 100 ng/ml of culture medium. ZO-1 (tight junction protein) expression is known to be affected with increasing amounts of TNF- α concentrations. Maintenance of tight junctions in epithelium is done by ZO-1. The expression of ZO-1 in HCE cells was visualized by immunostaining and confocal microscopy and the results are represented for 10 ng/ml and 100 ng/ml TNF- α concentrations in Figure 1.

ZO-1 expression was high and similar to control cells when HCE cells were treated with 10ng/ml TNF- α or lower. A concentration of 100 ng/ml of TNF- α decreased the ZO-1 expression and disrupted the tight junctions. Hence, concentration of TNF- α at 10 ng/ml or below were used to assess the expression of inflammatory cytokines in HCE cells in further experiments. mRNA expression of TNF- α also increased with the increasing concentrations of TNF- α (Fig.2a, bottom panel).

Changes in the expression of transcripts and the effect of cross-linker

HCE cells were treated with TNF- α at different concentrations and the induction of inflammatory cytokines IL-6, MMP-9 and the matrix gene Col1A1

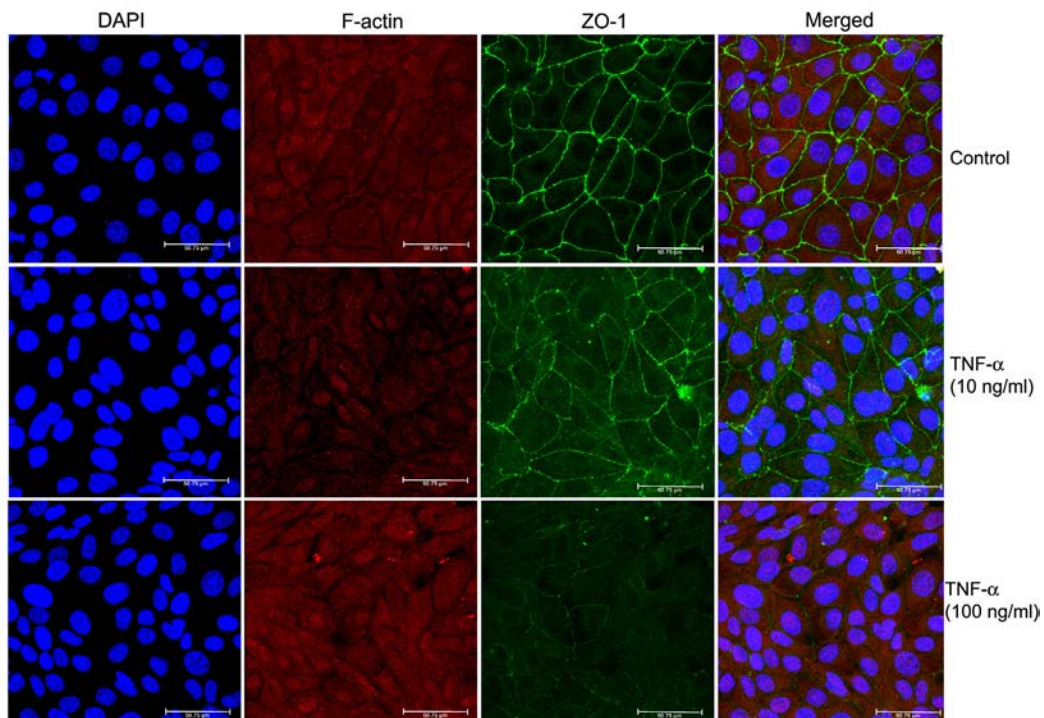


Figure 1: Effect of TNF- α on ZO-1 expression in HCE cells

were assessed by PCR. RNA from the control and treated cells was isolated at 6 hr time-point and reverse transcribed for PCR. GAPDH was used as an internal control for normalization of gene expression. IL-6 expression increased marginally with increasing concentrations of TNF- α . While the expression of MMP-9 increased until 10ng/ml TNF- α treatment when compared to the control, Col1A1 expression decreased with increasing concentrations of TNF- α (Fig. 2A and Fig.3). The changes in expression of transcripts were similar to those reported earlier for epithelial layer of keratoconus corneas (Shetty et al., 2015).

The concentration of cross-linker required for treatment of the HCE cells was optimized. Accordingly, 1/64th diluted cross-linker had more than 80% of the HCE cells viable while 1/32 dilution had around only 30% of the cells viable. TNF- α treated HCE cells were treated with the above two dilutions of the cross-linker and the changes in relative expression of mRNA levels were analysed (Fig. 2B and Fig.3). Accordingly, after treatment with the cross-linker (1/64 dilution), the expression of IL-6 and MMP-9 went up by more than 1.5-folds while the expression of Col1A1 decreased further when compared to the TNF- α induction (circled bars in Fig.3). Similar changes in gene expression were achieved by real-time PCR analysis before and after cross-linker treatment.

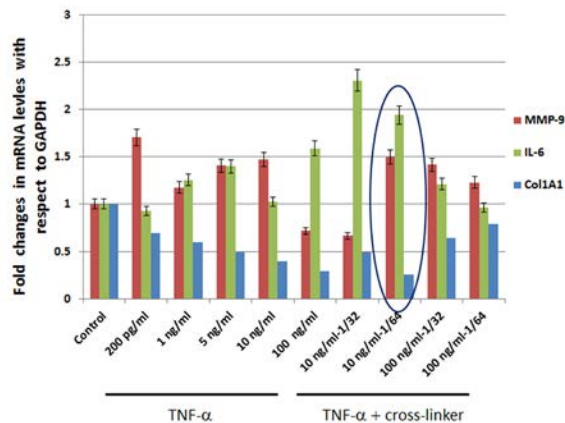
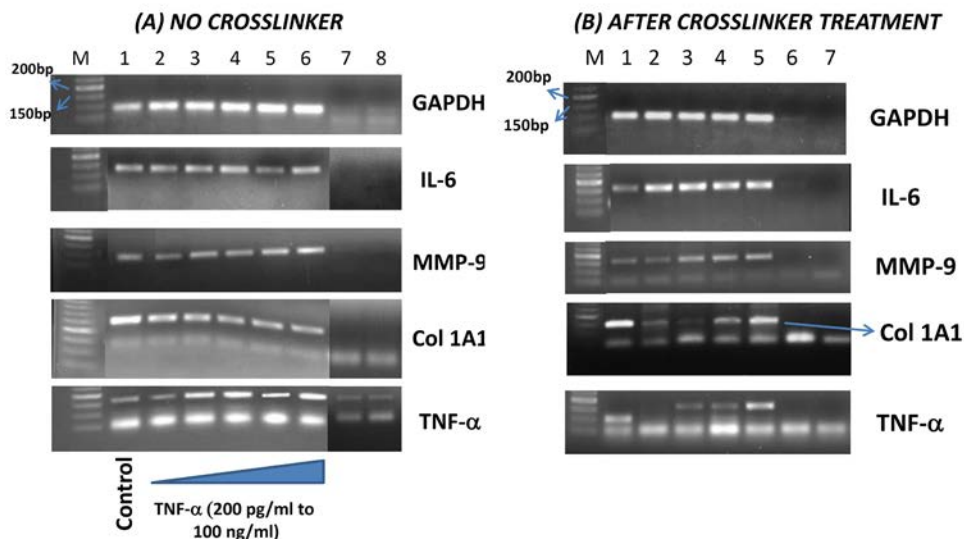


Figure 3: Quantitative levels of transcripts in HCE cells before and after cross-linker treatment

Conclusions

HCE cells could be stimulated in-vitro using TNF- α to induce changes in the expression of IL-6, MMP-9 and Col1A1 transcripts. This was similar to the changes observed during inflammatory conditions of keratoconus. While IL-6 and MMP-9 expression went up as a result of inflammation, Col1A1 expression decreased after TNF- α treatment. The gene expression of Col1A1, which is a major component of basement membrane in the epithelium went down during inflammation, suggesting that inflammation



Lane 1: Control ; Lane 2: 200 pg/ml; Lane 3: 1 ng/ml; Lane 4: 5 ng/ml
Lane 5: 10 ng/ml; Lane 6: 100 ng/ml; Lane 7: No RT; Lane 8: NTC

Lane 1: Control; Lane 2: 10 ng/ml+1/32 CXL;
Lane 3: 10 ng/ml+1/64 CXL; Lane 4: 100 ng/ml+1/32 CXL; Lane 5: 100 ng/ml+1/64 CXL; Lane 6: NoRT; Lane 7: NTC

Figure 2: Expression of transcripts in HCE cells before and after cross-linker treatment

Legend: CXL represents cross-linker solution at the indicated dilutions. (B) Cross-linker treatment is given after TNF- α induction at different concentrations. NoRT- No reverse transcriptase, NTC-No template control.

has an effect on this matrix gene. After cross-linker treatment, the gene expression of pro-inflammatory cytokines went up further, while the expression of Col1A1 further decreased. The cross-linker is further adding up the inflammatory response. Further experiments to analyse the activity of matrix-metalloproteases are being carried out.

References

- Pahuja N, Kumar NR, Shroff R, et al. Differential molecular expression of extracellular matrix and inflammatory genes at the corneal cone apex drives focal weakening in keratoconus. *Invest Ophthalmol Vis Sci* 2016;57:5372–5382.
- Shetty R, Ghosh A, Lim RR, Subramani M, et al. Elevated expression of matrix metalloproteinase-9 and inflammatory cytokines in keratoconus patients is inhibited by cyclosporine A. *Invest Ophthalmol Vis Sci* 2015; 56:738-750

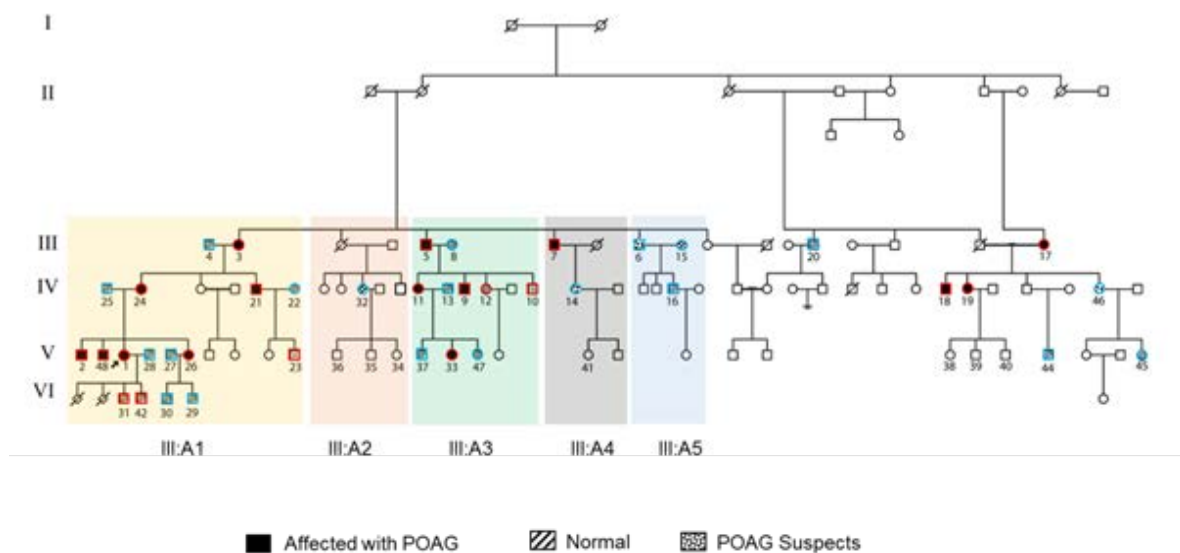
Screening the Kadaladi family with early onset Glaucoma for Myocilin gene mutations

Investigators : Prof. K. Dharmalingam (PI)
 Dr. S.R. Krishnadas
 Dr. Mohideen Abdul Kader
 Dr. D. Bharanidharan
 Technician : V. Saravanan
 Funding : Sun Pharma

Background

Glaucoma is a heterogenous group of ocular hypertensive diseases with a characteristic optic neuropathy and visual field loss, often associated with elevated intraocular pressure (IOP). Primary open angle glaucoma (POAG) is the most common type of glaucoma (Weinreb and Khaw, 2004; Leske, 2007) and leading cause of blindness in world. A recent meta analysis of POAG shows that the prevalence of 3.22% and an incidence of 0.38%. Juvenile onset open angle glaucoma (JOAG), is a form of primary open angle glaucoma, which affects even children as early as three years of age (Johnson et al., 1993; Dickens and Hoskins, 1996). It is relatively uncommon with a prevalence of 0.4 to 4% among glaucoma patients (Goldwyn and Waltman, 1970; Das and Bhomaj, 2001; Fung et al., 2013; Kwun et al., 2016). Many studies show JOAG is a monogenic disorder and myocilin mutations is the major cause of hereditary JOAG (Stone et al., 1997; Wiggs et al., 1998). MYOC mutations are associated with 2% to 4% of adult-onset POAG (Fingert 201), while 10% in juvenile-onset open angle glaucoma (JAOG) (Wang et al 2019). Unlike adult-onset POAG, JOAG patients with myocilin mutations reported to have high intraocular pressure (IOP), severe optic nerve damage and earlier age at onset (usually <40 years), which, if left untreated, results in severe visual impairment (Gupta et al., 2018). Thus, screening of MYOC mutations among JOAG patients is helpful in detecting the disease early in the family members. In this study, we aim to screen Myocilin Gene mutations

Figure 1. The pedigree chart of six generations of a Kadaladi family with glaucoma.



Colored boxes represents the four generations of families. Red outline are positive and Blue outline are negative for a heterozygous MYOC gene mutation at c.1440C>G (p.Asn480Lys).

in a large family from Kadaladi, Tamil Nadu since the proband age is 26 with high IOP and has the family history. Furthermore, many of family members are affected with similar clinical features. The clear family history and high IOP cases in the family indicates that MYOC gene mutations could have been involved in the pathogenesis [Wang et al 2019].

Results and Conclusions

40 members of the family were enrolled in this study who are related to the proband (Figure 1). Among the 40 individuals, 15 were clinically diagnosed with POAG and five were glaucoma suspects. Myoc mutation c.1440C>G in exon 3 was found in 20 members of this family. Among the carriers of this mutation 15 were glaucoma patients and two were glaucoma suspects and three were normal. The youngest with the confirmed glaucomatous condition was 10 years of age. Among the 18 carriers who were 10 years and above 17 are having the disease and this makes the penetrance of this mutation 94 % among the people above 10 years of age. The two normal individuals who carry the mutation were 1

and 4-year-old. The likelihood of these two children developing JOAG is very high. Only one carrier who is above 10 years of age and did not develop glaucoma was 25-year-old. These are the most interesting cases and need further study. We found three members (aged 50 yrs, (No.6 in the figure 2), 29 yrs (No. 14) and 38 yrs (No. 46). diagnosed with POAG suspects, did not carry any mutation in exon 3. However, we cannot rule out other mutations elsewhere in the myocilin gene. We notice in this study two patients with POAG suspects carrying myocilin gene mutation. The penetrance of the Asn480Lys mutation in this population is comparable to other reported values.

Conclusion

The genetic analysis shows that Asn480Lys MYOC mutation plays an important role in the management of autosomal dominant disease in the kadaladi family. The identification of mutation in young children will allow early treatment to prevent further progression of the disease.

OCULAR PHARMACOLOGY

Elevated intraocular pressure (IOP) is a major causative risk factor for the development and progression of most forms of glaucoma. Glucocorticoid (GC) induced ocular hypertension (GC-OHT) and glaucoma (GCG) are the secondary glaucoma associated with the long-term use of GC for the management of inflammatory eye diseases. Though the major form of glaucoma i.e. primary open angle glaucoma (POAG) shares clinical similarities with GC glaucoma, the molecular mechanism responsible for the disease pathogenesis is poorly understood.

The current glaucoma treatment attempts to lower the elevated IOP with anti-glaucoma medications and laser treatment. However, there is no specific treatment option available till date that could target the pathogenic mechanisms responsible for GC response. Therefore, the major research focus of our department is to investigate the molecular mechanisms responsible for GC induced OHT and glaucoma and to identify a newer molecular targets which specifically influence their molecular pathogenesis.

Role of microRNA in regulating glucocorticoid receptor signaling in steroid-induced ocular hypertension/glaucoma

- Investigator : Dr. S. Senthilkumari,
Department of Ocular Pharmacology,
- Co-Investigators : Dr. C. Gowripriya, Department of Immunology & Stem Cell Biology
Dr. D. Bharanidharan
Department of Bio-informatics
Dr. R. Sharmila, Glaucoma Clinic, Aravind Eye Hospital
- International Collaborator : Prof. Colin Willoughby, Faculty of Life & Health Sciences, University of Ulster, Northern Ireland, UK
- Mentors : Prof. VR. Muthukkaruppan, Research-Advisor, Department of Immunology and Stem Cell Biology
Dr. SR. Krishnadas, Glaucoma Clinic, Aravind Eye Hospital
Prof. K. Dharmalingam, Research-Director, Department of Proteomics
- Research Associate: Dr. R. Haribalaganesh
Junior Research Fellow: K. Karthivel
- Funding Agency : DBT/ Wellcome Trust India Alliance (Intermediate Fellowship (2017-2022))



Introduction

Glucocorticoid induced OHT and glaucoma are the serious side effects associated with the long term use of glucocorticoid therapy. GC-OHT occur in 40% of the susceptible individuals (GC responders) and those are not susceptible are GC non-responders (60%). Normal individuals with GC responsiveness are likely to develop a major form of glaucoma i.e. primary open angle glaucoma (POAG). More than 90% of the patients with POAG are GC responders which further aggravate their clinical symptoms leading to vision loss. The molecular mechanism responsible for the differential GC responsiveness is not clearly understood.

In this study, the role of microRNA (a small non-coding RNA which regulate the transcription of genes) in GC-induced ocular hypertension / glaucoma was investigated and identified a number of dys-regulated miRNA-mRNA pairs in cultured

human trabecular meshwork (HTM) cells with known GC responsiveness. It is believed that the identified dysregulated miRNA-mRNA pairs may have a crucial role in mediating differential GC responsiveness in humans. Further, these pairs can have the potential of developing them as a surrogate marker to determine GC responsiveness prior to treatment and also miRNA based therapeutics are of some potential use in the management of GC-OHT /glaucoma.

For this purpose, the primary HTM cells with known GC responsiveness was established using Human Organ Cultured Anterior Segment (HOCAS). In a paired eye, one eye was used to establish HOCAS system to characterize GC responsiveness after DEX treatment and the other eye was used to establish primary HTM cultures from eyes with identified responsiveness. Confluent cultures of DEX-responder and DEX non-responder HTM cells strains were then treated with either 100nM

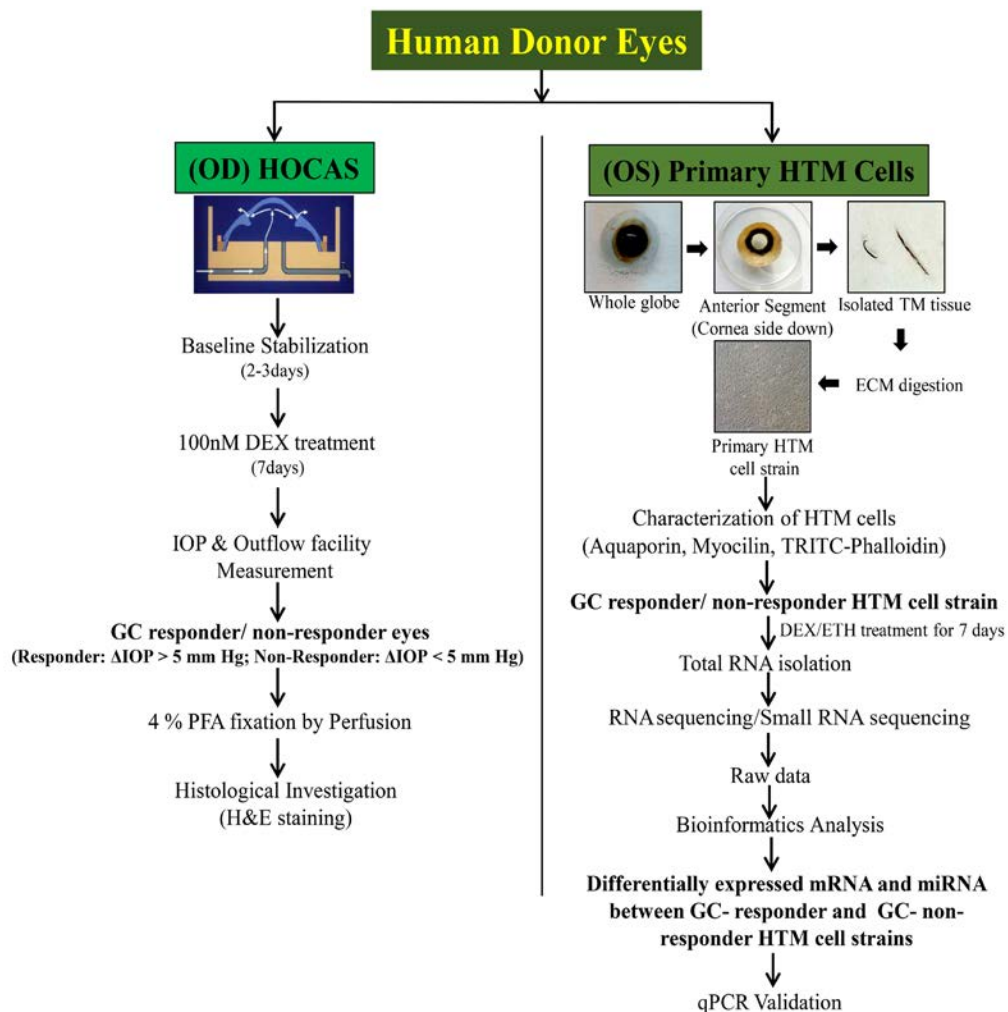


Figure : 1 Schematic representation showing work flow for this study

DEX or 0.1% ethanol (ETH) as a vehicle control for 7 days and subjected for RNA Sequencing. The detailed work plan is given in the following schematic representation (Figure 1).

Results

A. Genome-wide Transcriptome Analysis of Primary HTM cells with Known GC Responsiveness

A total of 16 paired eyes were used for this study with the mean (\pm) SD age of 62.38 ± 12.82 years. The mean (\pm) SD elapsed time between death and enucleation was 2.75 ± 1.58 h and the mean elapsed time between enucleation and culture was 38.44 ± 18.39 h.

In HOCAS, DEX treatment caused an elevated IOP in 7/16 eyes (43.75%) (Mean $\Delta(\pm$ SEM) IOP: GC responder eyes: 13.8 ± 3.4 mmHg and GC-non-responder eyes: 0.91 ± 0.4 mmHg) (Figure 2).

Based on the IOP response, the HTM cell strain was categorized as GC-responder and non-responder cell strains and characterized with aquaporin, myocilin and TRIC-Phalloidin (Figure 3).

Confluent cultured HTM cells were treated with 100nM DEX for 7 days and subjected for RNA Sequencing. The pre-processed high-quality reads were mapped with human reference genome using HISAT2. An average, 85.6 percentage of mRNA reads were aligned with reference genome from all cell strains used in the present study.

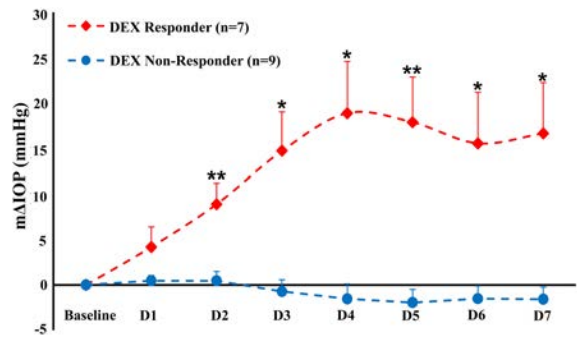


Figure 2: IOP graph of the anterior segment after treatment with 100nM DEX treatment. Out of 16 eyes treated, 7 eyes showed elevated IOP over the period of treatment. * $p < 0.05$; ** $p < 0.001$; Un-paired t-test.

The total number of genes identified in each strain ranged from 14,515 to 17,371. In total, 1622 (163 up-regulated; 462 down-regulated), 1082 (156 up-regulated; 542 down-regulated) and 556 (170 up-regulated; 107 down-regulated) genes were identified as significantly dysregulated in Group #1 (DEGs comparison between ETH and DEX-treated cell strains); Group #2 and #3 (DEGs comparison between ETH and DEX treated GC responder and GC non-responder cell strains) respectively. The expression of dysregulated genes from Group #1, Group #2 and Group #3 are represented in volcano plot (Figure 4).

In Group #2, SAA4 (FC: 4.75), FRG2C (5.27) and NTRK2 (3.39) were significantly up-regulated and UPK3A (-8.48), RLN1 (-8.01) were down-

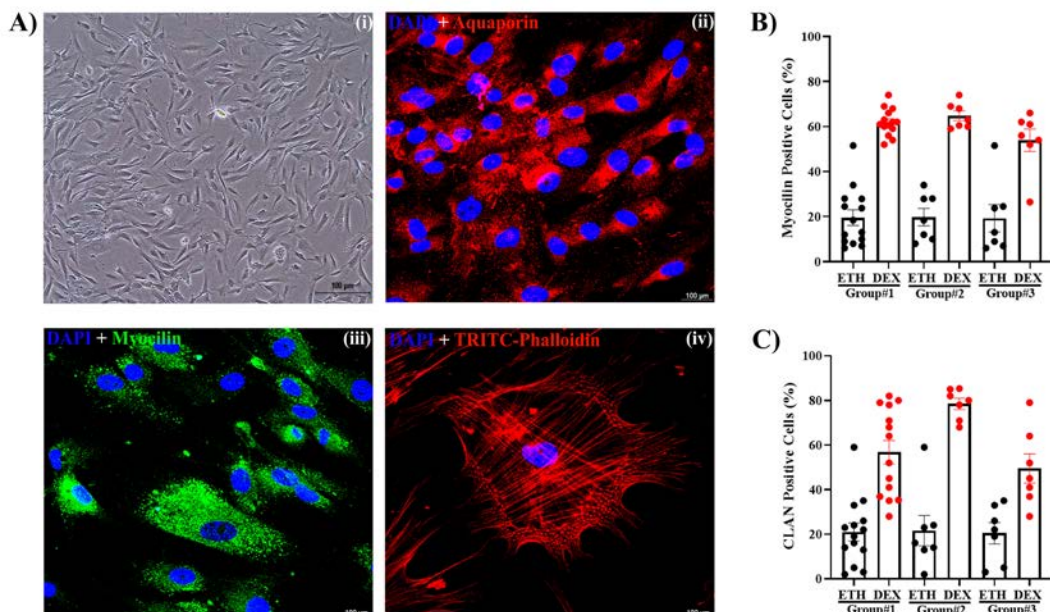


Figure 3. Characterization of primary HTM Cells. (a) (i) Representative phase-contrast image of HTM cells; (ii) Representative confocal image of HTM cells probed with aquaporin; (iii) myocilin and (iv) TRITC-Phalloidin after DEX treatment. Graph showing the percentage of (b) myocilin positive and (c) Cross Linked Actin Network (CLAN) positive cells in DEX and ETH treated primary HTM cells. Blue: DAPI; Green: Myocilin; Red: Aquaporin & TRITC Phalloidin

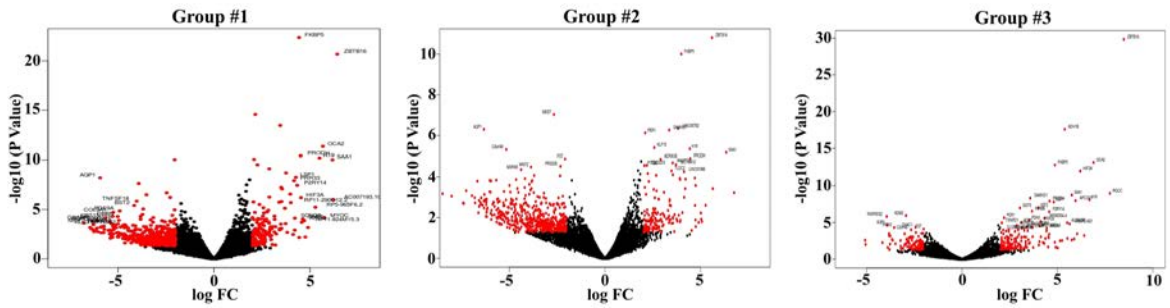


Figure 4. Volcano plot of Differentially Expressed Genes (DEGs). (a) The fold of change (\log_2) and p value ($-\log_{10}$) of the genes in group #1; (b) group #2 and (c) group #3 was shown in the plot. Note: Group #1: DEGs comparison between ETH and DEX- treated cell strains; Group #2 and #3: DEGs comparison between ETH and DEX treated GC responder and GC non-responder cell strains.

regulated. Similarly, in Group #3 (GC non-Responder group), FAM107A (4.44), STEAP4 (4.58), STOX1 (3.11) were significantly up-regulated and GRM5 (-5.03), SLC24A2 (-3.86) were down-regulated. The overlapping genes between GC-R and GC-NR

(Group #1) were SAA1, ZBTB16, FKBP5 and MYOC (up-regulated) and AQP1, LAMP3 (down-regulated). In total, 518, 205 and 96 genes were identified as uniquely expressed in Group #1, Group #2 and Group #3, respectively.

Table 1. List of Enriched Pathways for DEGs

Enriched Pathways	Group #1		Group #2		Group #3	
	NES	P value	NES	P value	NES	P value
Axon guidance	-1.4	0.104	-	-	-1.98	0.012
B Cell Receptor Signaling pathway	1.23	0.242	-0.97	0.491	-	-
Cell Adhesion Molecules Cams	-1.57	0.067	-1.29	0.188	-1.25	0.207
Chemokine Signaling Pathway	1.71	0.02	0.77	0.733	-	-
Cytokine Cytokine Receptor Interaction	-1.05	0.355	0.62	0.905	0.9	0.579
Drug Metabolism Cytochrome P450	2.15	0	1.98	0.007	1.69	0.021
ECM Receptor Interaction	-0.65	0.878	0.85	0.667	-	-
Insulin Signaling Pathway	1.21	0.28	1.04	0.39	-	-
JAK STAT Signaling Pathway	1.22	0.252	1.04	0.39	-	-
MAPK Signaling Pathway	0.86	0.617	1.25	0.22	1.3	0.161
Natural Killer Cell Mediated Cytotoxicity	1.53	0.07	0.86	0.611	-	-
P53 Signaling Pathway	-1.13	0.299	-1.71	0.002	-	-
Pathways in Cancer	1.09	0.373	-0.98	0.462	1.56	0.027
Regulation of Actin Cytoskeleton	1.08	0.375	1	0.424	0.86	0.668
T Cell Receptor Signaling Pathway	1.06	0.406	-1.03	0.439	-	-
TGF Beta Signaling Pathway	-1.77	0.01	-1.25	0.175	0.93	0.574
Tight Junction	-0.64	0.887	-1.41	0.105	-1.56	0.043
Vascular Smooth Muscle Contraction	1.19	0.271	0.88	0.597	0.82	0.681
VEGF Signaling Pathway	0.85	0.626	-1	0.448	-	-
WNT Signaling Pathway	-1.45	0.086	-0.73	0.818	-0.98	0.49
Apoptosis	-0.9	0.614	-	-	-	-
GAP Junction	-0.58	0.964	-	-	-	-
NOTCH Signaling Pathway	0.84	0.695	-	-	-	-
Taurine and Hypotaurine Metabolism	0.8	0.741	-	-	-	-
Toll like Receptor Signaling Pathway	0.93	0.54	-	-	-	-

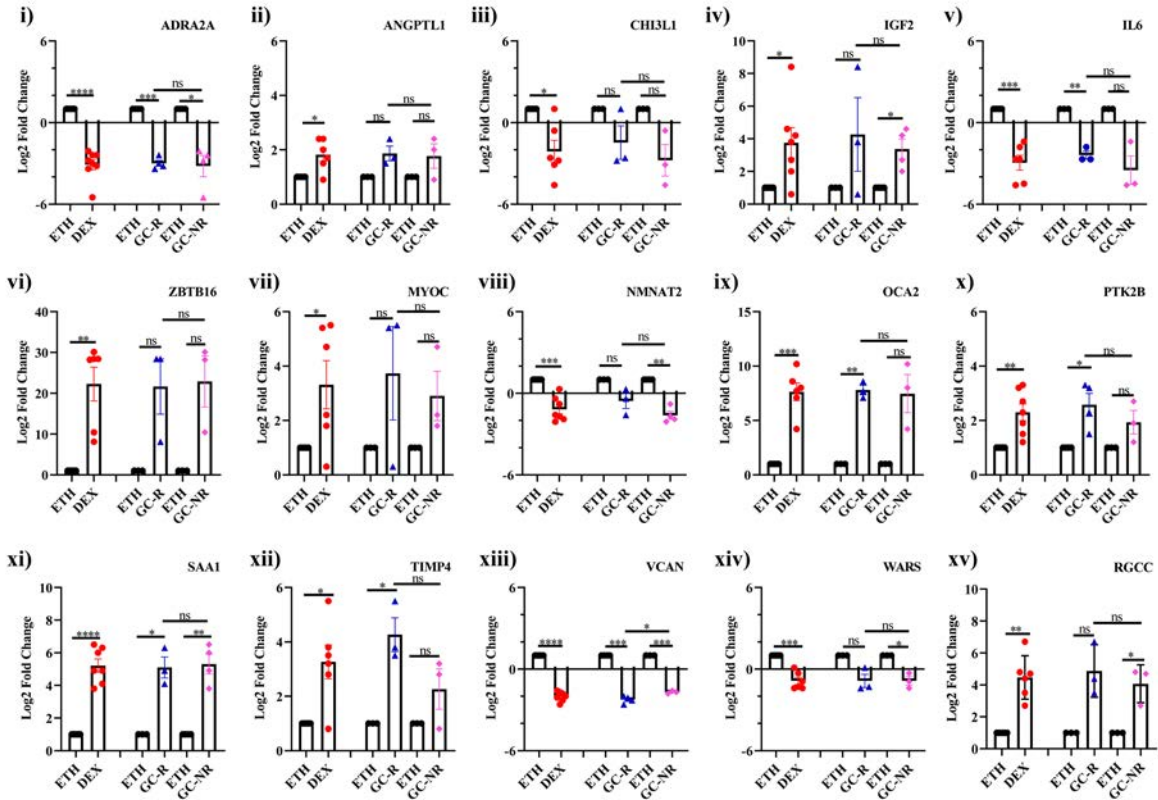


Figure 5A. qPCR validation of RNA Sequencing.
n = GC-R: 3-4; GC-NR: 3-4. **p* < 0.05; ***p* < 0.001; ****p* < 0.0001; *****p* < 0.00001; paired - *t* - test.

Pathway analysis for the DEGs resulted 109, 29 and 87 significantly altered pathways in Group #1, Group #2 and Group #3, respectively. The results of pathway analysis enriched in each group are represented in Table 1.

WNT signaling, MAPK signaling, TGF beta signaling, drug metabolism cytochrome, cell adhesion, pathways in cancer pathways were commonly enriched in all three groups. VEGF signaling, T cell receptor signaling, P53 signaling, Natural Killer (NK) cell mediated cytotoxicity, extracellular matrix (ECM) receptor interaction, chemokine signaling and B cell receptor signaling pathways were enriched in both Group #1 and Group #2. Interestingly, apoptosis, gap junction and notch signaling pathways were enriched only in Group #1, which indicates that these pathways might be an effect of dexamethasone induction.

Validation of DE genes by RT2-PCR Array

We used RT2-PCR array to validate the expression of 41 dysregulated genes selected from all three groups that were identified by RNA sequencing. Since, GAPDH and B2M showed significant changes

to treatment in at least one strain from each group and hence, ACTB was used as a referenced control (Figure 5A).

Out of 41 genes, the expression pattern of 15 genes matched with RNA sequencing data, which further confirming the reliability of these two techniques (Figure 5B).

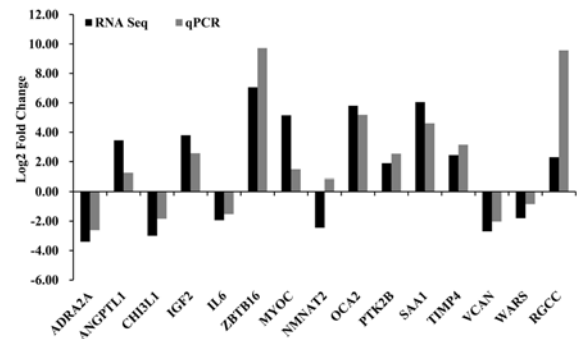


Figure 5B. Validation of RNA sequencing findings by qPCR.
 Values of Log₂ (Fold of change) : >0: up-regulation; = 0 non change; <0 down-regulation. *n* = 3-4.

B. Profiling of MicroRNAs in GC- Responder and GC-Non-responder primary HTM cells

In this study, the profiling of miRNAs in primary HTM cells with known GC responsiveness was carried out to identify the dys-regulated miRNAs which could dictate the differential response to DEX treatment in HOCAS-characterized GC-responsive and non-responsive HTM cells.

Cultured HTM cell strain with known GC responsiveness were treated with either 0.1%ETH (vehicle control) or 100nM DEX for 7 days. Total RNA was isolated by the TRIzol method. RNA quality and quantity were assessed by using Tape Station (Agilent) and Qubit 3.0, respectively. Additionally, the quality of RNA was observed by ratio of 28S and 18S ribosomal bands on 0.8 % agarose gel electrophoresis. The samples with RIN value more than 7 was used for small RNA sequencing.

In total, 9.1 to 17.2 million reads were generated from miRNA sequencing. Pre-aligned QC reports showed the quality score (phred score) of miRNA reads were ≥ 30 . An average of 97.2% reads from miRNA-seq data were aligned with human reference genome GRCh38. TMM normalization and EdgeR were employed for differential expression analysis.

Differentially expressed miRNAs between GC-Responder and GC-non-responder HTM cells:

An average, 808 miRNAs were identified from all samples with read count more than 9. In group #1, 26 dysregulated (21, up-regulated; 5, down-regulated) were identified. In group #2, out of 13 significantly dysregulated miRNAs, 5 were down-regulated and 7 were up-regulated with absolute fold of change (\log_2) of >1.5 whereas in group #3, 21 miRNAs were dysregulated in DEX treated cells compared to control and out 21 miRNAs, 15 were down-regulated

and 4 were up-regulated with absolute fold change (\log_2) of >1.5 (Figure 6).

The miRNAs, hsa-miR-483-5p, hsa-miR-483-3p, hsa-miR-675-5p, hsa-miR-675-3p, has-miR-5690, hsa-miR-6842-3p and hsa-miR-335-3p were identified as common miRNAs for all 3 groups with similar expression levels. Interestingly, hsa-miR-6512-5p (FC=2.7), hsa-miR-10396b-5p (FC=2.3), hsa-miR-1249-5p (FC=2.3), hsa-miR-10396a-5p (FC=2.2), hsa-miR-4488 (FC=1.6) were found to be up-regulated in group #1 whereas hsa-miR-10396b-5p (FC=2.7) and hsa-miR-10396a-5p (FC=2.6) were found to be up-regulated in group #3 only (Table 2).

Validation of DE miRNAs by qPCR

The expression of highly dysregulated miRNAs (n=9) from all three groups were further validated by qPCR. RNU6 served as a reference control. Out of 9 miRNAs, the has-miRNA 6842-3p and 5p were undetermined and in the remaining miRNAs, the DEX induced changes was observed only in 5 miRNAs and matched with miRNA-seq data (Figure 7A & 7B).

The hsa-miR-483-3p expression was found to be up-regulated in HTM cells after being treated with DEX. The previous study by Shen et al., 2015, showed the increased expression of hsa-miR-483-3p has an inhibitory effect on ECM production in HTMCs through down-regulating Smad4. Up-regulation of hsa-miR-335-5p reported with inhibition of TGF-B1-induced epithelial-mesenchymal transition in non-small cell lung cancer via ROCK1 (Wenwen et al., 2019). Interestingly, the up-regulation of hsa-miR-335-5p and TGF-B pathway down-regulation was observed in this present study. Further studies are underway to manipulate the validated miRNAs in HTM cells and the successful miRNA mimics/ inhibitors will be further evaluated in SI-OHT ex vivo model.

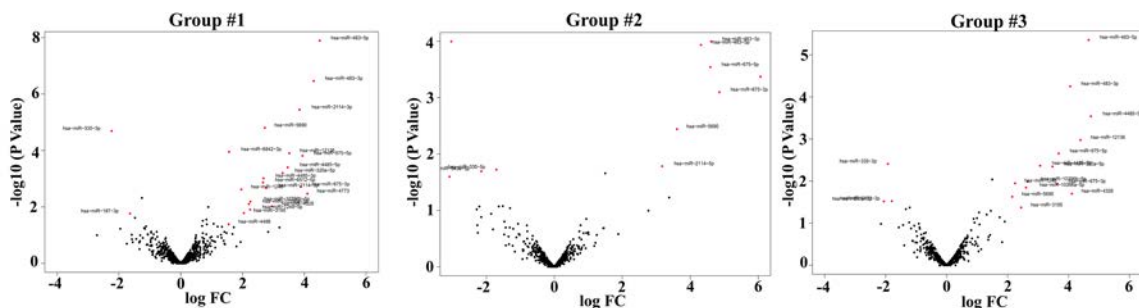


Figure 6. Volcano plot showing Group-wise Analysis of differentially expressed miRNAs. The fold of change (\log_2) and p-value ($-\log_{10}$) of the dysregulated genes in DEX treated cells as compared to vehicle control are shown in volcano plot. P value <0.05 was considered statistically significant (red color). Note: Group #1: DEGs comparison between ETH and DEX- treated cell strains; Group #2 and #3: DEGs comparison between ETH and DEX treated GC responder and GC non-responder cell strains.

Table 2: The list of DE miRNAs

Group	miRNA	Up-regulated			miRNA	Down-regulated		
		logFC	logCPM	p-value		logFC	logCPM	p-value
#1	hsa-miR-483-5p	4.5	1.02	0	hsa-miR-4645-3p	-1.1	-0.62	0.05
	hsa-miR-483-3p	4.3	3.13	0	hsa-miR-335-5p	-1.3	6.64	0
	hsa-miR-4773	4.1	-1.93	0	hsa-miR-6758-3p	-1.5	-1.17	0.02
	hsa-miR-675-5p	3.9	2.45	0	hsa-miR-187-3p	-1.6	0.2	0.02
	hsa-miR-675-3p	3.9	1.82	0	hsa-miR-335-3p	-2.2	8.49	0
	hsa-miR-2114-3p	3.9	-1.07	0				
	hsa-miR-12136	3.5	6.57	0				
	hsa-miR-4485-5p	3.5	0.3	0				
	hsa-miR-320a-5p	3.3	1	0				
	hsa-miR-4328	3.0	-0.94	0.01				
	hsa-miR-2114-5p	2.8	-1.05	0				
	hsa-miR-5690	2.7	-1	0				
	hsa-miR-4485-3p	2.7	2.84	0				
	hsa-miR-6512-5p	2.7	-1.09	0				
	hsa-miR-10396b-5p	2.3	-1.22	0.01				
	hsa-miR-1249-5p	2.3	-1.57	0.01				
	hsa-miR-10396a-5p	2.2	-1.24	0.01				
	hsa-miR-3195	2.0	-1.13	0.02				
	hsa-miR-1246	2.0	0.46	0				
	hsa-miR-6842-3p	1.6	1.77	0				
hsa-miR-4488	1.6	0.15	0.04					
#2	hsa-miR-2114-3p	6.1	-1.2	0.0	hsa-miR-335-5p	-1.7	6.8	0.0
	hsa-miR-675-3p	4.9	0.1	0.0	hsa-miR-549a-5p	-2.1	0.9	0.0
	hsa-miR-483-3p	4.6	2.9	0.0	hsa-miR-335-3p	-3.0	8.4	0.0
	hsa-miR-675-5p	4.6	1.2	0.0	hsa-miR-7151-3p	-3.1	-0.3	0.0
	hsa-miR-483-5p	4.3	0.8	0.0	hsa-miR-124-3p	-6.2	-0.8	0.0
	hsa-miR-5690	3.6	-1.3	0.0				
	hsa-miR-2114-5p	3.2	-0.8	0.0				
	hsa-miR-6842-3p	1.5	1.3	0.0				
#3	hsa-miR-4485-5p	4.7	1.0	0.0	hsa-miR-181b-2-3p	-1.2	0.8	0.0
	hsa-miR-483-5p	4.7	1.2	0.0	hsa-miR-486-3p	-1.3	2.4	0.0
	hsa-miR-12136	4.4	7.3	0.0	hsa-miR-6853-3p	-1.8	-0.7	0.0
	hsa-miR-4328	4.1	-0.4	0.0	hsa-miR-335-3p	-1.9	8.6	0.0
	hsa-miR-483-3p	4.0	3.4	0.0	hsa-miR-550a-3p	-2.1	-0.1	0.0
	hsa-miR-675-5p	3.7	3.1	0.0	hsa-miR-9-3p	-4.9	-1.3	0.0
	hsa-miR-675-3p	3.6	2.6	0.0				
	hsa-miR-320a-5p	3.5	1.8	0.0				
	hsa-miR-4485-3p	3.1	3.6	0.0				
	hsa-miR-10396b-5p	2.7	-0.7	0.0				
	hsa-miR-10396a-5p	2.6	-0.7	0.0				
	hsa-miR-3195	2.4	-0.7	0.0				
	hsa-miR-1246	2.2	1.0	0.0				
	hsa-miR-5690	2.1	-0.8	0.0				
hsa-miR-6842-3p	1.5	2.1	0.0					

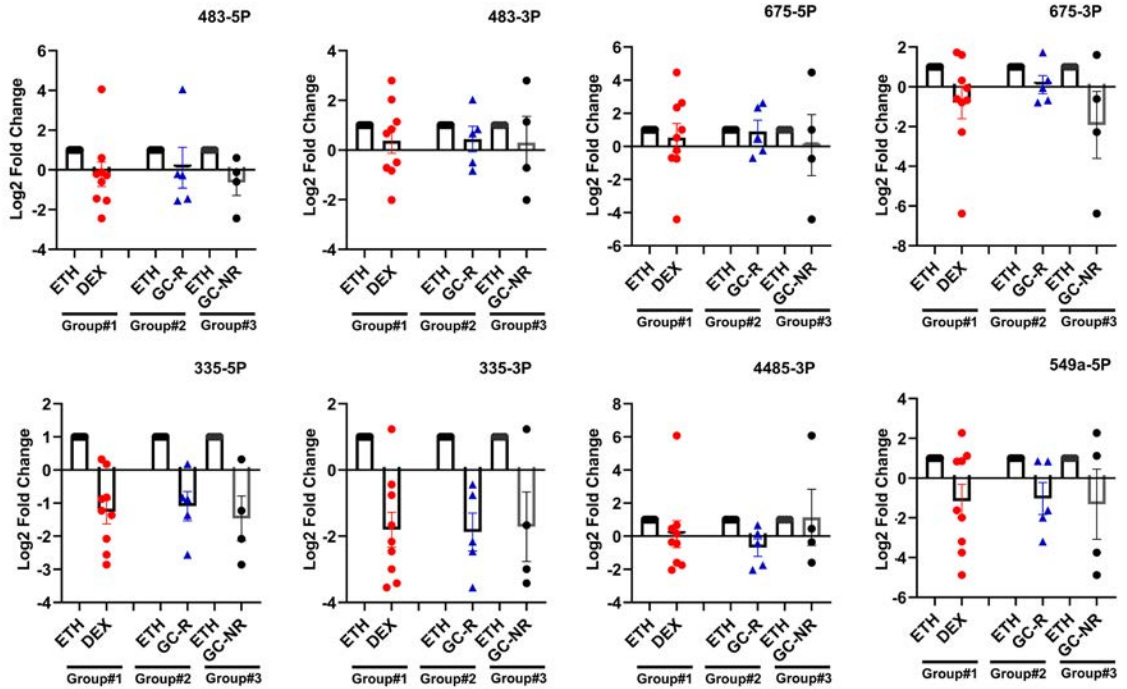


Figure 7A. Validation of miRNA sequencing by qPCR.

Primary HTM cells were treated with DEX or 0.1% ETH for 7 days. RNA was extracted and reverse transcribed for qPCR using U6 as an internal control. $2^{-\Delta\Delta Ct}$ method was used for calculation (n= Group #1: 9; Group #2: 4; Group #3: 5).

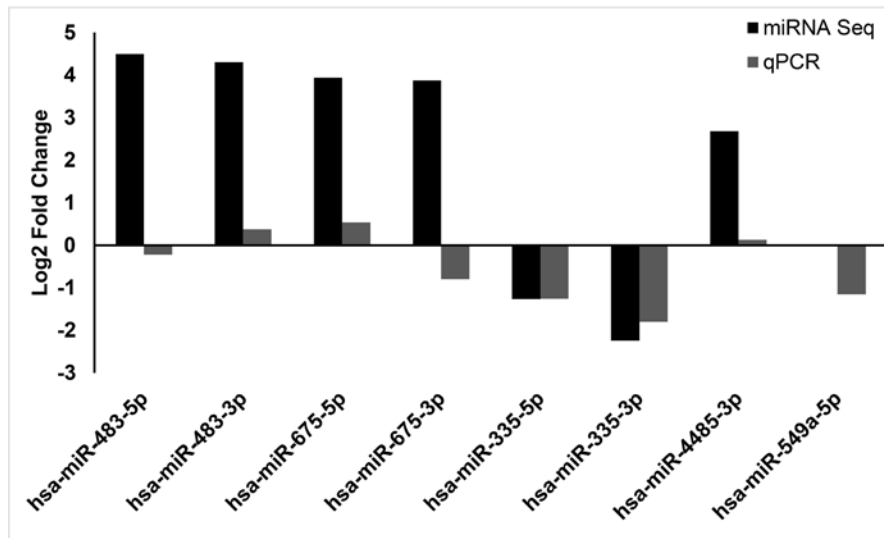


Figure 7B. Validation of miRNA sequencing by qPCR.

Values of Log₂ (Fold of change) : >0: up-regulation; = 0 non change; <0 down-regulation.
n = 4-5 (Group #2 and #3); n=9 (Group #1).

several steps to produce high-quality alignment files, and to detect definite variants. Initially, the quality of the raw reads obtained from SRA will be checked by FastQC and the low-quality reads, adapter contaminates will be trimmed by Cutadapt. Alignment of the reads with the reference genome will be performed using BWA and Novoalign. PCR duplicates will be removed using PiCard Tools with option provided by the user. The variants, single nucleotide variants (SNVs) and InDels will be identified by DeepVariant and strelka. Annovar tools performs annotation for all the variants. The variant prioritization step will be performed on the case-by-case basis. Therefore, we provide here the github online link : <https://github.com/bharani-lab/WES-pipelines/> for the details with filtering option. The default filtering methods as shown in figure 1.1 is better works for illumina whole exome/targeted sequencing data for Mendelian and Complex eye disorders. The stringent filtering strategy is better optimized with eye disease exome/targeted data sets, which involves heuristic filtering methods for pathogenic variant prioritization and machine learning methods using gene-based models.

In-house machine learning method for Pathogenic Variant Prioritization

A machine learning method was developed to identify Single Nucleotide Variants (SNVs) pathogenic variants associated with eye disease gene panel. 825 genes were collected as Eye Disease Associated Genes (EDAG) from OMIM database (Online Mendelian Inheritance in Man) and HGMD database (The Human Gene Mutation Database). The

dataset consisted of 5412 pathogenic nsSNVs and 8567 common variations. Using 34 attributes, 93% sensitivity was observed with random forest (RF) than support vector machine (SVM) learning method. In addition, the machine learning method to identify novel variants for eye diseases independent of gene-based knowledge is under constant development to improve the sensitivity (not shown).

Case Study: Whole Exome Sequencing to identify causative variants in patients with BEST disease

A trio south Indian family patients with BEST disease were sequenced using Illumina. A total of 21 pathogenic variants were identified through heuristic filtering and co-segregation analysis. Of these, a novel missense mutation (c.G310A p.D104N) in the BEST1 gene was prioritized as disease causing variant using our RF method and also observed the same with Varelect. Furthermore, structural analysis of the variant showed that destabilizing effect of the variant through breaking the hydrogen bond as shown in the figure 1.2.

2. Diagnostic markers for Intra-Ocular Tuberculosis

Investigators : Dr. D. Bharanidharan
 Dr. SR. Rathinam
 Dr. Lalitha Prajna
 Dr. M. Vidyarani
 Research Scholar : C. Swathi
 Funding : DBT

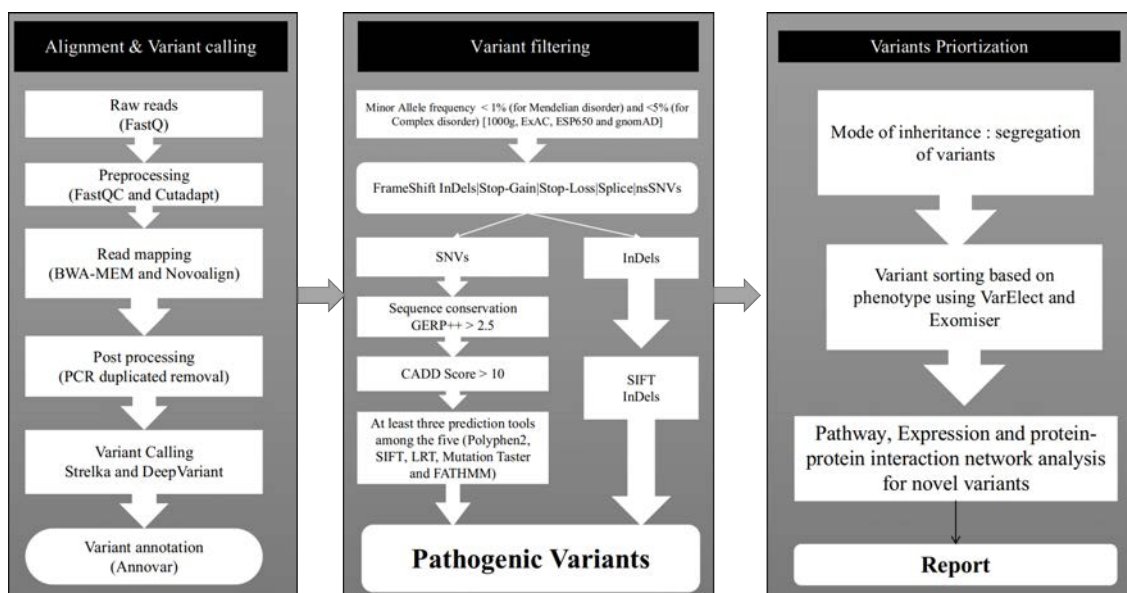


Figure 1.1. Variant calling pipeline workflow

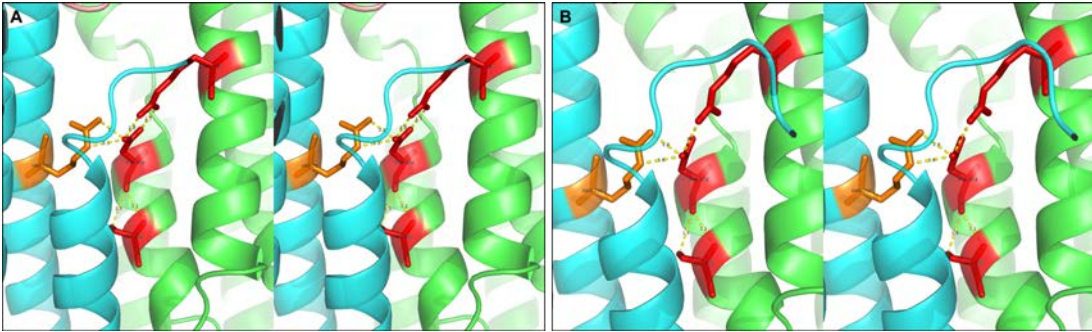


Figure 1.2 (A) represent the stereo image of wild type of BEST1 and (B) represent the stereo image of Mutant type of BEST1. The Yellow line indicates the hydrogen bond between the neighboring residues. The cyan blue represents the B chain and green represents the A chain of the BEST1.

Background

Ocular tuberculosis can present with extraocular or intraocular inflammation, the most common manifestation being uveitis. The differential diagnosis of Intraocular TB is challenging because it is a great mimicker of various uveitis entities. Moreover, the limited size of ocular fluids and the paucibacillary nature of ocular M. tuberculosis infection create additional barriers in the diagnosis. The diagnosis is only presumptive and corroborated by laboratory tests and therapeutic response to Anti-TB treatment (ATT). These leads to undiagnosed TB uveitis carry a risk of high visual morbidity. Moreover, overzealous ATT treatment in the absence of TB infection carries a significant risk of systemic side effects. Therefore, advanced molecular markers in the diagnosis of ocular tuberculosis are required.

In order to explore the molecular mechanisms of pulmonary tuberculosis infection and to discover potential diagnostic biomarkers, global gene expression profiles in peripheral blood have been investigated by several studies. Similarly, the potential use of microRNAs as diagnostic biomarkers has received much attention. MicroRNAs are

expressed in various ocular tissues and have been implicated in various eye diseases, owing to their distinct tissue and disease-specific regulation as well as high sensitivity and specificity. Expression of miRNAs targeting dysregulated proteins can complement RNA based biomarkers in ocular tuberculosis. This will be the first study to test the efficacy of molecular biomarkers in the diagnosis of ocular tuberculosis. Although various studies have discussed the potential use of mRNA and protein-based biomarkers in the diagnosis of pulmonary tuberculosis, none of them have addressed it in the context of ocular tuberculosis. Identification and validation of an integrated miRNA and mRNA signature in intraocular fluid samples will have potential diagnostic value in tuberculous uveitis patients.

Results and Conclusions

Small RNA deep sequencing on ultra-low-input RNA sample: Clinically suspected Ocular TB (OTB) samples confirmed with CT scan, Mantoux, PCR were selected for NGS. Four AH (two OTB, two cataract) and Six VH (three OTB, three Macular

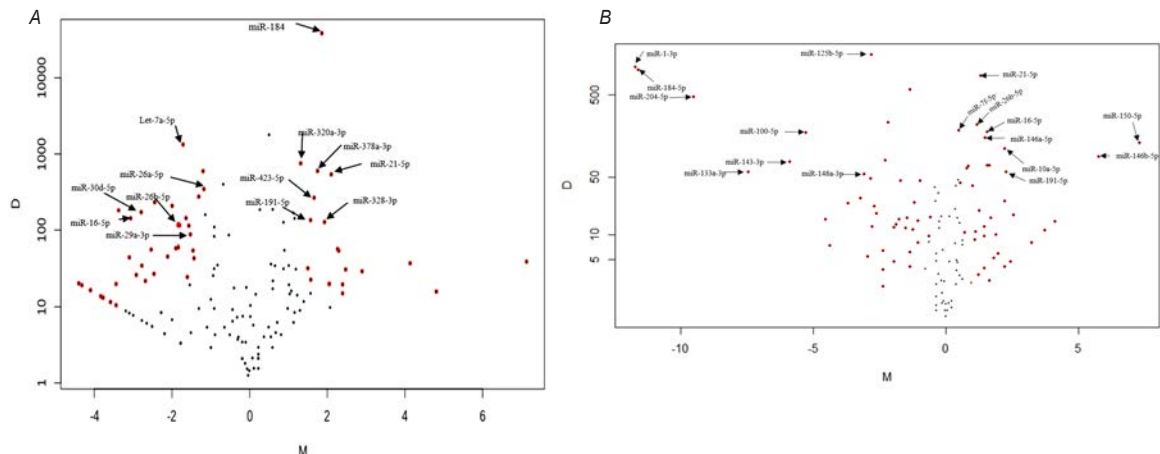


Fig.2.1 The volcano plot depicts the differential expression (DE) of microRNAs in AH (left - A) and VH (right - B) of TB samples compared to control samples.

hole) were sent for NGS. NGS was achieved with ultra-low input RNA samples (<100 ng and <500 ng of total RNA of AH and VH respectively) using GenXpro Kit, Germany. Data analysis was performed using in-house pipeline and other tools for differential expression analysis.

Fifty-six miRNAs with fold change 1.2 or greater were identified as significant differentially expressed (DE) in AH of ocular TB samples compared with cataract controls. 56 DE miRNAs in AH, 13 miRNAs were selected for further validation, based on their relative abundance and foldchange from the volcano plot (Fig 2.1 A) (Named ones). 17 miRNAs from VH data was selected as significantly differentially expressed (Fig 2.1 B) (Named ones).

Validation of differentially expressed miRNAs in AH using qPCR

Among thirteen miRNAs, three miRNAs hsa-miR-423-5p (Fold Change (FC), 3.1), hsa-miR-328-3p (FC, 0.8) and hsa-miR-21-5p (FC, 2.1) were selected based on qPCR data as shown below (Fig 2.2). Also, hsa-miR-16-5p (FC, 3.8) was selected, which reported to be differentially expressed in latent and active systemic tuberculosis patients.

Using predicted targets, among top 15 enriched pathways, five pathways mTOR signaling pathway, MAPK signaling pathway, PI3K-Akt signaling pathway, tuberculosis, and autophagy, were selected, which is of our interest in tuberculosis related pathways.

Based on the functional network analysis and literature report, fifteen genes (red text in fig 2.3) were selected for qPCR expression analysis in AH.

In conclusion, for the first time, the small-RNA sequencing from the low-volume of aqueous humor (AH) and vitreous humor (VH) of ocular TB patients, and cataract and Macular hole patients as controls was achieved. Potential ocular TB – specific miRNAs were identified and validated in AH samples. Four miRNAs miR-423-5p, miR-328-3p, miR-21-5p, and miR-16-5p were significantly differentially expressed in TB patients compared to

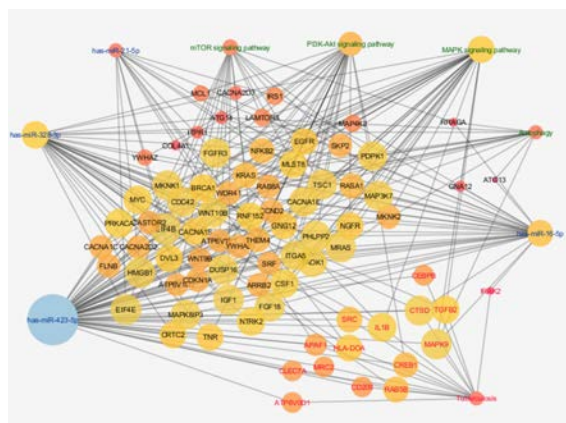


Fig.2.3 Target Genes and functional analysis for four selected miRNAs from AH samples

cataract controls using AH samples. Five enriched pathways mTOR signaling pathway, MAPK signaling pathway, PI3K-Akt signaling pathway, tuberculosis, and autophagy were identified based on the pathway analysis of four miRNAs predicted targets. Further, network analysis and TB-related literature identified fifteen genes that may have role in the ocular TB pathogenesis, requires expression analysis in ocular TB. Also several potential ocular TB-specific miRNAs were identified using VH, which requires validation to confirm their role as diagnostic markers.

3. Comparative genomics of bacterial pathogens isolated from keratitis patients

Investigators : Dr. D. Bharanidharan
Dr. Lalitha Prajna
Research Scholar : K. Kathirvel, O. Ruthra
Funding : AEH

Background

Bacterial keratitis, often caused by *Pseudomonas aeruginosa* and methicillin-resistant *Staphylococcus aureus* (MRSA), has a complex pathogenesis process. Majority of times in spite of adequate medical management the ulcer does not heal and

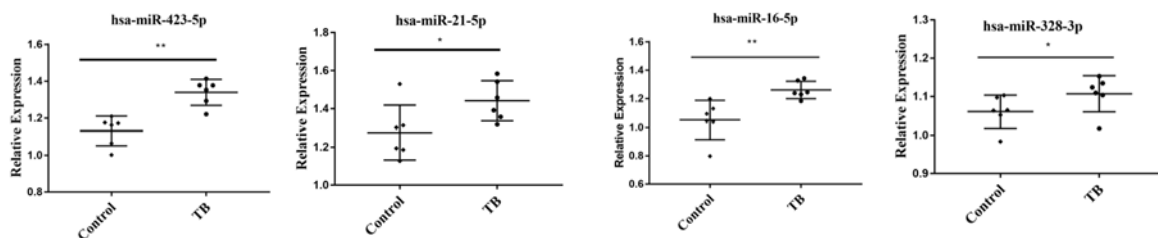


Fig.2.2 Relative expression values of four miRNAs in TB patients (N=6) compared to cataract controls (N=6).

Median values are shown by horizontal lines. P-value was calculated using the Mann-Whitney test. *P<0.05, ** P<0.01, ns= non significant

may require a corneal transplant. Several virulence factors, multiple drug resistance mechanisms and altered host response has been implicated in the treatment failure. Comparative genomics through de novo assembly of next-generation sequencing and third-generation sequencing methods of ocular bacterial pathogens will show genetic features specific to the causative organism. Further insights would show that these strain-specific features may response to the host immune system, which may indeed affect the outcome of the disease. Our genome analysis of ocular *P. aeruginosa* strains from keratitis patients highlighted that strains with MDR/XDR carry *exoU* and non-MDR carry *exoS* as their major virulence in keratitis.

In addition, the presence of flagellar genes in non-MDR strains that alters the host immune response may impact the clinical outcome. On the other hand, we sequenced four ocular MRSA strains using Oxford Nanopore MinION sequencer and also used Illumina Nextseq500 sequencer reads along with MinION reads to benchmark genome assembly under various conditions. After evaluation, we found that only MinION-based assembly could not be suitable for the comparative genomics studies, but we could obtain the acceptable assembly along with Illumina reads. Next, we compared the complete genomes to investigate the genetic features and molecular characteristics including antibiotic resistance, virulence factors, and diversity using various bioinformatics tools.

Results and Conclusion

Our findings exhibited that each isolate incorporated one circular chromosome of approximately ~2.8 Mbp with a mean GC content of 32.7%, one plasmid sequence carrying the antibiotic resistance, virulence, cadmium heavy metal resistance gene, and mobile genetic elements (MGEs). Resistance towards the different classes of antibiotics like fluoroquinolone, tetracycline, β -lactam, aminoglycoside, folate pathway inhibitors, lincosamides, and macrolides

antibiotics was seen. Moreover, virulence genes encoding enterotoxin, exfoliative toxin, hemolysin, biofilm production, superantigens, and several exotoxins have been detected (Figure 3.1).

AMRF3 and AMRF5 are highly homologous and belonged to the ST772 lineage, while AMRF4 and AMRF6 belonged to the ST2066 lineage, there was

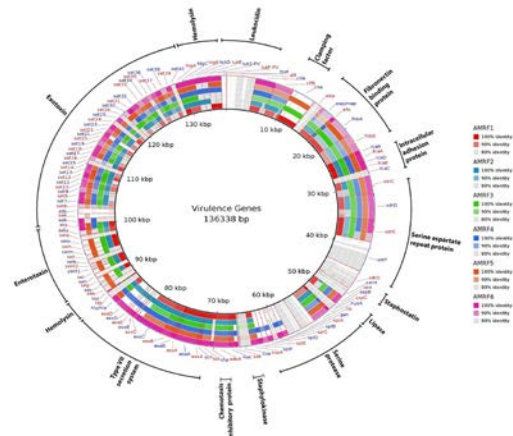


Figure 3.1: Circular representation of four Ocular MRSA genome major virulence genes compared against VFDB: White bar in circles represent the absence of respective virulence genes in ocular MRSA genome. White bar in circles represent the absence of respective virulence genes in ocular MRSA genome.

concordance amongst the sequence typing and virulence & antibiotic resistance gene profile in four MRSA isolates. Phandango analysis (Fig 3.2) showed three different clades from six ocular MRSA isolates, one contained AMRF3 and AMRF5 (ST772), and the other contained AMRF4 and AMRF6 (ST2066), one another clade contained AMRF1 and AMRF2 (ST22 and ST672).

In conclusion, this study showed all four MRSA isolates are multi-drug resistant, highly virulent, and diverse in the term of genotypic characteristic. This MRSA isolates genomic data could be used to monitor the transmission of ocular infection, evolutionary relationship, genetic diversity, and as a model genome during the clinical diagnosis of ocular MRSA strains and its future research.

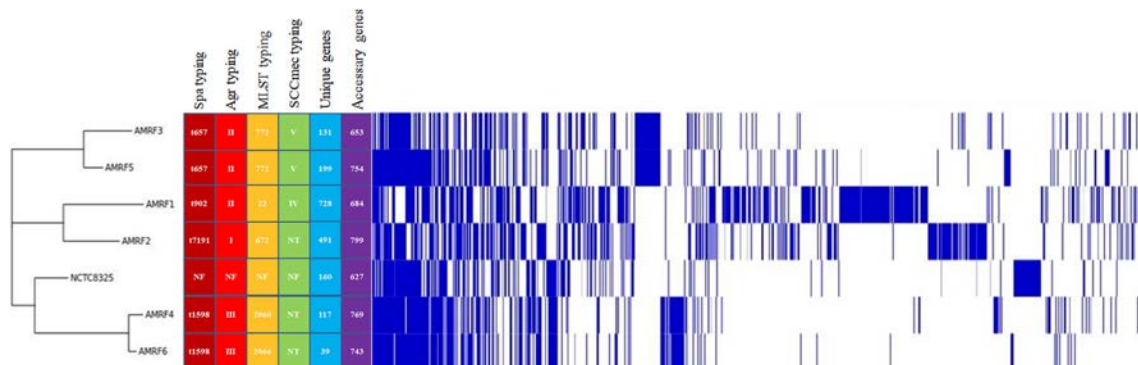


Figure 3.2. Phandango plot of assessor genomes of all six strains including their resistance and MLST, SCCmec, Spa and Agr typing. The strains were arranged phylogenetically based on the acquired resistance gene similarity (blue).

OCULAR MICROBIOLOGY

Major focus of the department is to understand the pathogenesis of ocular pathogens and its host interactions. The conventional microbiological methods along with molecular tools and next generation sequencing were employed for this purpose. As a part of routine diagnosis molecular methods such as PCR, Real Time PCR, DNA bar coding and Multi locus sequence analysis are used for the identification of ocular pathogens such as bacteria, fungus, Acanthamoeba spp., Mycobacterium spp., Toxoplasma, Microsporidia and virus such as HSV, VZV and CMV. Currently, pathogen aureus methicillin resistant Staphylococcus aureus (MRSA), extended spectrum β -lactamase producers (ESBL), *Pseudomonas aeruginosa*, and Acanthamoeba spp., is the major focus of our research.

Clinical association and characterization of type three secretory system, biofilm formation and antibiotic resistance of *Pseudomonas aeruginosa* isolated from Keratitis patients

Investigator : Dr. S. Lalitha Prajna,
Research Associate: Dr. R. Siva Ganesa
Karthikeyan
Technician : A. Selva Pandiyan

Introduction

Pseudomonas aeruginosa is a Gram-negative opportunistic pathogen and a common cause of bacterial corneal infections. *P. aeruginosa* corneal infections have poor clinical outcome and are more

difficult to treat than other bacterial infections. *P. aeruginosa* has arsenal of virulence mechanisms among which, biofilm formation and type three secretory systems (TTSS) are extensively studied. TTSS allows the *P. aeruginosa* to inject the effector proteins directly into the cytosol of target cells when came into contact. Neutrophils are the primary innate immune cells essential for controlling the *P. aeruginosa*. Using the TTSS *P. aeruginosa* can escape from infiltrating neutrophils by inhibiting phagocytosis and reactive oxygen species burst. TTSS has four effector toxins such as Exo (exoenzyme) S, ExoT, ExoU and ExoY. These toxins affect DNA synthesis, endocytosis, phagocytosis, vesicle trafficking, cell necrosis, apoptosis and interrupt wound healing process. In natural condition, ExoY do not have significant impact on the virulence nature of *P. aeruginosa*. Only ExoS, ExoT and ExoU are demonstrated as primary effectors associated with *P. aeruginosa* infection. In addition, associations of antibiotic resistance with the TTSS were also reported. The high expression of TTSS in cornea also aid in development of stronger biofilm on the corneal surface, which further protects the organism from neutrophils as well as antibiotic treatments. There are only very fewer clinical studies were reported characterizing the virulence factors and its association with clinical outcome of the disease.

Results and conclusion

In the current study, 50 corneal ulcer patients infected with *P. aeruginosa* were included. *P. aeruginosa* were isolated from corneal scraping, which were confirmed by standard microbiological methods



followed by VITEK system and 16S rDNA gene bar coding. The study group consists of 27 (54%) female and 23 (46%) male patients with mean age of 47.16 ± 16.7 years. The major symptom of patient when reported to the clinic includes, pain, redness, watering, photophobia and defective vision. The major predisposing factor of corneal trauma was reported in 21 patients out of which, 8 (16%) was reported due to the fall of foreign bodies, 8 (16%) were vegetative matters and others 5 (10%). After treatment, ulcer was healed in 40 (80%) patients and 10 (20%) patients were did not respond to the treatment resulting in corneal thinning, perforation and progression to endophthalmitis. In one patient the entire eye got infected leading to complete removal of the eye. Even though, majority of the patients corneal ulcer were healed, vision status (based on best corrected visual acuity) was improved only in 24 (48%) patients, no change was observed in 9 (18%) and worse in 17 (34%) patients.

Among the 50 isolates *exoST* genotypes were identified in 24 (48%) isolates and found to be predominant followed by *exoUST* 7 (14%), *exoS* in 5 (10%), *exoT*, and *exoUT* in 4 (8%), two isolates (4%) were found to be have *exoU* genotype and 4 (8%) did not had any of the effector genes. The release of the exotoxin effectors was analyzed by culturing the organisms in calcium deficient environment and identified by western blot. *ExoST* and *ExoT* expression was identified in 16 (32%) and 10 (20%) respectively, followed by 7 (14%) *ExoUT* phenotype, 6 (12%) *ExoS*, one (2%) *ExoU*, one (2%) *ExoUST* and 9 (18%) isolates did not express any of the exotoxin (Figure 1). The organism expresses *ExoU* or *ExoUT* are categorized as cytotoxic strains, *ExoS* or *ExoST* or *ExoT* as invasive, *ExoUST* as both cytotoxic and invasive and non-expressing organisms as nil phenotypes. Eight (16%) isolates were

identified as cytotoxic, 32 (64%) as invasive, only one strains (2%) was identified as both invasive and cytotoxic. The nine (18%) isolates did not express any of the exotoxin even though some of them had the exotoxin genes.

Strong biofilm formation was observed in 39 (78%) isolates, 7 (14%) isolates forms moderate biofilm, one isolates (2%) form weak and three isolates (6%) did not form biofilm. The antibiotic resistance was measured by standard disc diffusion method. Among the tested antibiotics, highest resistance (66%) was observed for the cephotaxime followed by moxifloxacin (24%), amikacin (8%), 6% resistance each to ciprofloxacin, ofloxacin, gatifloxacin and gentamicin, levofloxacin (4%) and least resistance of 2% was observed for ceftazidime and tobramycin. All the cytotoxic strains were resistance to the ceftidime and tobramycin, 67% resistance was observed for ofloxacin and 50% resistance for levofloxin and amikacin. The invasive strains, 75% were resistance to moxifloxacin followed by 67% resistance was observed to cephotaxime, ciprofloxacin and gatifloxacin. Overall TTSS negative isolates were found to be sensitive to most of the tested antibiotics, highest resistance of 25% was observed to the amikacin followed by 12% resistance was observed to cephotaxime (Figure 2).

Only 6 (19%) of patients infected with invasive strains and 4 (50%) patients was infected with cytotoxic phenotypes were observed with worse clinical outcome. Based on the best corrected visual acuity, one patient (11%) from negative phenotypes, three patients (38%) from cytotoxic and 13 (41%) patients infected with invasive pathogen were observed with worse vision outcome (Figure 3). The clinical outcome in patients infected with cytotoxic isolates had higher risk for poorer clinical outcome (Odds ratio 19 with 95% CI 0.8303 to 434.8

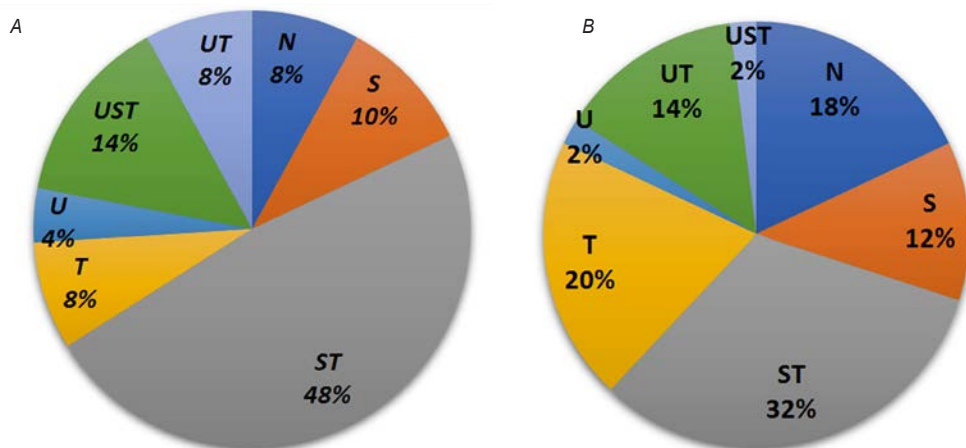


Figure 1: Number of isolates positive for exozymes genes *exoU*, *exoS*, and *exoT* identified by PCR (A); exozyme production in calcium deficient environment identified by western blot (B).

P value - 0.0294) than invasive strain infected individuals (Odds ratio 4.66 with 95% CI 0.2388 to 90.94 P value -0.309).

Conclusion

In conclusion, most of the *P. aeruginosa* isolates had TTSS and also able to form biofilm. Cytotoxic strains have shown clinical outcome as well as they are resistance to multiple antibiotics. For implementing any treatment strategy in addition to the antibiotic resistance nature, virulence factors must also taken into account. The targeted therapy of blocking the biofilm formation and TTSS systems can enable neutrophils to eliminate the bacteria. Understanding

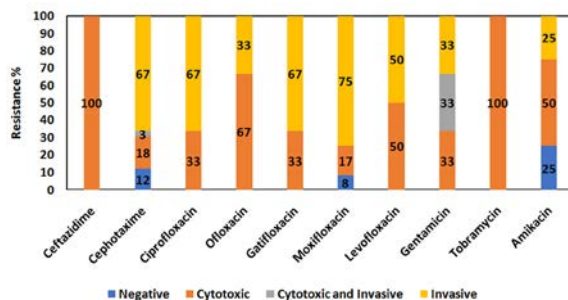


Figure 2: The antibiotic sensitivity profile identified by disc diffusion methods and the zone of inhibition interpreted as per the CLSI standards. The numbers in each bar represent the resistance percentage of TTSS isolates calculated among the total number of organism resistance for that specific antibiotic.

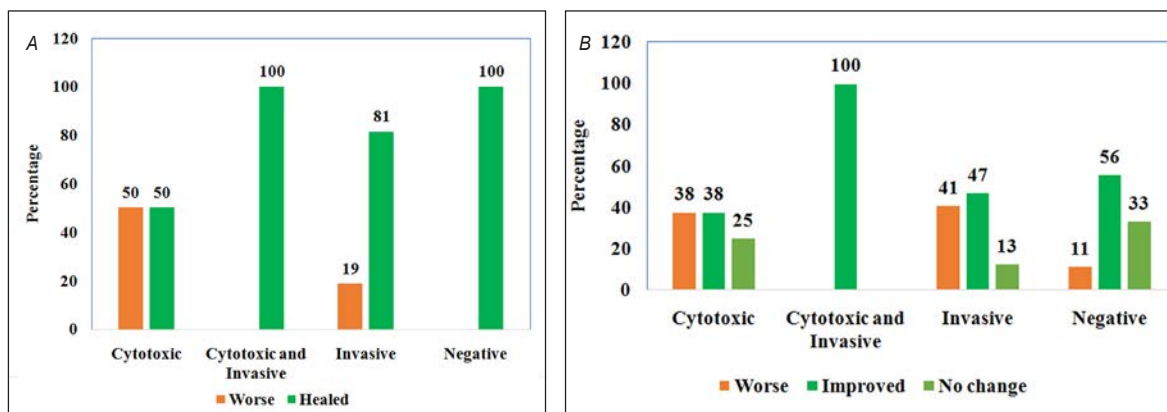


Figure 3. The data in each bar represents the percentage of patients healed or worse clinical outcome (A); Worse or improved vision status based on the best corrected visual acuity (B).

the virulence nature will aid in better understanding of disease pathogenesis as well aid in development of targeted treatment for better clinical and visual improvement.

Contribution of Macrophage Migration Inhibitory Factor (MIF) in the immunopathology of human microbial keratitis and its utility in disease management

Investigator : Dr. Swagata Ghosh
 Co-Investigator : Dr. N.V. Prajna
 Clinician Scientist : Dr. Lalitha Prajna
 Team Members : Athulya G. Shankar,
 Dr. Ninad Mudaraddi
 Funding Agency : Sun Pharma

Introduction and background

Microbial keratitis is an infectious eye disease caused by a variety of microbial pathogens that drive severe

inflammation and damage to the cornea, often leading to blindness. The incidence of infectious microbial keratitis has increased in the developing world to an epidemic proportion. In spite of providing adequate treatment, the outcome is often poor where patients fail to respond and are left with moderate or worse visual impairment requiring expensive surgical intervention that is often unsuccessful.

The severity of infection associated ocular morbidity is determined not only by the virulence of the pathogen but also by the extent to which the host immune defence is induced. The initial infection triggers the innate immune cells like neutrophils and macrophages to infiltrate the site of infection necessary for the clearance of the invading pathogen, but, unresolved inflammation causes excessive tissue destruction and severe keratitis. Most of our current available therapy are directed towards targeting the pathogen while unabrogated host inflammation remains to be one of the major challenges in treating eye infection. Therefore, there is a continued need for immunosuppressive drugs for infectious keratitis.

The Macrophage Migration Inhibitory Factor (MIF) is an upstream mediator of host inflammation. Unlike other cytokines, MIF is constitutively expressed in immune cells and epithelial lining of tissues and released upon contact with the pathogens. It triggers the expression of a wide range of pro-inflammatory molecules which further amplifies the inflammatory response by inducing large and continuous influx of immune cells at the site of infection. Therefore, MIF has been a prime target for reducing inflammatory damage in a number of autoimmune and inflammatory diseases, however, the scope of immunosuppression by targeting MIF in eye infection remains fairly unexplored.

Hypothesis

Human MIF drives inflammation and corneal damage in infectious microbial keratitis.

The specific objectives addressing the hypothesis are as follows: 1) To evaluate MIF protein levels in the tear samples of keratitis patients with i) *A. flavus*, ii) *P. Aeruginosa*, or iii) *Acanthamoeba* sp. infection compared to the uninfected controls; 2) To determine how tear MIF levels correlate with downstream inflammatory cytokines (IL-8, TNF- α ,) and the disease outcome. 3) To determine the effect of MIF inhibitor 4-IPP and anti-MIF neutralizing antibody *in vitro* on corneal epithelial cell derived IL-8 release upon infection with *Acanthamoeba* or *A. flavus* or stimulation with patient tear.

Proposed experiments and expected outcome

Tear samples from early stage patients (within 7 days of infection) with microbial keratitis involving bacteria (*P. aeruginosa*), fungus (*A. flavus*) and amoeba (*Acanthamoeba* sp) as well as uninfected controls will be collected and MIF, IL-8 and TNF- α levels will be quantified by ELISA. Comparisons will be made between uninfected controls and each infection group as well as between infection groups. Data will be analysed for correlation between MIF levels with downstream pro-inflammatory cytokine expression. Patients will be followed for disease progression during therapy and outcome will be graded. Preliminary data analysis will be done for correlation between MIF expression level and disease prognosis/ outcome. In-vitro infection model will be used for analysing MIF, IL-8 and TNF- α secretion from human corneal epithelial cells by ELISA upon infection with the pathogen as well as upon stimulation with patient tear containing high concentration of MIF. The same will be carried out in presence of a MIF inhibitor (4-IPP) or a neutralizing antibody against human MIF. The results will help us conclude if MIF is involved in the inflammatory response during infection, if

it might have any disease prognostic value and a 'proof of concept' for the inhibition of secreted MIF to be a strategy for abrogating epithelial cell-derived inflammatory signals.

Work in progress

While *A. flavus in vitro* infection model is well established in the proteomics labs, *Acanthamoeba* trophozoite infection was never been attempted in the institute. For diagnostic purposes *Acanthamoeba* is cultured in non-nutrient agar (NNA) plates with bacterial (*E. coli*) overlay which cannot be used for infecting human corneal epithelial cells *in vitro*. Therefore, we initiated axenic (bacteria free) liquid culture procedure in the lab. For this, NNA - *E.coli* overlaid plates were used for subculturing patient isolates of *Acanthamoeba* strains, which excyst and multiply in the presence of *E.coli*, followed by encystation once *E.coli* is limiting. Thus the cysts are amplified and harvested in saline solution for treatment with 3% HCL overnight to get rid of any contaminating microbes. Treated cysts are washed and used for inoculating a liquid Peptone-Yeast extract-Glucose based (PYG) medium in T-75 tissue culture flasks. Flasks are incubated at 30C where excystation happens in a span of 24-48 hours. Once, the trophozoites show about 10% confluency, excess suspended cysts are discarded by changing the media and the flasks are incubated until it reaches about 90% confluency with trophozoites.

Once 90% confluency is attained we harvest the trophozoites to add to a confluent monolayer

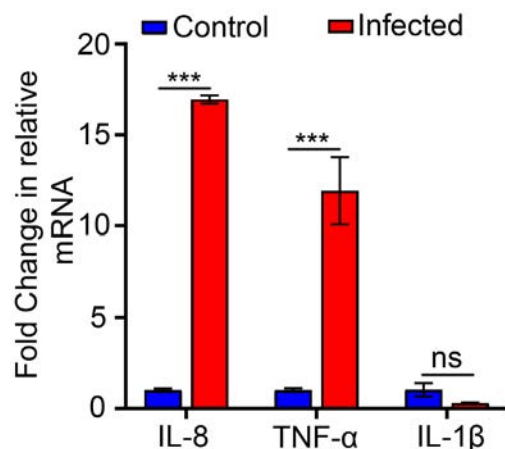


Fig 1. IL-8 and TNF- α gene expression is increased in human corneal epithelial cells upon infection with *Acanthamoeba* trophozoites. Total RNA from human corneal epithelial cells cultured in RPMI medium with and without *Acanthamoeba* trophozoites for 16 hours were analysed by real time PCR for the expression of human IL-8, TNF- α and IL-1 β genes. Gene expression was measured relative to the housekeeping control HPRT. Fold changes in relative gene expression were calculated in infected samples over the uninfected controls. Data represent Mean \pm SD, ***P<.001.

of human corneal epithelial cells, ideally with MOI of one or more. In our experiment so far, we were able to infect with MOI of 0.4, however we observed a 16- and 12-fold increase in the expression of IL-8 and TNF- α genes respectively, whereas IL-1 β gene expression showed a decreasing trend, after 16 hours of infection (Fig 1.) compared to the uninfected controls. This data implies that specific pro-inflammatory cytokines are induced upon *Acanthamoeba* infection to the cells. We also investigated if MIF gene expression is increased and found that there is no significant change in the MIF expression level. However, the basal level

expression of MIF transcripts were found to be high, suggesting that MIF is constitutively expressed in these cells. Therefore, it is likely that the secretion of the preformed MIF is triggered upon encounter with the amoeba, which is also implied by the elevation of expression of the cytokines, hallmark of MIF pathway activation in the host cells. Next, we will assess MIF release in the culture medium with and without *Acanthamoeba* infection by ELISA. Thus, a new *in vitro* pathogen infection model has been established in our lab providing infrastructure for our upcoming experiments.

CONFERENCES / MEETINGS

45th Annual meeting of the Indian Society of Human Genetics

Sri Ramachandra University, Porur, Chennai, Feb 13, 2020

Dr. P.Sundaresan

- Genomics for clinical Ophthalmology

All India Ophthalmic Conference (AIOC) and Indian Society of Human Genetics (ISHG) Meeting

Gurugram, Haryana, Feb 14, 2020

Dr.P. Sundaresan

- Glaucoma: Hereditary patterns based on gene mutations and chromosome alterations.



Dr.P.Sundaresan with Dr.Harminder Singh Dua, UK.

Annual Meeting of Association for Research in Vision and Ophthalmology (ARVO) 2020

Baltimore, USA. May 3-7, 2020 (Virtual)

P. Saranya, Department of Immunology and Stem cell Biology

- Identification and characterization of adult tissue resident stem cells in human anterior lens epithelium (poster).

Balaji Sekaran, Department of Molecular Genetics

- Chemotherapy sustained cancer stem cells and genomic alterations facilitate therapeutic resistance in retinoblastoma (poster).

18th Research Advisory Committee Meeting

March 14, 2020

During the meeting, faculty members of AMRF presented their work and received feedback. Research scholars presented their findings as posters and interacted with the committee members. Best poster was selected for Prof. VR.Muthukkaruppan Endowment award.

Invited talk

Alagappa University, Karaikudi , September 23,2020

Prof. VR.Muthukkaruppan and Dr. Gowri Priya Chidambaranathan visited Department of Biotechnology, Alagappa University, Karaikudi and gave a talk on "Biology of adult stem cells and their clinical applications".

Prof.VR.Muthukkaruppan and Dr. Gowri Priya at Alagappa University





18th Research Advisory Committee Meeting



AWARDS

Best poster presentation

Ms. O.Rudhra JRF, Department of Microbiology got first prize in poster presentation for the research work titled “Identification of Causative Organism of Infectious keratitis using NGS method” at the International Conference on Synergy of Sciences (ICSS-2020) during February 27- 29, 2020 at SASTRA Deemed University, Thanjavur.

Ph.D awarded by Madurai Kamaraj University

Ms. S.Yogapriya, Department of Immunology and Stem Cell Biology

Thesis: Understanding the role of trabecular meshwork stem cells in the maintenance of tissue homeostasis in normal and glaucomatous human eyes

Guide: Dr. Gowri Priya Chidambaranathan

Prof. VR. Muthukkaruppan Endowment Award 2020

Students & colleagues of Prof.VR.Muthukkaruppan, Advisor, Aravind Medical Research Foundation created an Endowment in his name in 2014 out of which an award will be given to the best researcher at the Institute every year. The award is given based on the scientific merit of abstracts and presentation by the research scholars. This award carries a certificate and cash prize of Rs.25,000/-

Ms. S.Yogapriya, Department of Immunology and Stem Cell Biology, won the award for her outstanding research work on “Functional characterization of human trabecular meshwork stem cells identified based on two-parameter analysis”.

Ph.D defense (virtual)

Mr. K.Thirumalai Raj, Senior Research Fellow, Department of Molecular Genetics defended his Ph.D thesis titled “Characterization of genetic and transcriptional alterations in Retinoblastoma” through video conferencing on October 12, 2020.



Ms. S. Yogapriya receiving Prof.VR. Muthukkaruppan Endowment Award 2020

PUBLICATIONS 2020 - 2021

XIONG ZHU *et al.*,

- "Identification of Novel Mutations in the FZD4 and NDP Genes in patients with Familial Exudative vitreoretinopathy in South India"

Genet. Test Mol Biomarkers 2020;24(2): 92-98

LAVANYA KALAIMANI, BHARANIDHARAN DEVARAJAN, UMADEVI SUBRAMANIAN, VANNIARAJAN AYYASAMY, VENKATESH PRAJNA NAMPERUMALSAMY, MUTHUKKARUPPAN VEERAPPAN, GOWRI PRIYA CHIDMABARANATHAN

- "MicroRNA profiling of highly enriched human corneal epithelial stem cells by small RNA sequencing"

Scientific Reports 2020;10:7418

SEKARAN BALAJI, RADHAKRISHNAN SANTHI, USHA KIM, VEERAPPAN MUTHUKKARUPPAN, CHIDAMBARANATHAN GOWRI PRIYA, AYYASAMY VANNIARAJAN

- "Cancer Stem Cells with Overexpression of Neuronal Markers Enhance Chemoresistance and invasion in Retinoblastoma"

Current Cancer Drug Targets 2020;20(9):710-719

MOHAMMED RAZEETH SHAIT MOHAMMED, SANDHYA KRISHNAN, RABBIND SINGH AMRATHLAL, JEYA MAHESHWARI JAYAPAL, VENKATESH PRAJNA NAMPERUMALSAMY, LALITHA PRAJNA, DHARMALINGAM KUPPAMUTHU

- "Local Activation of the Alternative pathway of complement system in Mycotic Keratitis patient tear"

Front Cell Infect Microbiol 2020;10: 205

SOUNDARARAJAN ASHWINBALAJI, RAVINARAYANAN HARIBALAGANESH, SUBBAIAH KRISHNADAS, VEERAPPAN MUTHUKKARUPPAN, SRINIVASAN SENTHILKUMARI

- "SB772077B (SB77) Alleviated the Aqueous Outflow Resistance Mediated by Cyclic Mechanical Stress in Perfused Human Cadaveric Eyes"

Sci Rep 2020;10: 10202

SARAH SZE WAH WONG, IRENE DANIEL, JEAN-PIERRE GANGNEUX, JEYA MAHESHWARI JAYAPAL, HÉLÈNE GUEGAN, SARAH DELLIÈRE, PRAJNA LALITHA, RAJASHRI SHENDE, TARUNA MADAN, JAGADEESH BAYRY, J. IÑAKI GUIJARRO, DHARMALINGAM KUPPAMUTHU, VISHUKUMAR AIMANIANDA

- "Differential interactions of serum and bronchoalveolar lavage complement proteins with conidia of airborne fungal pathogen *Aspergillus fumigatus*"

Infect immune 2020 Jun 22 (E Pub)

SEKARAN BALAJI, AYYASAMY VANNIARAJAN

- "Implication of Pseudo Reference Genes in Normalization of Data from Reverse Transcription-Quantitative PCR"

Gene 757 (2020)

THENNARASU SHANTHINI, SEKARAN BALAJI, USHA KIM, VEERAPPAN MUTHUKKARUPPAN, AYYASAMY VANNIARAJAN

- "Genetic characterization of a patient with an unusual presentation of waardenburg syndrome Type 4 and retinoblastoma"

Pediatr blood cancer 2020

SR. RATHINAM, GOWRI PRIYA CHIDAMBARANATHAN

- "Corneal melt in leptospirosis"

Ophthalmic Image 2020; 68(9): 1970

KATHIRVEL KANDASAMY, KANNAN THIRUMALMUTHU, NAMPERUMALSAMY VENKATESH PRAJNA, PRAJNA LALITHA, VIDYARANI MOHANKUMAR, BHARANIDHARAN DEVARAJAN

- "Comparative genomics of ocular *Pseudomonas aeruginosa* strains from keratitis patients with different clinical outcomes"

Genomics 112 (2020) 4769-4776

EKATERINA YONOVA-DOING WANTING ZHAO, ROBERT P. IGO JR, CHAOLONG WANG, PERIASAMY SUNDARESAN, KRISTINE E. LEE, GYUNGAH R., ALEXESSANDER COUTO ALVES, XIAORAN CHAI, ANITA S. Y. CHAN, MEI CHIN LEE, ALLAN FONG, AVA G. TAN, CHIEA CHUEN KHOR, EMILY Y. CHEW, PIRRO G. HYSI, QIAO FAN, JACQUELINE CHUA, JAEYOON CHUNG, JIEMIN LIAO, JOHANNA M. COLIJN, KATHRYN P. BURDON, LARS G. FRITSCHER, MARIA K. SWIFT, MARYAM H. HILMY, MIAO LING CHEE, MILLY TEDJA, PIETER W. M. BONNEMAIJER, PREETI GUPTA, QUEENIE S. TAN, ZHENG LI, ERANGA N. VITHANA, RAVILLA D. RAVINDRAN, SOON-PHAIK CHEE, YUAN SHI, WENTING LIU, XINYI SU, XUELING SIM YANG SHEN, YA XING WANG, HENGTONG LI, YIH-CHUNG THAM, YIK YING TEO, TIN AUNG, KERRIN S. SMALL, PAUL MITCHELL, JOST B. JONAS, TIEN YIN WONG, ASTRID E. FLETCHER, CAROLINE C. W. KLAVER, BARBARA

E. K. KLEIN, JIE JIN WANG, SUDHA K. IYENGAR, CHRISTOPHER J. HAMMOND & CHING-YU CHENG
- *“Common variants in SOX-2 and congenital cataract genes contribute to age-related nuclear cataract”*

Commun Biol. 2020 Dec 11;3(1):755

POIGAIALWAR GOWRI, SHANMUGAM MAHESH KUMAR, AYYASAMY VANNIARAJAN, DEVARAJAN BHARANIDHARAN, PERIASAMY SUNDARESAN
- *“A hospital-based five-year prospective study on the prevalence of Leber’s hereditary optic neuropathy with genetic confirmation”*

Molecular Vision 2020; 26:789-796

SEN, SAGNIK, KANNAN SARASWATHI, SHANMUGAM ULAGANATHAN, RAJAN RENU, BABU NARESH AYYASAMY VANNIARAJAN

- *“Variable Phenotypes of Gyrate Atrophy in Siblings with a Nonsense Mutation in OAT Gene”*

Ophthalmic Genetics 2020 (E Pub)

RAVINARAYANAN HARIBALAGANESH, CHIDAMBARANATHAN GOWRI PRIYA, RAJENDRABABU SHARMILA, SUBBIAH KRISHNADAS, VEERAPPAN MUTHUKKARUPPAN, COLIN E. WILLOUGHBY, SRINIVASAN SENTHILKUMARI

- *“Assessment of differential intraocular pressure response to dexamethasone treatment in perfusion cultured Indian cadaveric eyes”*

Scientific Reports | (2021) 11:605

HARIHARAN GNANAM, SIVA GANESA KARTHIKEYAN RAJAPANDIAN, RAMESHKUMAR GUNASEKARAN, SWASTHIKKA ROSHNI PRITHIVIRAJ, RAM SUDARSHAN RAVINDRAN, SAGNIK SEN AND LALITHA PRAJNA

- *“Molecular species profiling of Nocardia species causing Endophthalmitis by Multi locus sequence analysis (MLSA): a ten-year perspective”*

Journal of Medical Microbiology. 2020 May; 69(5):728-738. DOI 10.1099/jmm.0.001180.

APPAVU SELVA PANDIYAN, RAJAPANDIAN SIVA GANESA KARTHIKEYAN, GUNASEKARAN RAMESHKUMAR, SAGNIK SEN & PRAJNA LALITHA
- *“Identification of Bacterial and Fungal Pathogens by rDNA Gene Barcoding in Vitreous Fluids of Endophthalmitis Patients”*

Seminars in Ophthalmology 2021, DOI:10.1080/08820538.2020.1864416

NARESH BABU KANNAN , SAGNIK SEN , PRAJNA LALITHA , CHITARANJAN MISHRA , GUNASEKARAN RAMESHKUMAR , GNANAM HARIHARAN , RAJAPANDIAN SIVA GANESA KARTHIKEYAN & KIM RAMASAMY.

- *“Challenges in Post-cataract Surgery Nocardia Endophthalmitis: Management Strategies and Clinical Outcomes”*

Ocular Immunology and Inflammation, DOI: 10.1080/09273948.2020.1826536

MILLS B, RADHAKRISHNAN N, SIVA GANESA KARTHIKEYAN RAJAPANDIAN, RAMESHKUMAR G, LALITHA P, PRAJNA NV.

- *“The role of fungi in fungal keratitis. Exp Eye Res. 2021 Jan;202:108372.*

HAZARIKA M, NAMPERUMALSAMY VP, SRINIVASAN S.

- *“Drug reservoir function of voriconazole impregnated human amniotic membrane: An in vitro study”.*

Indian J Ophthalmol 2020 (Accepted).

WONG SSW, VENUGOPALAN LP, BEAUSSART A, KARNAM A, MOHAMMED MRS, JAYAPAL JM, BRETAGNE S, BAYRY J, LALITHA P, KUPPAMUTHU D, LATGÉ JP, AIMANIANDA V.

- *“Species-specific immunological reactivities depend on the cell-wall organization of the two Aspergillus, Aspergillus fumigatus and A. flavus”.*

Front Cell Infect Microbiol. 2021. (Manuscript accepted for publication)

ONGOING RESEARCH PROJECTS

No	Projects	Funded by	Investigators	Research Scholar
PROTEOMICS				
1.	Study on Human mycotic keratitis	AMRF & AEH	Dr. N. Venkatesh Prajna Dr. Lalitha Prajna Dr. J. Jeya Maheshwari Dr. K.Dharmalingam Dr.O.G.Ramprasad	G. Hariharan S. Nishanti V.Renuka
2.	Prospective Multicenter discovery and validation of diagnostic circulating and urinary biomarkers and development of sensor(s) to detect sight threatening diabetic retinopathy - Biomarker and Biosensor study in UK and India (Indo-UK collaborative project)	Research Councils UK	Dr. K. Dharmalingam Dr. R.Kim Dr. J. Jeya Maheshwari	K.R. Shruthi Mahalakshmi Subash KK
3.	Proteome profiling of serum microparticles in diabetes and diabetic retinopathy patients: Towards identification and validation of predictive biomarkers	Department of Health Research (DHR)	Dr.J. Jeya Maheshwari Dr.K.Dharmalingam Dr.R.Kim	P. Vignesh
4.	Prediction of treatment outcome in fungal keratitis patients	Cognizant Foundation	Dr. K.Dharmalingam Dr. J. Jeya Maheshwari Dr. Bharanidharan D Dr. N. Venkatesh Prajna Dr. Lalitha Prajna	T.S.Pon Yazhini
5.	Development of aptamer-based assays for diagnosis of infectious keratitis and absolute quantitation of proteoform markers of diabetic retinopathy	Sun Pharma	Dr. J. Jeya Maheshwari Prof. K. Dharmalingam Dr. N. Venkatesh Prajna Dr. R. Kim	Sandhya L
6.	Screening the Kadaladi family with early onset Glaucoma for Myocilin gene mutations	Sun Pharma	Prof. K. Dharmalingam Dr. S.R. Krishnadas Dr. Mohideen Abdul Kader Dr. D. Bharanidharan	Sr.Technician: V. Saravanan
7.	Interaction of pathogenic fungi with Human Corneal Epithelial cells.	ICMR-SRF	Dr. K.Dharmalingam	A. Divya
8.	Understanding the mechanism of action of a novel chemical cross-linker designed to treat keratoconus	ICMR	Dr.O.G.Ramprasad Prof. K. Dharmalingam Dr. N.Venkatesh Prajna Dr. Naveen Radhakrishnan	T.M.Nasrin Banu
9.	Identification of druggable targets for attenuating the progression of pterygium development	Sun Pharma	Dr. Daipayan Banerjee Dr. Vishnu Teja Dr.N. Venkatesh Prajna Dr. K.Dharmalingam	Aadithiya T Gr
10.	Role of Retinol Binding Protein 3 (RBP3) in progression of Diabetic Retinopathy (DR) and evaluate its potential as a DR biomarker in Type 2 diabetic patients.	VISTA	Dr. Daipayan Banerjee Dr. Sagnik Sen Dr.R.Kim Dr. K.Dharmalingam	Aadithiya T Gr

MOLECULAR GENETICS				
11.	Molecular genetics of macular corneal dystrophy (MCD) in Indian population	DST INSPIRE Fellowship	Dr. P.Sundaresan Dr. N. Venkatesh Prajna	M.Durga
12.	Molecular genetics of ABCA4 gene in autosomal recessive Cone rod dystrophy and Retinitis Pigmentosa	Aravind Eye care system	Dr. P.Sundaresan Dr. Rupa Anjanamurthy	R. Kadarkarai Raj
13.	Understanding the molecular mechanisms of chemoresistance in retinoblastoma	CSIR-NET	Dr.A.Vanniarajan	T.S. Balaji
14.	Molecular characterization of tumor progression in retinoblastoma	DST INSPIRE Fellowship	Dr. A.Vanniarajan	T.Shanthini
15.	Identification and validation of deregulated cancer pathways in retinoblastoma	SERB	Dr. A. Vanniarajan	Anindita Rao
16.	Translational Genomics of Ocular Cancers	Aravind Eye Foundation	Dr. Usha Kim Dr. A. Vanniarajan Dr. D. Bharanidharan Dr. R. Shanthi Dr. VR. Muthukkaruppan	K.Saraswathi
17.	COE LEAD: Translational Genomics of paediatric eye diseases	DBT	Dr. P. Sundaresan Dr. A. Vanniarajan Dr. D. Bharanidharan Dr. P. Vijayalakshmi Dr. R. Kim Dr. Usha Kim	Dr. Roopam Gowri Poigalwar A.S.Sree Viswarubhiny
18.	COE PR-I: Molecular analysis of mitochondrial diseases with ophthalmic manifestations	DBT	Dr. P. Sundaresan Dr. A. Vanniarajan Dr. P. Vijayalakshmi	A.Aloysius Abraham
19.	COE PR-II: Epigenetic mechanisms underlying tumor progression in retinoblastoma	DBT	Dr. A. Vanniarajan Dr. D. Bharanidharan Dr. VR. Muthukkaruppan Dr. Usha Kim	K. Jeya Prakash A. Mohamed Hameed Aslam
20.	COE PR-III: Functional validation of novel candidate genes using alternate model	DBT	Dr. P. Sundaresan Dr. A. Vanniarajan	C. Prakash
21.	COE R&D: Computational methods for whole exome/genome sequencing of paediatric eye diseases	DBT	Dr. D. Bharanidharan Dr. P. Sundaresan Dr. A. Vanniarajan	K. Manoj kumar
22.	Molecular Genetics of Juvenile X-linked Retinoschisis in South Indian Population	Lady Tata Memorial trust	Dr. P. Sundaresan	Susmita Chowdhury
23.	Molecular characterization of ocular lymphoma for improved disease prognosis	Lady Tata Memorial trust	Dr. A. Vanniarajan	K. Saraswathi
24.	Targeted Modulation of E2F3 and KIF14 pathway in Retinoblastoma refractory to existing chemotherapeutic drugs	Sun Pharma	Dr. A. Vanniarajan Dr. Usha Kim Prof. K. Dharmalingam	R. Sethu Nagarajan

IMMUNOLOGY AND STEM CELL BIOLOGY				
25.	Characterization and Functional Evaluation of Trabecular Meshwork Stem Cells in Glaucoma Pathogenesis	SERB UGC-JRF	Dr. C. Gowri Priya Dr. S. Senthikumari Dr. Neethu Mohan Dr. SR.Krishnadas Prof. VR. Muthukkaruppan	R. Iswarya
26.	Characterization of adult human lens epithelial stem cells in the maintenance of tissue homeostasis throughout life and their functional status in cataractous lens	SERB	Dr. Madhu Shekhar Dr. C. Gowri Priya Chidambaranathan Dr.Haripriya Aravind Dr. Muthukkaruppan Veerappan	S. Sivaprakash
27.	Understanding the Role of Trabecular Meshwork Stem Cells in The Maintenance of Tissue Homeostasis in Normal and Glaucomatous Human Eyes	Lady Tata Memorial trust	Dr. Gowri Priya Chidambaranathan	S. Yogapriya
28.	MicroRNAs specific to corneal epithelial stem cells	CSIR-SRF	Dr. Gowri Priya Chidambaranathan	K. Lavanya
29.	Characterization of adult human lens epithelial stem cells, their niche and their role in the maintenance of tissue homeostasis	Lady Tata Memorial trust	Dr. Gowri Priya Chidambaranathan	P. Saranya
30.	Identification and Characterization of adult human retinal pigment epithelial stem cells	CSIR-SRF	Dr. Gowri Priya Chidambaranathan	A.Waseema
OCULAR PHARMACOLOGY				
31.	Role of miRNA in the regulation of Glucocorticoid Receptor (GR) signalling and Development of New therapeutics for Steroid-induced glaucoma	Wellcome-DBT /India Alliance Intermediate Fellowship (2017-2022)	Dr. S. Senthikumari Dr. C. Gowri Priya Dr. D. Bharanidharan Dr. R. Sharmila	R. Hari balaganesh K. Kathirvel
BIOINFORMATICS				
32.	Diagnostic Markers for Ocular Tuberculosis	DBT	Dr. D.Bharanidharan Dr. SR.Rathinam Dr. Lalitha Prajna Dr. M. Vidyarani	O.Ruthra
33.	Identification of Dysregulated MicroRNAs In Ocular Fluids as Diagnostic Markers for Intraocular Tuberculosis	ICMR-SRF	Dr.D.Bharanidharan	Swathi Chadalawada
34.	Computational Methods For Whole Exome/Genome Sequencing Of Paediatric Eye Diseases	DBT-COE, R&D	Dr.D.Bharanidharan Dr.A.Vanniarajan Dr.P.Sundaresan	K.Manojkumar

35.	Comparative genomics of Methicillin-Resistant Staphylococcus aureus (MRSA) and Pseudomonas aeruginosa ocular isolates from keratitis patients with different clinical outcomes	AEH	Dr. D. Bharanidharan Dr. Lalitha Prajna	K.Kathirvel O.Ruthra
36.	Role of Human Corneal MiRNAs in the onset and severity of Fungal Keratitis	ICMR	Dr. D. Bharanidharan Dr. K. Dharmalingam Dr. N. Venkatesh Prajna Dr. Lalitha Prajna	Shreya Dinesh
MICROBIOLOGY				
37.	Clinical significance of the Type Three Secretory System, Biofilm formation and Antibiotic Resistance of the Pseudomonas aeruginosa isolated from Keratitis patients	AEH	Dr. R. Siva Ganesa Karthikeyan	A. Selva Pandiyan
38.	Identification of Bacterial and Fungal Pathogens by rDNA Gene Barcoding in Vitreous Fluids of Endophthalmitis Patients	AEH	Dr. Lalitha Prajna	A. Selva Pandiyan
39.	Clinical and demographic study of non-tuberculous mycobacterial ocular infections in South India	AEH	Dr. Lalitha Prajna	A. Selva Pandiyan
40.	Contribution of Macrophage Migration Inhibitory Factor (MIF) in the immunopathology of human microbial keratitis and its utility in disease management	Sun Pharma	Dr. Swagata Ghosh Dr. N. Venkatesh Prajna	Athulya Shankar



Much has been done, but much remains to be done... we look to the future with renewed strength to continue the mission of providing quality eye care and hope that some of what we have learned will be useful to other eye care workers around the world.

G. Venkataswamy

ARAVIND MEDICAL RESEARCH FOUNDATION

DR. G. VENKATASWAMY EYE RESEARCH INSTITUTE

1, Anna Nagar, Madurai 625 020, Tamilnadu, India.

Phone: (0452) 435 6550

www.amrf.org.in



ARAVIND EYE CARE SYSTEM